NTNU
Norwegian University of
Science and Technology

The Compressor Recycle System

Bjørn Ove Barstad

Master of Science in Engineering Cybernetics
Submission date: August 2010
Supervisor: Jan Tommy Gravdahl, ITK

Norwegian University of Science and Technology
Department of Engineering Cybernetics

Problem Description

Surge is an instability occurring in compression systems. In the oil-, gas- and process industries, this problem is handled by using a recycle loop, ensuring higher flow through the compressor and thereby preventing surge. The main topic of this work should be analysis of this recycle control system.

Assignment:

1) Give a brief overview of compressors and the surge control problem.
2) Investigate the use of approximations of compressor maps, and present a method for numerical representation of the compressor map in simulations.
3) Propose a dynamical model of a compression system with a recycle loop
4) Propose a control law, and perform a stability analysis of the recycle control system.
5) Investigate if it is possible to use the recycle loop as a means for active surge control.

Assignment given: 11. January 2010
Supervisor: Jan Tommy Gravdahl, ITK

Abstract

The compressor recycle system is the main focus of this thesis. When the mass flow through a compressor becomes too low, the compressor can plunge into surge. Surge is a term that is used for axisymmetric oscillation through a compressor and is highly unwanted. The recycle system feeds compressed gas back to the intake when the mass flow becomes too low, and thereby act as a safety system.

A mathematical model of the recycle system is extended and simulated in SIMULINK. The mathematical model contains the compressor characteristic, which is a function that defines the axisymmetric behavior through a compressor at different flows. The compressor characteristic is often modeled as a third order equation, but here it is modeled as a bivariate cubic spline approximation of measurement points. It is shown how a typical industry-setup of the recycle system works to avoid surge.

The recycle system is proven to be stable independent of recycle flow, as long as the slope of the compressor characteristic is negative. Three control laws have been derived by the use of block backstepping. The simplest one of them guarantees semiglobal exponential stability.

Contents

List of Figures

Preface

This master thesis describes my work during my last semester at the Norwegian University of Science and Technology. It has been carried out at the Department of Engineering Cybernetics.

I would like to thank my supervisor during the period, professor Jan Tommy Gravdahl.

The thesis was typeset using LaTeX. All computations and simulations were done using MATLAB and SIMULINK.

Bjørn Ove Barstad

Chapter 1

Introduction

1.1 Motivation

Centrifugal compressors are used everywhere. They are used in the oil and gas industry to move gas through pipes, in refineries and plants, and in pumping gas back to oil reservoirs to increase the pressure in a well which increases oil production. They are used in aerospace to pressurize the fuselage at high altitudes and even as gas turbines, although beaten by the greater capability of mass flow by the axial compressor. It is the only option to supercharge and turbocharge in the automobile industry. They are also used in air conditioners and blowers. (Lüdtke, 2004)

The recycle system ensures stable operation of the centrifugal compressor by recycling gas back to the intake when the mass flow becomes too low. It currently belongs to the surge/stall avoidance scheme, where the unstable operating areas are avoided. The efficiency of the recycle system compared to newer, but not so accepted, active surge/stall control schemes is poor. Recycle systems often runs with considerable margin. That is, the recycle valve is opened long before there is any danger of moving into the instability area. The efficiency of a recycle system operating in the avoidance scheme is therefore low, since compressor system efficiency is highest when operating close to instability.

1.2 Thesis Outline

The thesis starts with an introduction to continuous flow compressors. In this chapter, general theory are presented. The instability problems of compressors are presented, along with a compressor model. Its focus is on centrifugal compressors, since it is the type of compressor used in the recycle system. The following chapter is a thorough examination of the compressor characteristic, unique to each compressor type and setup. It defines the axisymmetric characteristic through a compressor. The main focus of the chapter is approximations of this characteristic. In chapter 4 the recycle system is presented. It has an introduction to surge/stall avoidance and active surge/stall control. In chapter 5 different Lyapunov methods is conducted for the recycle system. The thesis ends with a discussion and a final conclusion.

1.3 Source Code

The ZIP-file attached contains all the MATLAB and SIMULINK files used in the report. It contains all the files needed to run the approximation procedure, and all the files needed to run all the simulations presented in this thesis. The main code and diagrams are also found in the appendix.

Chapter 2

Theory of Continuous Flow Compressors

2.1 Compressors

A gas compressor increases the pressure of a gas by mechanically decreasing its volume and pressing the molecules together. This can be explained by the ideal gas law

$$p = \rho RT \tag{2.1}$$

where p is pressure, ρ is the density, R is the specific gas constant and T is temperature, which states that an increase in pressure results from an increase in density. Density is $\rho = \frac{m}{V}$, where m is mass and V is volume, so a reduction in volume would result in an increase in density and pressure.

According to Nisenfeld (1982), compressors can be divided into four general types

1. Axial-flow
2. Centrifugal
3. Reciprocating
4. Rotary

Reciprocating and rotary compressors work by the means of reducing the physical volume occupied by the gas, and then discharge the gas at higher pressure. These compressors will not be considered further. The other two,

axial-flow and centrifugal, are known as continuous flow compressors (Gravdahl and Egeland, 1999), or turbo compressors. They work by the principle of accelerating the gas to high velocity, and then decelerating the gas in diverging channels, converting kinetic energy into potential energy. This conversion can be explained by the Bernoulli equation

$$\frac{v_1^2}{2} + \frac{p_1}{\rho} + z_1 g = \frac{v_2^2}{2} + \frac{p_2}{\rho} + z_2 g \tag{2.2}$$

Although this equation is valid only for stationary frictionless flow along a streamline for an incompressible fluid, it illustrates the principle of the conversion as follows. Let point 1 be in the high velocity area, and point 2 in the low velocity area. At point 1 the velocity and the kinetic energy is high. At point 2 the velocity is greatly reduced by diffusion, and therefore the pressure at point 2, the potential energy, must be increased. The energy consuming part of a continuous flow compressor is the energy needed to accelerate the gas in the first place. This is managed by some drive unit.

2.2 The Centrifugal Compressor

Every centrifugal compressor consists of two principal parts. The impeller and shaft, called the rotor, and the casing which the rotor is mounted in. The casing directs the flow into the impeller. The impeller can be viewed as a fan which imparts high velocity to the gas. The gas is decelerated in diverging channels with a rise in pressure. The deceleration is obtained by diffusion, and consequently the part of the casing containing the diverging channels is called the diffusor. The diffusor exit flow is collected in the volute, which most effectively leads the gas away.

A supercharger is shown in Figure 2.1. When centrifugal compressors are mounted in cars to improve performance, they are called superchargers when the drive unit is the crankshaft, and turbochargers when the drive unit is a turbine wheel spun by exhaust.

The working principle is as follows. Some force spins the impeller, and gas gets dragged down in the impeller eye. The gas is whirled around in the impeller. The centripetal acceleration is obtained by a pressure head, so half of the pressure rise is typically obtained in the impeller. The rest of the pressure rise is obtained in the diffuser, which can be vaned or vaneless. The pressure rise in the diffuser is obtained by gas diffusion. The job for the volute is to most effectively lead the pressurized gas away, without considerable

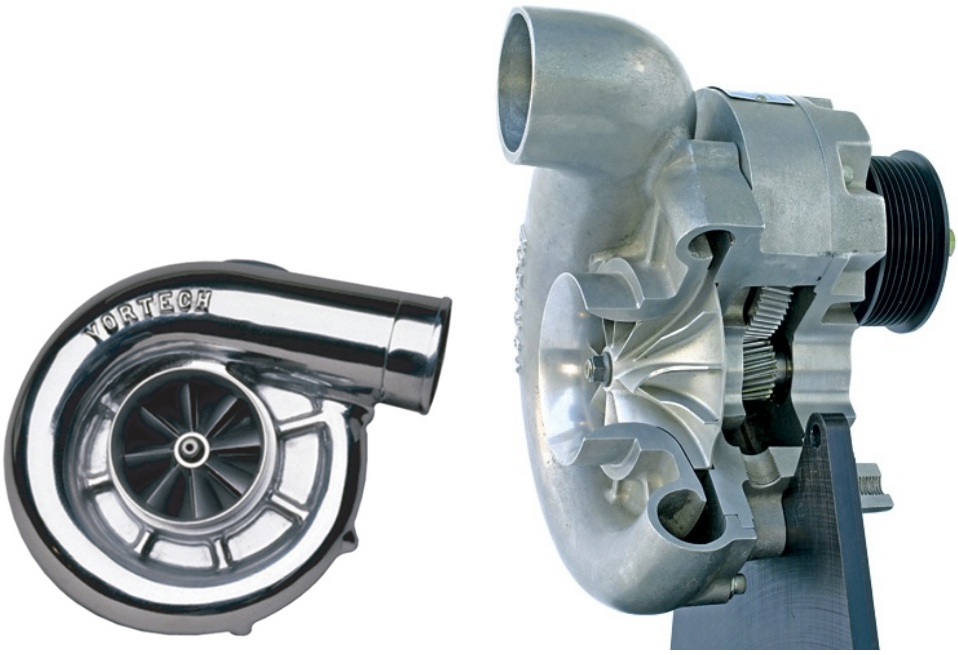

(a) Front (b) Cutaway

Figure 2.1: Centrifugal compressor (www.superchargersonline.com, www.vortechsuperchargers.com, feb. 2010)

losses. Some of the components of a centrifugal compressor is shown in Figure 2.2.

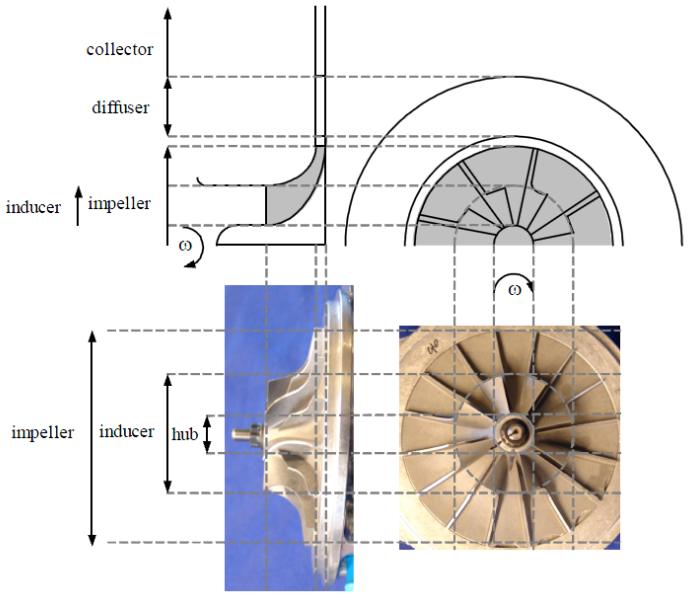

Figure 2.2: Components in a centrifugal compressor (Bøhagen, 2007)

Centrifugal compressors can be very big, and the forces involved are great. A compression system can consist of multiple stages of compressors, where the pressurized gas from one compressor is fed to the intake of another. The axial compressor actually consists of multiple stages. Although the pressure rise for a centrifugal compressor beats one stage in an axial compressor, several centrifugal compressors are often mounted together in a stage setup in the industry. In Figure 2.3(b) it is seen that there is mounted an axial compressor behind a two stage centrifugal compression system.

2.3 Operating Range Limitations

Towards high mass flow, the compressor is limited by choking. Towards low mass flow, the stable operating region is bounded due to the occurence of aerodynamic flow instabilities, surge and rotating stall. According to Willems et al. (1999), these instabilities can lead to failure of the compressor system because of the large mechanical and thermal load in the blading, and limit

(a) Large impellers

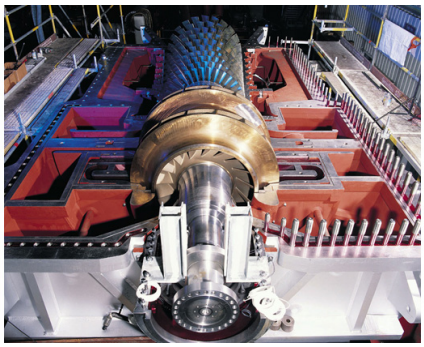

(b) Multiple stages

Figure 2.3: Large variants of centrifugal compressors (www.siemens.com, mar. 2010)

its performance and efficiency. Suppressing these phenomena improves life span and performance of the machine. There are also other instabilities, such as vibration in the materials, but these will not be considered further.

2.3.1 Stonewall

When sonic velocity is reached in some component, the compressor cannot pump more gas (Nisenfeld, 1982). This is called stonewall, or choking. Sonic velocity is reached when the Mach number is equal to unity (White, 2008):

$$\mathrm{Ma} = \frac{v_{gi}}{a_g} \tag{2.3}$$

Here, v_{gi} is the velocity of the gas relative to the impeller blade, and a_g is the speed of sound in the gas. According to Nisenfeld (1982), it is common to design the compressor such that the Mach number at design flow will not exceed 0.85 or 0.90.

2.3.2 Rotating Stall

Rotating stall occurs when one or more of the airfoils of the compressor stalls, without destabilizing it. This happens because the foil is loaded beyond its lifting capacity, e.g. when turbulent gas enters the compressor. When an airfoil stalls, the lift drops off markedly, drag increases markedly, and generally a separation bubble forms on the upper surface of the foil (White, 2008). The stalled airfoils create pockets of somewhat stagnant air, called *stall cells*. This causes a situation of abnormal airflow. The compressor continues to deliver compressed gas, but at reduced effectiveness.

The stall cells rotate around the circumference of the impeller at a fraction of the rotor speed. According to Gravdahl and Egeland (1999) the speed of the stall cells may be 20-70% of the rotor speed, affecting the next airfoils around the impeller as each encounters the cell. Another type of rotating stall is when the stall cells cover the complete circumference of the impeller, but only a part of its radius, with the remainder of the impeller continuing to deliver compressed gas. Rotating stalls can also propagate to include the entire impeller.

Once again, according to Gravdahl and Egeland (1999), rotating stall reduces the pressure rise and is likely to induce vibration in the blades as stall cells

rotate at a fraction of the rotor speed. However, rotating stall is a more common problem in axial compressors, and its importance in centrifugal compressors is a matter of debate.

2.3.3 Compressor Surge

Compressor surge is a breakdown in compression which can result in a reversal of flow, and possibly a violent expulsion of previously compressed gas out through the intake. This happens because the compressor is unable to work against the already compressed gas behind it.

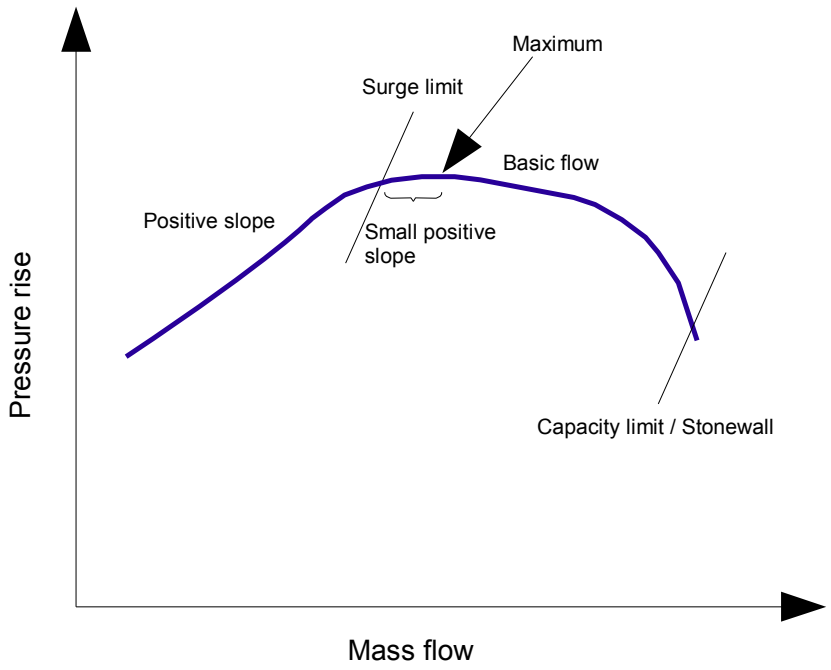

Figure 2.4: Compressor characteristic for constant compressor speed

A typical *compressor characteristic* (performance curve), for a compressor at constant speed, is shown in Figure 2.4. The compressor characteristic typically shows the pressure rise developed across the compressor as a function of mass flow. The pressure developed by the compressor is a function of the density of the gas being pumped, the diameter of the impeller, and the speed of the compressor. The shape of the curve is a function of the angle of the

blade in the impeller, the tip speed of the blade, and the gas velocity relative to the blade. (Nisenfeld, 1982)

Imagine the compressor operating at a negative slope of the characteristic, in the basic flow area of the chart. A reduction in mass flow here would yield higher pressure rise, and this would encourage higher mass flow. This is a self compensating, stable system. Now imagine the compressor operating at a positive slope of the characteristic. A reduction in mass flow here would yield lower pressure rise, and this again would encourage a further reduction in mass flow. So this is an unstable system. For surge to occur, positive compressor characteristic slope is necessary. Actually, it is possible to operate in the positive slope area without surge to occur as long as the slope is lesser than some small, positive value:

$$\frac{\partial \psi(\phi)}{\partial \phi} < k \tag{2.4}$$

where ψ is the pressure rise, ϕ is the mass flow, and k is the small, positive value.

Surge occurs when the pressure generated by the compressor, or the impeller, is less than the pressure in the system downstream. It is an axisymmetrical oscillation of flow through the compressor, and is characterized by a limit cycle in the compressor characteristic (Gravdahl and Egeland, 1999).

Figure 2.5 illustrates a surge cycle. The surge point (1) is where the flow becomes unstable. Lets imagine that the throttle is closed a little bit further, lower mass flow occurs, and since we are at the surge point, there is lower discharge pressure. The "flow momentum" is decreased along with the discharge pressure being lower than the system pressure downstream. In the case of a deep cycle this causes flow reversal (2), which ends in zero flow (3). At this point the discharge pressure is building up again, along the mass flow, to (4) and then to (1). Then, the cycle repeats.

Figure 2.5 shows a deep surge, where the flow is reversed. This is one type of surge, and the other is mild/classic, where the flow is not reversed and the cycle is inside the positive flow area of the chart. Experiments show that the surge frequency is of the same magnitude as the Helmholtz frequency of the system, with deep surge frequencies well below, Gravdahl and Egeland (1999).

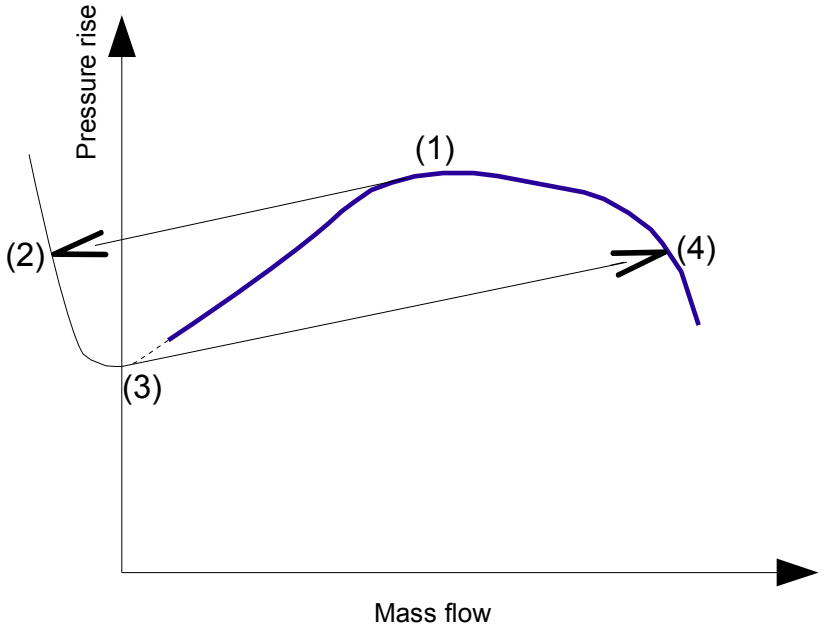

Figure 2.5: Compressor characteristic with deep surge cycle

2.3.4 Coupled Stall & Surge

According to Gu et al. (1999), often surge and rotating stall are coupled (classic surge) although each can occur without the other. During classic surge, the compressor may pass in and out of rotating stall during a surge cycle, with rotating stall characteristics appearing to be quite similar to those obtained during steady-state operation. The conclusion is that rotating stall and surge, though coupled, are well defined individually. It has been pointed out by many that rotating stall occurs at the compressor characteristic maximum. Rotating stall can also push the system into surge. Recall that steady operation with regards to surge is possible in some small positive slope area of the characteristic, but since stall which can induce surge occurs at the maximum, the surge point is often approximated to the maximum. This has been well accepted in the literature.

2.4 The Compressor Model

Axial and centrifugal compressors mostly show similar flow instabilities, according to Gravdahl and Egeland (1999). In this section a multispeed model for centrifugal compressors is presented. When the speed is assumed constant, the model reduces to the dimensional model of Greitzer (Greitzer, 1976), originally developed for axial compressors, but shown valid also for centrifugal compressors by Hansen et al. (1981). The compression system is modeled as in Figure 2.6, with a compressor, a duct of length L, a plenum of volume V_p, a throttle, and a drive unit imparting a torque on the compressor.

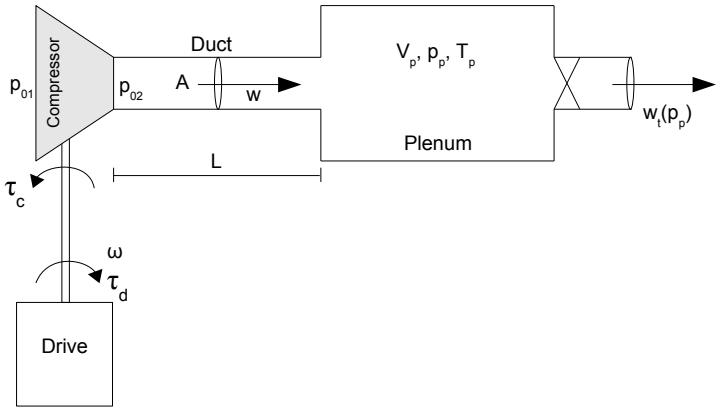

Figure 2.6: The compressor system

The expression for the pressure is found from the mass balance applied on the plenum. The expression for the massflow is found from the momentum balance applied on the duct, and the expression for the shaft dynamics is found from the angular momentum relation. The model is

$$\dot{p}_p = \frac{a_p^2}{V_p}(w - w_t) \tag{2.5}$$

$$\dot{w} = \frac{A}{L}(\Psi_c(w, \omega)\, p_{01} - p_p) \tag{2.6}$$

$$\dot{\omega} = \frac{1}{J}(\tau_d - \tau_c) \tag{2.7}$$

where p_p is the pressure in the plenum, w is the mass flow and ω is the angular speed of the impeller, a_p is the speed of sound of the gas in the plenum, V_p

is the volume of the plenum, w_t is the mass flow through the throttle, A and L is the cross sectional area and the length of the duct, respectively, Ψ_c is the important compressor characteristic, p_{01} is the ambient pressure, J is the moment of inertia of the drive unit, τ_d is the drive torque, and τ_c is the torque on the shaft from the impeller blades. The model (2.5)-(2.7) was first presented in Gravdahl and Egeland (1999), although the two first equations are the model of Greitzer (1976) in dimensional form, and the whole model is similar to the model presented in Fink et al. (1992).

We're going to investigate the torque acting on the impeller blades. From the angular momentum balance it can be written as

$$\tau_c = w\left(r_2 C_{\theta 2} - r_1 C_{\theta 1}\right) \tag{2.8}$$

where r_1 and r_2 is the radius at the inducer and the impeller exit, respectively, and $C_{\theta 1}$ and $C_{\theta 2}$ is the tangential velocity of the gas at the inducer and the impeller exit, respectively. It is customary to assume that the velocity at the impeller inlet is zero, that is no pre-whirl, such that (2.8) becomes

$$\tau_c = w r_2 C_{\theta 2} \tag{2.9}$$

Consider the velocity triangle at the impeller exit in Figure 2.7.

The tangential velocity at the impeller exit can by trigonometric considerations be written as

$$\begin{aligned} C_{\theta 2} &= U_2 - C_{a2}\cot\beta_{2b} \\ &= \left(\underbrace{1 - \frac{C_{a2}}{U_2}\cot\beta_{2b}}_{\mu}\right) U_2 \end{aligned} \tag{2.10}$$

where μ is the flow coefficient. In practice the flow coefficient is less than the ideal value due to slip. The slip factor can be introduced in (2.10) as

$$C_{\theta 2} = \underbrace{\sigma\left(1 - \frac{C_{a2}}{U_2}\cot\beta_{2b}\right)}_{\mu} U_2 \tag{2.11}$$

where σ is the slip factor, typically slightly less than unity. For radial vanes we have $\cot\beta_{2b} = 0 \Rightarrow \mu = \sigma$. With $U_2 = r_2\omega$, (2.9) can be written as

$$\tau_c = w r_2^2 \mu \omega \tag{2.12}$$

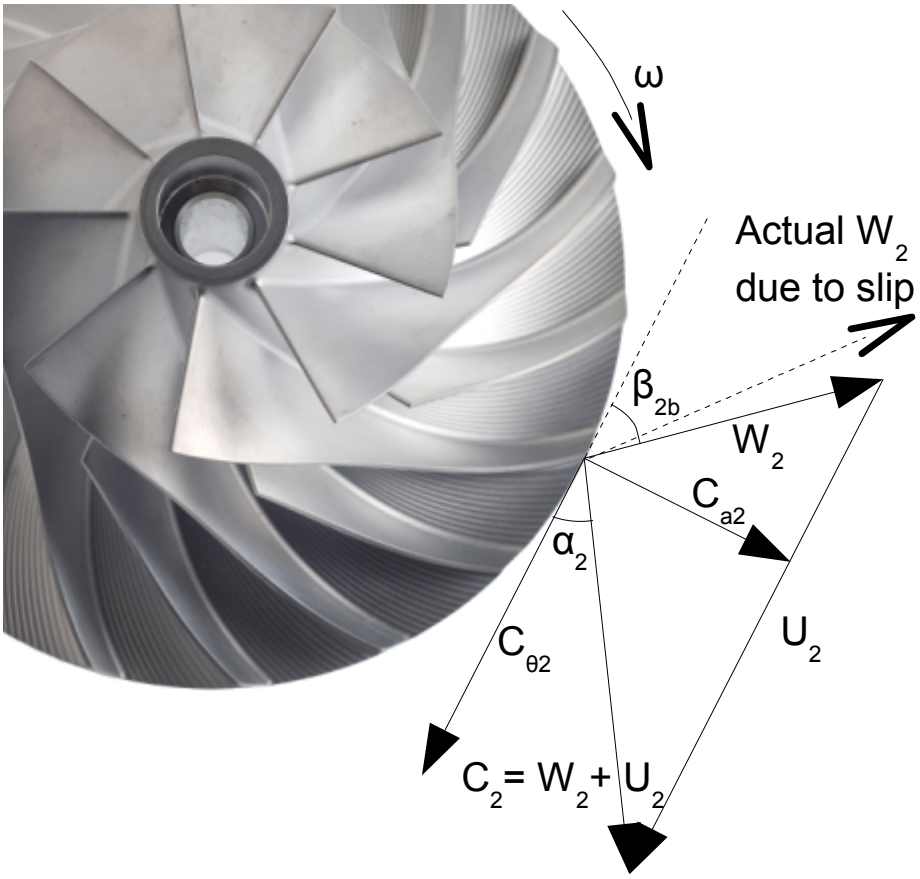

Figure 2.7: Velocity triangle at the impeller exit

In the case of compressor deep surge, we'll have reversal of flow. The final equation for the torque acting on the impeller blades is

$$\tau_c = |w| r_2^2 \mu \omega \tag{2.13}$$

The model uses the pressure ratio of the compressor Ψ_c, the compressor characteristic. It is a property of the compressor and there are multiple ways to express it. One of them, derived from enthalpy transfer in Egeland and Gravdahl (2002), is

$$\Psi_c(w, \omega) = \left(1 + \frac{\mu r_2^2 \omega^2 - \frac{1}{2} r_1^2 (\omega - \alpha w)^2 - k_f w^2}{a_p T_{01}}\right)^{\frac{\kappa}{\kappa - 1}} \tag{2.14}$$

The values in (2.14) is hard to find, and often an approximation based on measurement data is used for Ψ_c.

The model (2.5)-(2.7) is one-dimensional and capable of predicting surge. Rotating stall is two-dimensional, with its circumferential pattern, and thereby require a two-dimensional model. This is done in Moore and Greitzer (1986) where the Moore-Greitzer model is presented. However, (2.5)-(2.7) could be augmented with another state, where rotating stall is manifested by a lower but stable mass flow through the system. According to Gravdahl and Egeland (1999), rotating stall is believed to have little effect on centrifugal compressors. Since this master thesis is concerned with centrifugal compressors, where the importance of rotating stall is a matter of debate, the state for rotating stall will be omitted.

2.4.1 Valves

The flow through the throttle $w_t(p_p)$ in the model (2.5)-(2.7) is modeled as flow through a valve. Flow through a valve can be modeled as flow through a restriction or orifice. That is

$$w = C A_2 \sqrt{2\rho (p_1 - p_2)} \tag{2.15}$$

where w is the mass flow through the orifice, C is the flow coefficient, A_2 is the area of the orifice opening, ρ is the density of the fluid, and $p_1 - p_2$ is the pressure drop across the orifice. The derivation of (2.15) is found in Appendix A.1.

In general, (2.15) is only valid for incompressible flow. Gas is indeed not incompressible, which is dealt with here. Gas flow through a valve can be modeled as isentropic nozzle flow. That is

$$w = \frac{A_2 p_1}{\sqrt{RT_1}} \sqrt{\frac{2\kappa}{\kappa - 1} \left(\frac{p_2}{p_1}\right)^{\frac{2}{\kappa}} \left(1 - \left(\frac{p_2}{p_1}\right)^{\frac{\kappa-1}{\kappa}}\right)} \tag{2.16}$$

where κ is the ratio of the heat capacity c_p at constant pressure to the heat capacity c_v at constant volume, R is the specific gas constant, T_1 and p_1 is the temperature and the pressure at the inlet of the nozzle, respectively, and p_2 and A_2 is the pressure and the area at the outlet of the nozzle, respectively. (2.16) is the same as equation 9.47 in White (2008), where the final result is just presented without its derivation, stating that the algebra is convoluted. Its derivation is nevertheless given here, in Appendix A.2.

A comparison between (2.15) with a flow coefficient of $C = 0.93$, and (2.16) at 20^o C yields the result shown in Figure 2.8. The gas is air.

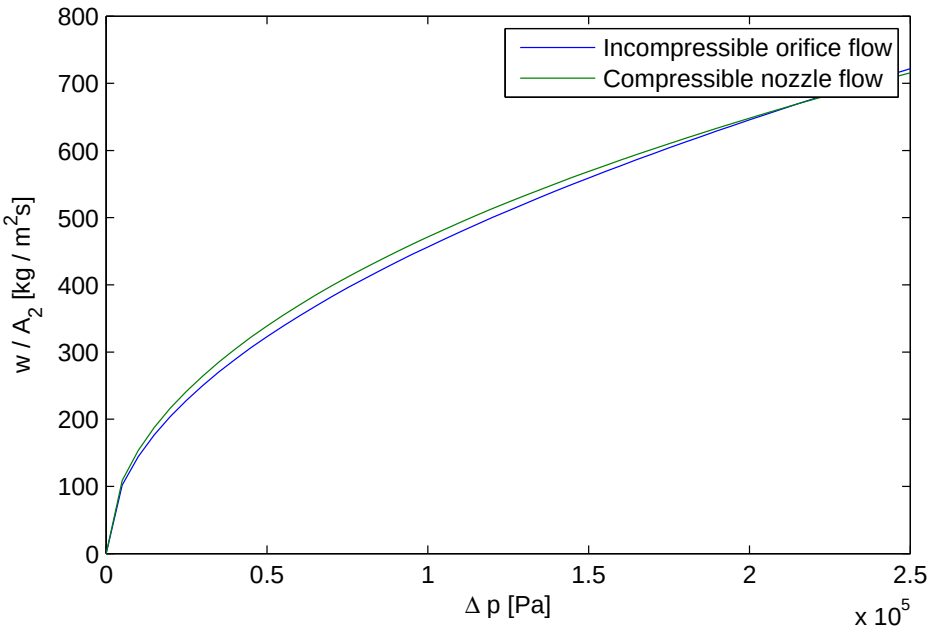

Figure 2.8: Comparison of incompressible- and compressible flow through a valve.

From the figure it is seen that the difference between the two models is small. Assuming incompressible flow in a small area around the orifice is

not necessarily any bad idea, even for a compressible fluid. As standard, (2.15) will be used to model gas flow through a valve due to its simplicity. Using a flow coefficient of $C = 0.65$ is a good approximation to some loss of energy, which happens in practice. For air we then have $C\sqrt{2\rho} \approx 1$, and (2.15) becomes

$$w = A_2\sqrt{p_1 - p_2} \tag{2.17}$$

To be able to control the flow through the valve, the orifice area A_2 can be adjusted from 0 to 100%. The final model for the flow through the throttle is

$$w_t = A_{t\%}\sqrt{p_p - p_{01}} = k_t\sqrt{\Delta p} \tag{2.18}$$

To be able to account for the special case $p1 < p2$ in (2.17), the following modification is done

$$w = \operatorname{sgn}(p_1 - p_2)\, A_2\sqrt{|p_1 - p_2|} \tag{2.19}$$

The *sign* function is not continuous, but can be approximated as

$$\operatorname{sgn}(x) = \lim_{\zeta\to\infty} \tanh(\zeta x) \tag{2.20}$$

as well as the absolute value

$$|x| = x \cdot \operatorname{sgn}(x) = x \lim_{\zeta\to\infty} \tanh(\zeta x) \tag{2.21}$$

The flow through the throttle is now given as

$$w_t = \tanh(\zeta(p_p - p_{01}))A_{t\%}\sqrt{(p_p - p_{01})\tanh(\zeta(p_p - p_{01}))} \tag{2.22}$$

2.4.2 Stability of the Model

By assuming constant speed for the impeller, the compressor characteristic Ψ_c only varies with mass flow. Equilibrium points for the system (2.5)-(2.6) are given as

$$w^* = w_t(p_p^*) \tag{2.23}$$
$$p_p^* = \Psi_c(w^*)p_{01} \tag{2.24}$$

That is, the mass flow is equal to the throttle flow, and the plenum pressure is equal to the pressure developed by the compressor.

According to Khalil (2002), the qualitative behavior of a nonlinear system near an equilibrium point can be determined via linearization with respect to that point. Assuming constant speed for the impeller, linearization of (2.5)-(2.6) yields

$$\dot{x} = Ax \tag{2.25}$$

where $x = [p_p \ w]^T$ and the Jacobian evaluated at the equilibrium point is

$$A = \left[\begin{array}{cc} \frac{\partial f_1}{\partial p_p} & \frac{\partial f_1}{\partial w} \\ \frac{\partial f_2}{\partial p_p} & \frac{\partial f_2}{\partial w} \end{array} \right] \Bigg|_{x=p} = \left[\begin{array}{cc} -\frac{a_p^2}{V_p} \left. \frac{\partial w_t}{\partial p_p} \right|_{p_p^*} & \frac{a_p^2}{V_p} \\ -\frac{A}{L} & \frac{A}{L} p_{01} \left. \frac{\partial \Psi_c}{\partial w} \right|_{w^*} \end{array} \right]$$

Defining $k_1 = \frac{a_p^2}{V_p}$, $k_2 = \frac{A}{L}$, $a = p_{01}$, $\partial_1 = \left. \frac{\partial w_t}{\partial p_p} \right|_{p_p^*}$ and $\partial_2 = \left. \frac{\partial \Psi_c}{\partial w} \right|_{w^*}$, A becomes

$$A = \left[\begin{array}{cc} -k_1 \partial_1 & k_1 \\ -k_2 & k_2 a \partial_2 \end{array} \right]$$

The characteristic polynomial is given by $\det(\lambda I - A) = 0$, calculated as

$$\lambda^2 + (k_1 \partial_1 - k_2 a \partial_2)\lambda + k_1 k_2 (1 - a \partial_1 \partial_2) = 0 \tag{2.26}$$

The eigenvalues are

$$\lambda = \frac{-(k_1 \partial_1 - k_2 a \partial_2) \pm \sqrt{(k_1 \partial_1 - k_2 a \partial_2)^2 - 4 k_1 k_2 (1 - a \partial_1 \partial_2)}}{2} \tag{2.27}$$

From Theorem 4.7 Khalil (2002), we can deduce the following.

- *The equilibrium point is asymptotically stable if* $\mathrm{Re}\lambda_i < 0$ *for all eigenvalues of A.*
- *The equilibrium point is unstable if* $\mathrm{Re}\lambda_i > 0$ *for one or more of the eigenvalues of A.*

It is seen from (2.27) that if either $(k_1 \partial_1 - k_2 a \partial_2)$ or $(1 - a \partial_1 \partial_2)$ is negative, we have an unstable system. If the latter applies,

$$\begin{aligned} \frac{1}{p_{01}} \left(\left. \frac{\partial w_t}{\partial p_p} \right|_{p_p^*} \right)^{-1} &< \left. \frac{\partial \Psi_c}{\partial w} \right|_{w^*} \\ \Rightarrow \left. \frac{\partial \Psi_t}{\partial w_t} \right|_{p_p^*} &< \left. \frac{\partial \Psi_c}{\partial w} \right|_{w^*} \end{aligned} \tag{2.28}$$

that is, the slope of the compressor characteristic becomes bigger than the slope of the throttle characteristic, the system is unstable. The system is in this case termed *statically unstable* and tends to happen a distance to the left of the compressor characteristic, if it happens at all. If the first applies,

$$\left.\frac{\partial \Psi_c}{\partial w}\right|_{w^*} > \frac{k_1}{k_2 a} \left.\frac{\partial w_t}{\partial p_p}\right|_{p_p^*} \tag{2.29}$$

the system is also unstable. In this case the system is termed *dynamically unstable* and tends to happen just to the left of the peak of the compressor characteristic. Particulary the result that can be extracted from (2.29) is that dynamic instability implies

$$\left.\frac{\partial \Psi_c}{\partial w}\right|_{w^*} \left.\frac{\partial \Psi_t}{\partial w_t}\right|_{p_p^*} > \frac{k_1}{k_2 a^2} \tag{2.30}$$

The expression to the right tends to be small. We know that $\left.\frac{\partial \Psi_t}{\partial w_t}\right|_{p_p^*}$ is strictly increasing, so for higher mass flows and pressures, the point of instability moves towards the compressor characteristic maximum, the peak. However, the most important result implied by the eigenvalues is found in the lemma below.

Lemma 2.1 *Let $x = x^* = [p_p^* \; w^*]^T$ be an equilibrium point for the nonlinear compressor system*

$$\dot{x} = \begin{bmatrix} \dot{p}_p \\ \dot{w} \end{bmatrix} = \begin{bmatrix} \frac{a_p^2}{V_p}(w - w_t) \\ \frac{A}{L}(\Psi_c(w)\, p_{01} - p_p) \end{bmatrix} = f(x)$$

where the flow through the throttle is modeled as (2.22)*, and the compressor characteristic Ψ_c is assumed continuously differentiable. Then $f : D \to R^2$ will be continuously differentiable for $p_p > p_{01}$, where D is a neighborhood of the equilibrium point. Let*

$$A = \left.\frac{\partial f}{\partial x}(x)\right|_{x=x^*}$$

Then,

The equilibrium point is asymptotically stable if the slope of the compressor characteristic $\left.\frac{\partial \Psi_c}{\partial w}\right|_{w^*}$ is negative or zero. ◇

Proof: When using (2.22) to model the throttle, its slope ∂_1 for a given plenum pressure is always positive $\forall\ p_p > p_{01}$. The assumption that the plenum pressure always is greater than the ambient pressure is true, except for some special cases that will be ignored, including startup. Lets assume that the slope of the characteristic at a given mass flow ∂_2 is negative or zero. The result is that $k_1\partial_1 - k_2 a\partial_2 > 0$ and $(k_1\partial_1 - k_2 a\partial_2)^2 - 4k_1k_2(1 - a\partial_1\partial_2) < k_1\partial_1 - k_2 a\partial_2$. That means that $\mathrm{Re}(\lambda_i) < 0\ \forall\ i$. The rest follows from the proof of Theorem 4.7 in Khalil (2002). □

Although the surge line is given by (2.30), and that in theory we can steadily operate in some positive slope region, this tends not to be the case during simulations. During simulations the system goes into surge at approximately the compressor characteristic maximum. The reason for this could be that the right hand side of (2.30) is very low, and once entered the positive slope region from the right, surge occurs quickly because the value of the slope of the positive compressor characteristic is very limited.

Chapter 3

The Compressor Performance Map

3.1 Introduction & Motivation

The compressor characteristic is also called the performance curve of a compressor. It shows how the pressure developed by the compressor varies with mass flow for a given compressor speed. Generally, at high flows the pressure developed is low. When the flow decreases, the pressure increases until the instability point is reached. The compressor then goes into stall/surge. The performance curve is different for different types of compressors and system setups. The performance curve is dependent on a lot of variables. Among other things it changes for different settings for the inlet guided vanes, it changes for different gas densities, and it changes for different speed settings. When multiple curves are drawn for different speeds, it is also called the performance map of a compressor. In this report the expression "compressor characteristic" is also used for the performance map, dependent on both the mass flow and the speed. In Figure 3.1 a typical performance map of a multispeed compressor system is shown.

Consider the compressor shown in Figure 3.2. The pressure rise over the compressor is defined as

$$P_c(\phi) = p_{02} - p_{01} \tag{3.1}$$

where ϕ is the mass flow through the compressor, p_{01} is the suction pressure,

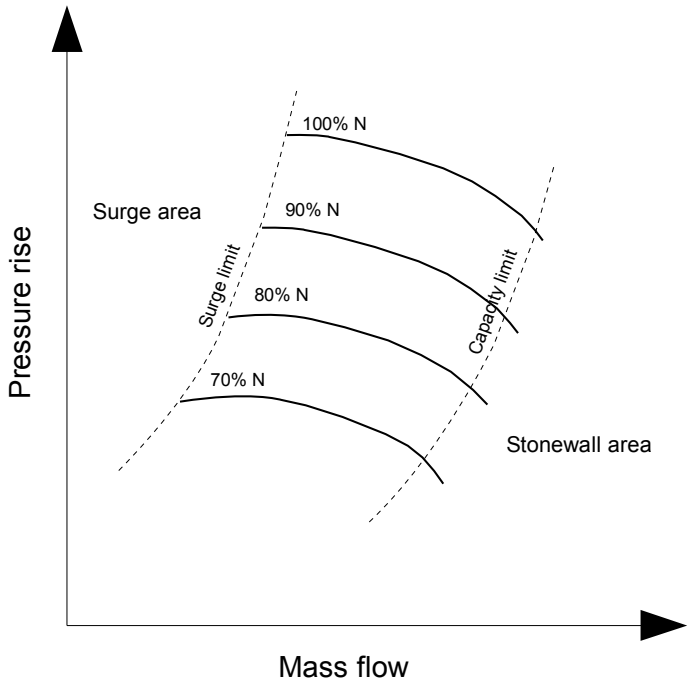

Figure 3.1: Typical performance map of a multispeed compressor system

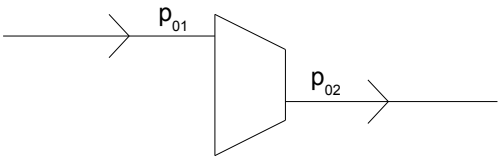

Figure 3.2: Illustration of the pressure rise and pressure ratio of a compressor

and p_{02} is the discharge pressure. The pressure ratio is defined as

$$\Psi_c(\phi) = \frac{p_{02}}{p_{01}} \tag{3.2}$$

For purposes of control design, the ordinate of the performance map can be pressure rise, pressure ratio, or simply the discharge pressure. It is emphasized that if the discharge pressure is used, constant suction pressure is assumed. (Nisenfeld, 1982)

Moore and Greitzer (1986) uses a cubic as the compressor characteristic, referring to Figure 3.3. The ordinate is nondimensional pressure rise and the abscissa is nondimensional flow.

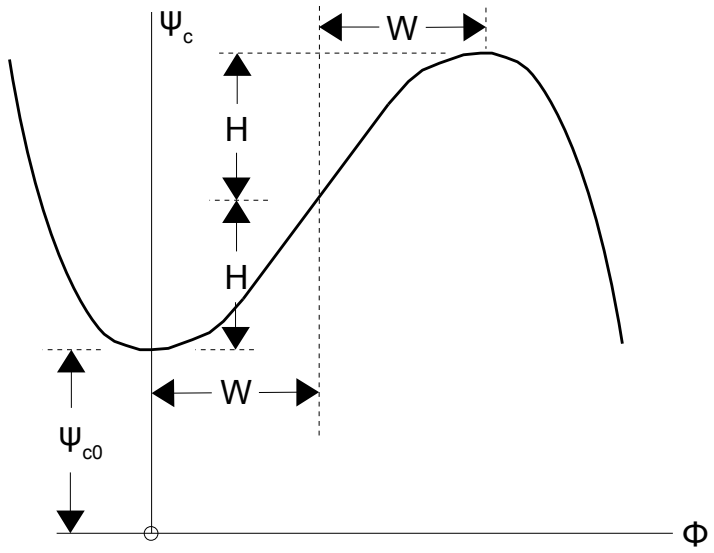

Figure 3.3: Notation used in definition of cubic axisymmetric compressor characteristic

The equation for this cubic approximation is

$$\psi_c(\phi) = \psi_{c_0} + H\left[1 + \frac{3}{2}\left(\frac{\phi}{W} - 1\right) - \frac{1}{2}\left(\frac{\phi}{W} - 1\right)^3\right] \tag{3.3}$$

where ψ_{c_0}, H and W are parameters. Earlier work done in Koff (1983) and Koff and Greitzer (1984) implied that the axisymmetric characteristic of a compressor is a smooth S-shaped curve. It was this result that motivated

the simple cubic approximation of the performance curve. It has found wide acceptance in the literature, and is used in numerous papers concerning compressor surge and stall. The expression for the characteristic is only valid for a given speed, and is in pressure rise form.

Gravdahl and Egeland (1999) derives the compressor characteristic by calculating the energy transfer and losses. It is valid for multiple speeds, and is in pressure ratio form. The equation is given as

$$\Psi_c(w,\omega) = \left(1 + \frac{\mu r_2^2\omega^2 - \frac{1}{2}r_1^2(\omega - \alpha w)^2 - k_f w^2}{a_p T_{01}}\right)^{\frac{\kappa}{\kappa-1}} \tag{3.4}$$

where w is dimensional mass flow and ω is dimensional compressor speed. It does not inherit an S-form, and will have to be modified for use during deep-surge simulations. Finding the values for the parameters in (3.4) can be hard, or even impossible. For instance, no one knows exactly the value of the energy transfer coefficient μ. In practice it varies with a lot of other parameters. However, the parameters in (3.4) can be tweaked such that the curve nearly complies with real measurement points. This is a very difficult task. Motivated by this, an approximation of the measurement points is often used as the compressor characteristic. A third order polynomial fit is often used, such that in Egeland and Gravdahl (2002). (3.3) could also be viewed as a third order fit. The reason for this is that a third order fit captures much of the general performance properties of compressors, with its S-form. However, it is also widely recognized as only being very roughly true of real compressors. (Drummond and Davison, 2009)

In this chapter we're pursuing new methods of approximating the compressor map, which hopefully will be more accurate than the third order approximation. The chapter is angled towards a rather practical perspective, with its use of MATLAB and SIMULINK.

3.2 Previous Work on Approximations

Some measurements are shown in Figure 3.4. These are points of pressure ratios for different mass flows and speeds. Take a look at how the form of the speedlines is changing with increasing impeller speed. Certainly a challenging identification scheme. The measurements actually origins from the compressor map of Vortech S-trim superchargers. (www.vortechsuperchargers.com)

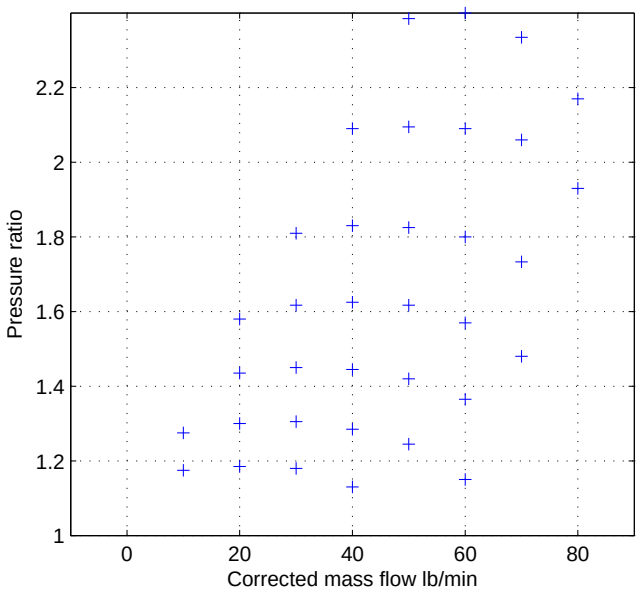

Figure 3.4: Measurements

Egeland and Gravdahl (2002) uses a method where approximations of the measurements in the figure based on polynomial curve fitting is done, to make the characteristic continuous in both mass flow and speed. Two stages are required. First, each speedline is approximated as

$$\Psi_c(w) = c_0 w^3 + c_1 w^2 + c_2 w + c_3 \tag{3.5}$$

with the MATLAB function "polyfit". Points for negative- and zero flow are needed for each speedline. Zero flows are calculated with Equation 13.50 in Egeland and Gravdahl (2002), and negative flow points are chosen such that the 3rd order polynomial obtains the right form. w is the mass flow and c_i, $i = 0, 1, 2, 3$ are the coefficients corresponding to a given rotational speed. Next, the coefficients are approximated as

$$c_i(N) = c_{i0} N^3 + c_{i1} N^2 + c_{i2} N + c_{i3} \tag{3.6}$$

where N is the rotational speed. The approximation can now be written as

$$\Psi_c(w, N) = c_0(N) w^3 + c_1(N) w^2 + c_2(N) w + c_3(N) \tag{3.7}$$

The result of the approximation is compared to the measurements in Figure 3.5.

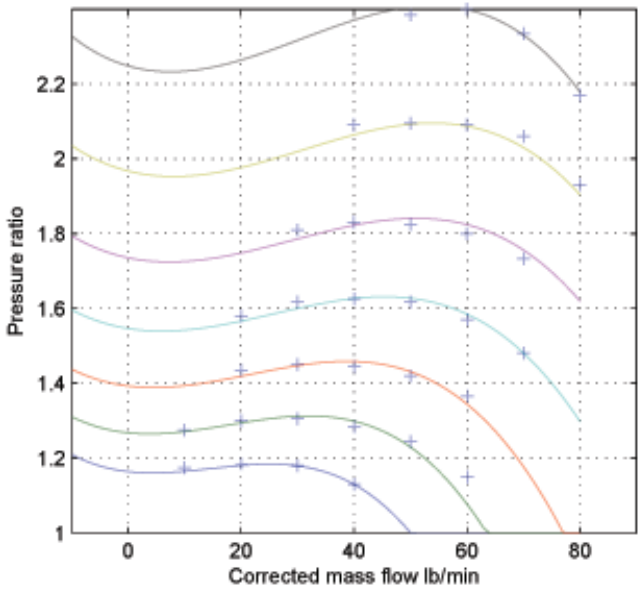

Figure 3.5: The polyfit identification procedure compared to measurements

As we can see from the figure, the speedlines do not correspond to the points very well. More importantly is where the surge line of the approximated speedlines is located. As explained before in this report, a good approximation to the surge point is the characteristic maximum. In Figure 3.5 it is seen that the maximum of the approximated speedlines are in most cases located a bit to the right compared to the measurement maximum. The approximation inherits a false location for the surge point. Since one of the goals of surge control research potentially is to increase the efficiency by allowing the system to operate close to the surge line, it can be argued that a better identification procedure is needed.

The details of how the polyfit approximation procedure is done is found in the ZIP-file at "approximation/polyfit".

3.3 The Spline Procedure

In this section MATLAB's *Spline Toolbox* is used. This is a toolbox which includes a collection of algorithms for data fitting, interpolation, extrapolation, and visualization. (de Boor, 2010)

3.3.1 Introduction to splines

Splines are simply smooth piecewise polynomials. In other words, a spline is a special function made up by polynomials, which merges smooth together. According to www.mathworks.com it has become the standard tool for modeling arbitrary functions. Spline interpolation is preferred over polynomial interpolation due to its exactness, even for low-degree polynomials. It can represent functions over large intervals, since it avoids Runge's phenomenom[1].

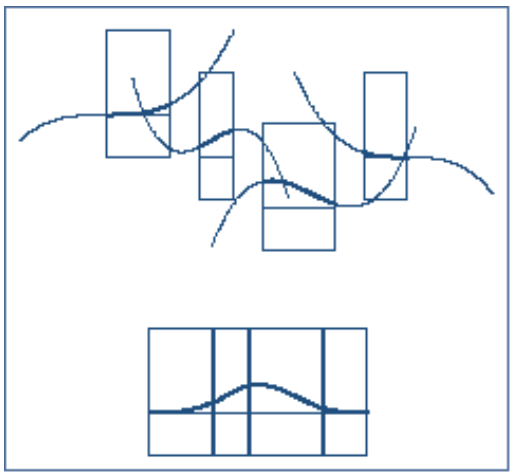

Figure 3.6: A cubic spline and the four polynomials from which it is made (www.mathworks.com, March 2010)

In Figure 3.6 a cubic spline is shown. That the spline is cubic simply means that the polynomials from which it is made is of 3rd order.

There are different forms to represent a spline. A Spline represented by the *ppform* provides a description in forms of breakpoints and coefficients. A spline represented by the *B-form* appears as a linear combination of B-splines, by the knot sequence and B-spline coefficients.

Further, it is possible to generate a multivariate spline. That is, a spline in multiple dimensions, as tensor products[2] of univariate splines.

[1]For higher degrees, the error (how much the approximation differs from the approximated curve/function) between- and especially past interpolation points gets worse.

[2]A bilinear operation: combining elements of two vector spaces into an element in the third

3.3.2 Bivariate Cubic Spline Approximation

Here, a bivariate cubic spline interpolation and extrapolation of the compressor characteristic will be done. The procedure starts with loading the measurements into MATLAB. Here, the measurements in Figure 3.4 will be used. The measurements are further augmented with points for negative- and zero flow. The next step is the approximation procedure. The main command used is `pp = csape({x,y}, z, conds)`, which is (bivariate) cubic spline interpolation with end conditions. It returns the ppform of a cubic spline. `x` is a vector containing the location of points along the mass flow axis, `y` is a vector containing the location of points along the speed axis, and `z` is a matrix where `z(i, j)` equals the pressure rise for the mass flow `x(i)` and the speed `y(j)`.

Since `z` is a matrix, gridded data is needed. We have to have a pressure ratio point at all mass flow locations used for all speedlines. This is not the case for the initial measurements. As we move up through speedlines, the mass flow locations are gradually shifted to the right. The data have to be prepared before using the `csape` command. The preparation starts with cubic spline interpolation for each speed with the command `spp = spline(X, Y)`, where `X` is a vector containing the mass flow points, and `Y` is a vector containing the pressure rise points. After a cubic spline is generated for each speed, missing mass flow points are extracted from the spline with the command `fnval(spp, wp)`, where `spp` is the cubic spline for one speed and `wp` is the mass flow. Observe that the extracted points from the spline are approximated points.

The `csape` command also has an optional parameter `conds` where end conditions can be specified. As default the end conditions are set to "Match end-slopes" (`conds = {'clamped', 'clamped'}`). It means that if we're trying make the spline generated with `csape`, `pp`, return a value for the pressure rise outside the range specified by the vector `x`, it will approximate a value based on the slope the approximated speedline had at the last mass flow point. It also means that if we're trying to obtain values of a speedline beyond the highest, an approximated value will be returned based on the slope of the "approximation through speedlines" at the last speedline.

Values for the pressure ratio at different mass flows and speeds can be obtained with the command `fnval(pp, {<massflow>, <speed>})`. The details of the spline approximation procedure is found in Appendix B.1.1, and in the ZIP-file at "approximation".

3.3.3 Results

The result of the spline approximation compared to the measurement points is shown in Figure 3.7.

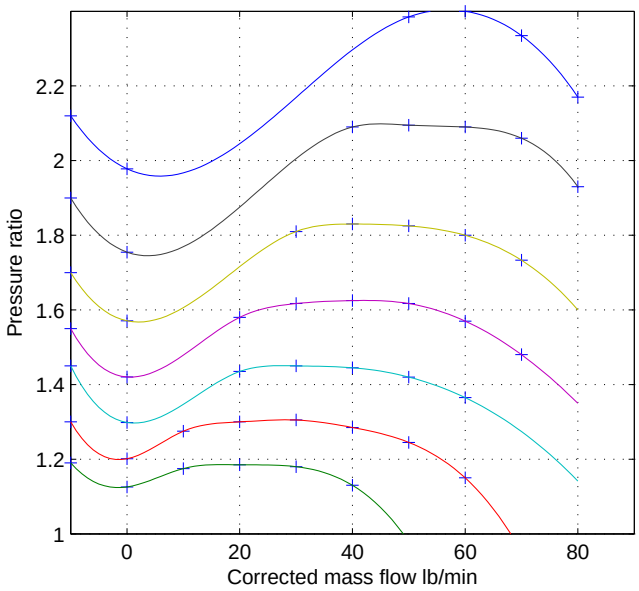

Figure 3.7: The spline approximation compared to measurements

When comparing Figure 3.5 and Figure 3.7 one thing comes clear. As is seen from the figure comparing the spline approximation to the measurements, the approximated speedlines goes exactly through the measurement points. The spline approximation is able to embed the highly nonlinear properties of the compressor characteristic. That is, the form of each speedline varies. One of the few things that is even close to linear is the surge line, although that is also a simplification. The result also implies that the characteristic maximum of the dotted measurements is inherited by the approximation. As a more fancy figure which illustrates that the approximation is continuous in both mass flow and speed is shown in Figure 3.8.

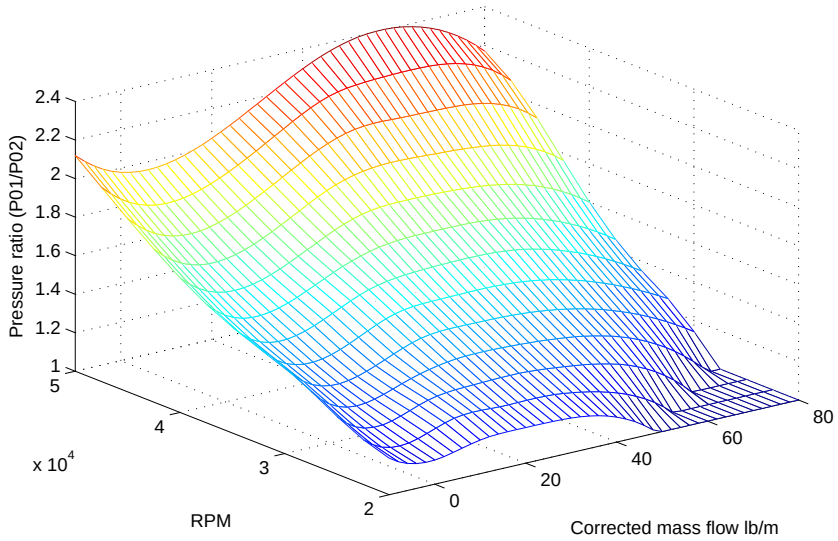

Figure 3.8: The bivariate cubic spline approximation

3.4 Verification by Simulation

To verify the new approximation procedure, the model presented in the introduction will be simulated with the new model of the compressor characteristic. The model, stated again, is

$$\dot{p}_p = \frac{a_p^2}{V_p}(w - w_t) \tag{3.8}$$

$$\dot{w} = \frac{A}{L}(\Psi_c(w,\omega)p_{01} - p_p) \tag{3.9}$$

$$\dot{\omega} = \frac{1}{J}(\tau_d - \tau_c) \tag{3.10}$$

$$w_t = \tanh(\zeta(p_p - p_{01}))\, k_t \sqrt{(p_p - p_{01})\tanh(\zeta(p_p - p_{01}))}\Big|_{\zeta \gg 0} \tag{3.11}$$

where the cubic bivariate spline is embedded into the compressor characteristic $\Psi_c(w,\omega)$. The reason why w_t is modeled as it is, or not as $w_t = k_t\sqrt{p_p - p_{01}}$ is to allow for reversed flow through the valve. It is strictly for simulation purposes during deep surge, since the flow through the throttle never should reverse in any other mode. The cubic bivariate spline in ppform is a struct in MATLAB with the following form

```
pp =

       form: 'pp'
     breaks: {[-10 0 10 20 30 40 50 60 70 80 90 100]  [20000
         25000 30000 35000 40000 45000 50000]}
      coefs: [1x44x24 double]
     pieces: [11 6]
      order: [4 4]
        dim: 1
```

and obviously, there is a whole lot of data that must be accessed at each time step of a simulation. The simulation setup in SIMULINK is found in Appendix C.1, and the initialization file is found in Appendix B.2.1. All the files needed to run the simulation is found in the ZIP-file at "model_plain". The result of a simulation using the bivariate spline as the compressor characteristic is shown in Figure 3.9. The model is being simulated for 12 seconds, the drive torque is set to 3 nm, and the throttle is being gradually closed from 2 seconds. The pressure and the efficiency of the system increases with decreasing throttle opening and mass flow. The speed of the impeller increases due to lesser load on the blades. The efficiency continues to increase until the system becomes unstable and begins to oscillate, the system has entered surge.

3.5 Concluding Remarks

Modeling the compressor characteristic by a bivariate cubic spline approximation seems to be very accurate with regards to measurement points. By calculating pressure ratios for zero flow and choosing pressure ratios for negative flow, the familiar S-form is obtained. The approximation performs well during simulations in SIMULINK, and it is in this manner a tool for more accurate simulations of compressor systems. The complexity of the compressor characteristic function drastically increases with its use, since it holds much more information compared to third order polynomial fitting. It is easy to make new approximations. The only thing that will have to be done is importing new measurements. The compressor characteristic shown in Figure 3.7 will be used in simulations throughout this report unless stated otherwise.

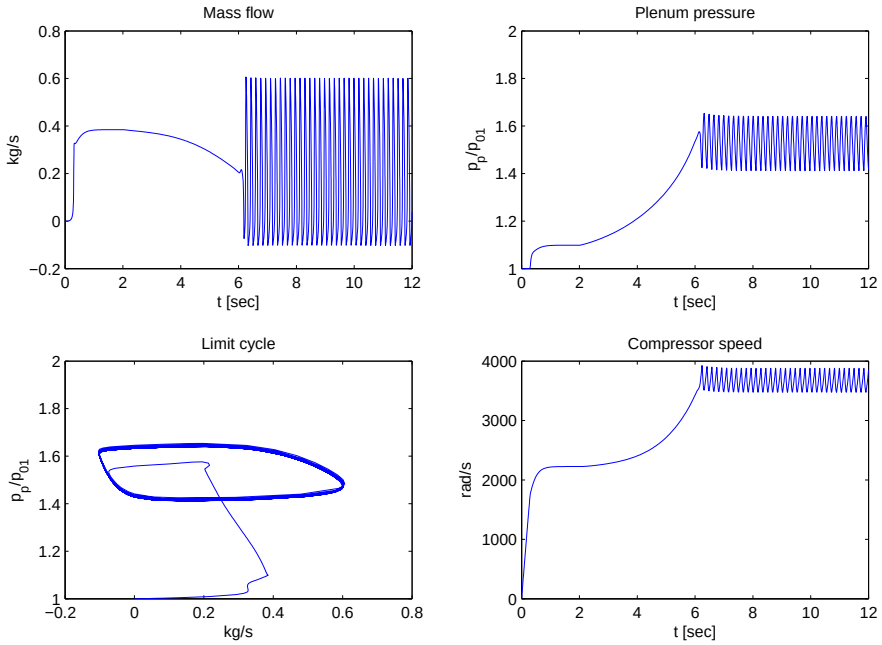

Figure 3.9: The result of a simulation in SIMULINK

Chapter 4

The Recycle System

4.1 Surge/Stall Avoidance and Active Surge/Stall Control

As previously mentioned, surge and rotating stall are highly unwanted phenomena in a continuous flow compressor system. The effects are several and can be dangerous. Due to lower pressure rise and oscillations, surge/stalls lead to loss of compressor performance. Because of the large mechanical and thermal load in the blading, the entire compressor system including nearby objects can be damaged. At present, the only remedy to get out of rotating stall is to shut down the engine and restart it again (Gu et al., 1999). That can lead to catastrophic outcomes for an airplane.

Always operating far away from the surge line would be safe, at high mass flows and low pressures, but this area is not where the efficiency is highest. The most efficient area of operation is where the pressure rise is highest, close to the surge line. A compression system is also generally prone to aerodynamic instabilities, surge and rotating stall. As such, according to Badmus et al. (1991), it is not surprising that there has been considerable effort directed towards design of control schemes to ensure stable operation of the compression system.

The proposed schemes can be categorized according to whether they strive to simply avoid unstable compressor operation by maintaining compressor operation at a safe margin from the region of unstable operation for the uncontrolled system, or whether they instead actively stabilize, or control, compressor operation near or within this same region (Badmus et al., 1991).

The first scheme is called *surge/stall avoidance* and the latter is called *active surge/stall control*. Surge/Stall avoidance has gained most acceptance in the industry.

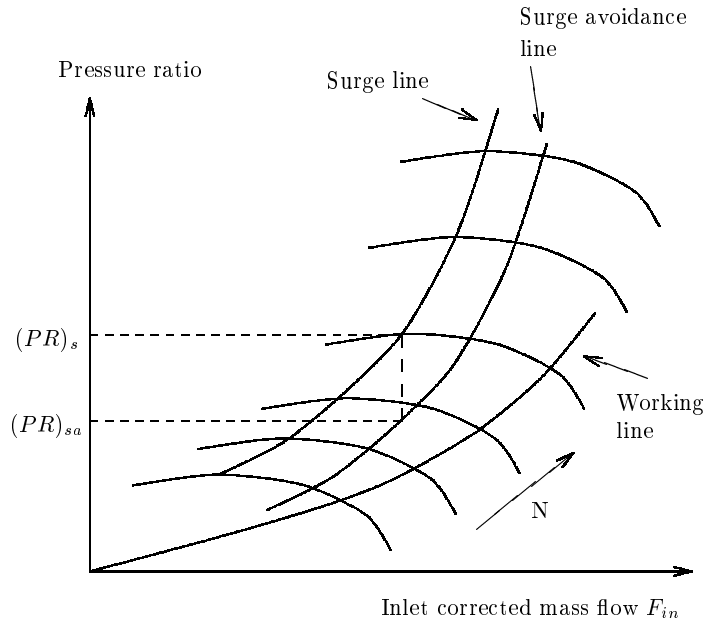

Figure 4.1: Surge margin (Gravdahl and Egeland, 1999)

Referring to Figure 4.1, by using the surge avoidance scheme, the compressor is prevented from operating beyond the surge line or some area close to it. This is achieved by e.g. recirculation of flow back to the intake, or by a bleed valve located downstream of the compressor. The surge avoidance line, also called the surge control line, is often chosen with considerable margin. 10 to 25 percent is not unusual. There are several reasons for this. First of all, the surge line is in many cases not well known. This is due to the fact that compressor maps from manufacturers not comply well with each individual setup. Secondly, the valves typically used in avoidance setups are slow. With the control line close to the surge line this can lead to surge even before the valves react. The distance between the surge line and the surge avoidance line is called *surge margin*.

According to Gravdahl and Egeland (1999), there are many different ways of defining the surge margin. One of them is

$$SM_1 = \frac{PR_s - PR_{sa}}{PR_{sa}} \tag{4.1}$$

where PR_{sa} is the pressure ratio at the surge avoidance line for a given speed, and PR_s is the pressure ratio at the surge line for the same mass flow. Another considers the change in outlet corrected mass flow, that is

$$SM_2 = \frac{F_{out,sa} - F_{out,s}}{F_{out,sa}} \tag{4.2}$$

The advantage of using (4.2) is that we get a measure of how much the mass flow can be changed before surge is encountered. Another variant uses inlet corrected mass flow, since it is easier to measure.

$$SM_3 = 1 - \left(\frac{(p_{0,out}/p_{0,in})_{sa}}{(p_{0,out}/p_{0,in})_s} \cdot \frac{F_{in,s}}{F_{in,sa}} \right) \tag{4.3}$$

Staroselsky and Ladin (1979) discusses three different forms for defining the surge control line. The optimal form would be to have the surge control line parallel to the surge line, such as in figure 4.1. Another form is to let the slope of the avoidance line be less than the slope of the surge line. The result can be surge at low speeds, and insufficient actuation at high speeds. The third form is to set the avoidance line vertical, but that could yield insufficient actuation at low speeds, and surge at high.

The working principle of a surge avoidance scheme is as follows. When the working point of the compressor system is located right to the surge control line, nothing is done. As the working point slides over the control line, some actuation device forces it to stay to the right. Another approach is to consider the working point ”safe” or ”unsafe”. When the working point of the compressor system is considered ”safe”, nothing is done. It is considered safe when the point is located right of the surge control line, or has a velocity in the map below a threshold. When the working point is considered ”unsafe”, some actuation device moves the working point back into the safe area. The working point is considered unsafe when sliding over the surge control line from the right, or has a velocity towards the control line that is considered too high. As previously mentioned, the actuation device can be a recycle line or a bleed valve, among others. A bleed valve is commonly used as actuation in gas turbines, both for power generation and propulsion. The high energy bleed flow is not entirely wasted as it can be used for e.g. cabin heat.

Another scheme is *surge detection and avoidance*, according to Gravdahl and Egeland (1999). The actuation device is started after surge has been detected. Since the instabilities can propagate quickly, and the actuation devices often are slow, this scheme is not very accepted.

4.2 Recycle Lines

As actuation with the surge avoidance scheme, recycle lines are frequently used in the industry. Botros and Henderson (1994) groups surge avoidance for centrifugal compressors with recycle into four categories[1]:

- **Conventional anti-surge control:** These are "foolproof" antisurge systems developed over the years, and are based on measurements of the differential pressure across the compressor and compressor inlet flow. One is called the flow-delta-p system, treated in detail in Nisenfeld (1982), pages 135-142. The output of the flow transmitter, ΔP_0, is shown to be proportional to the differential pressure ΔP_c. A linear relation is used to describe the surge avoidance line

$$\Delta P_0 = k_1 \Delta P_c + k_2 \tag{4.4}$$

  where k_1 and k_2 are constants.

- **Flow/rotational speed (Q/N) technique:** Nondimensionalizes the flow Q with the rotational speed N and the pressure head H. The surge avoidance line is thus reduced to a point where $(Q/N)_c$ is constant. If the measured flow/speed $(Q/N)_{measured}$ is lower than the value at the avoidance point $(Q/N)_c$, the recycle valve is opened.

- **Microprocessor and PLC based controller:** Mostly of the new designed antisurge systems are of this class, because of the nowadays great availability of computer-based controllers. It is based on direct comparison of the compressor operating point, the compressor characteristic and the surge avoidance line. One way to achieve this is by calculating the mass flow and the differential pressure across the compressor. That again requires temperature measurements, pressure measurements and the use of the compressor characteristic.

- **Control without flow measurement:** Because the signal from the flow transmitter often is noisy, inaccurate, and in some cases nonlinear and non-repeatable and also introduce a pressure drop, it is advantageous to avoid flow measurement in the surge avoidance scheme. This can be accomplished by using a $(H/N^2)_c$ ratio instead of $(Q/N)_c$ as in the Q/N-technique. This is possible provided the compressor characteristic is steep enough.

[1] This is also stated in Gravdahl and Egeland (1999)

Cooling is important in the recycle scheme. As the gas is compressed its temperature rises, according to the ideal gas law. The high-temperature gas is then recycled back into the intake, through the recycle valve. Although there may be some cooling of the high pressure gas as its pressure drops across the control valve, the gas will still have a higher temperature than the fresh gas being fed to the compressor, Nisenfeld (1982). The temperature at the intake increases which in turn would yield a further increase in temperature when the gas is compressed again. This is a reinforcing loop which clearly needs a counteract. That is achieved with a cooler, placed either upstream or downstream of the recycle valve. Economics may dictate where to place it, but placing it upstream may result in condensing of the high pressure gas. That is why there generally is a suction knock-out pot placed before the intake, to gather the condensate.

The recycle line may in theory be used in the active surge/stall control scheme. It can then be viewed as an extension to the plenum volume, where the recycle valve will have to be very fast to make this work. It is a major topic of this report, where this issue is investigated in the stability analysis chapter.

4.3 Previous Work on Modeling the Recycle System

The previously modeled compressor system in Figure 2.6 is augmented with the recycle line in Figure 4.2.

Applying the mass balance (Equation 3.20 in White (2008)) on plenum 1 yields

$$\left(\frac{dm}{dt}\right)_{syst} = 0 = \frac{d}{dt}\left(\iiint_{CV} \rho dV\right) + \iint_{CS} \rho(\vec{V_r}\cdot\vec{n})dA \tag{4.5}$$

$$\Rightarrow \frac{d}{dt}\left(\rho_1 V_1\right) = w_f + w_r - w \tag{4.6}$$

Now lets assume that the gas is ideal and isentropic. That means ignoring the molecular size of the gas along with intermolecular forces, since the gas is ideal. Since the process is assumed isentropic, there is no energy losses due to viscosity or heat conduction. The following relation can be deduced from Equation 9.15, White (2008)

$$dp = a^2 d\rho \tag{4.7}$$

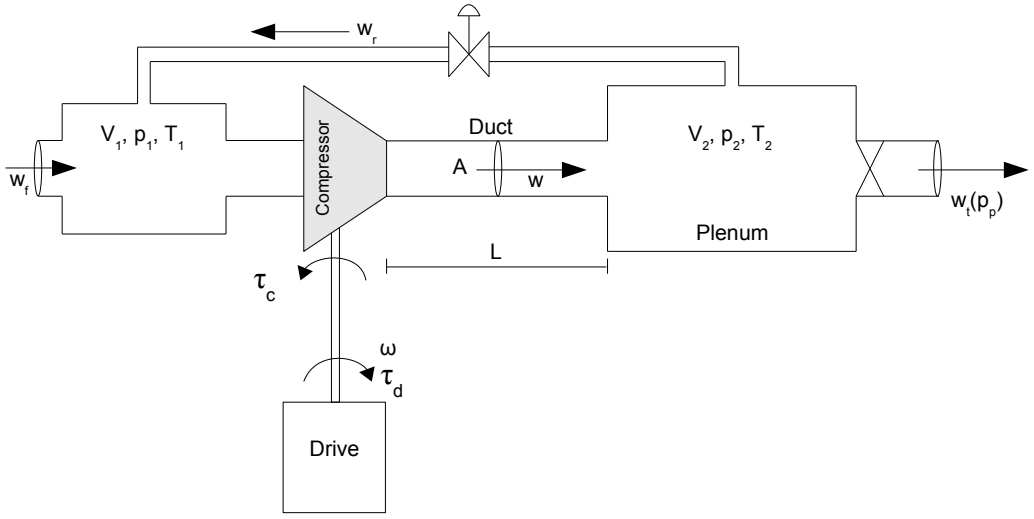

Figure 4.2: Compressor system with recycle

where $a = \sqrt{\kappa RT}$ is the speed of sound in the gas. Insertion of (4.7) into (4.6) yields

$$\frac{d}{dt}(p_1) = \frac{a^2}{V_1}(w_f + w_r - w) \tag{4.8}$$

Similarly for plenum 2 we get from applying the mass balance on volume 2

$$\frac{d}{dt}(p_2) = \frac{a^2}{V_2}(w - w_r - w_t) \tag{4.9}$$

Along with calculation of the momentum balance applied on the duct, and the angular momentum relation applied on the shaft, we get

$$\dot{p}_1 = \frac{a^2}{V_1}(w_f + w_r - w) \tag{4.10}$$

$$\dot{p}_2 = \frac{a^2}{V_2}(w - w_t - w_r) \tag{4.11}$$

$$\dot{w} = \frac{A}{L}(\Psi_c(w, \omega)\, p_1 - p_2) \tag{4.12}$$

$$\dot{\omega} = \frac{1}{J}(\tau_d - \tau_c) \tag{4.13}$$

The mass flow through the valves, that is the throttle and the recycle line, is modeled as

$$w = c\sqrt{\Delta p} \tag{4.14}$$

where c is a constant and Δp is the pressure drop across the valve. Special cases where the flow through the valve is reversed is ignored. (4.10)-(4.13) is the same model as derived in Egeland and Gravdahl (2002), pages 504-505.

4.4 Expansion of the Model

During simulations in SIMULINK, the model (4.10)-(4.13) behaved strange. The feed flow was set to constant. The feed flow range is very limited, and once a value too high or too low is entered, the simulation failed. Of course, knowing the speed and operating point in the compressor map would be necessary to conclude about a reasonable range of values. The reason the simulation failed is that the pressure in volume 1 becomes too high due to the constant supply of "air molecules". This seems unreasonable in reality. The feed flow should be dependent on the compressor somehow.

The problem is that constant feed flow doesn't make any sense. The feed flow should be dependent on the compressor, which it ain't when the feed flow is constant. When the compressor tries to pump more gas, the feed flow should increase, and vice versa. It could be argued that volume 1 should model all the piping upstream, as volume 2 actually aims to model all the piping downstream. But it makes more sense to let volume 1 model a little suction volume, which actually exists in reality as a means to gather condensate. The flow through the entrance of the suction volume would then open up to be modeled as flow through an orifice, just as the other valves. The feed flow would then be modeled as

$$w_f = c_f \sqrt{p_{upstream} - p_1} \tag{4.15}$$

and the input to the system would be pressure controlled. The system is now shown in Figure 4.3.

4.5 Open-Loop Simulation

In this section the model (4.10)-(4.13) is simulated in SIMULINK with the valves modeled as

$$w_t = \tanh\left(\zeta(p_2 - p_{01})\right) c_t \sqrt{(p_2 - p_{01})\tanh\left(\zeta(p_2 - p_{01})\right)}\Big|_{\zeta \gg 0} \tag{4.16}$$

$$w_f = c_f \sqrt{p_{upstream} - p_1} \tag{4.17}$$

$$w_r = c_r \sqrt{p_2 - p_1} \tag{4.18}$$

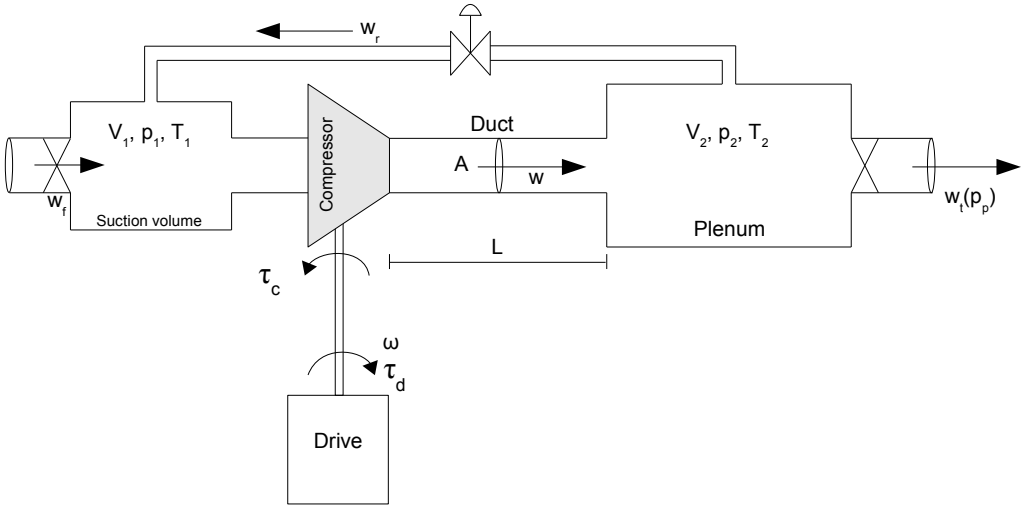

Figure 4.3: Compressor recycle system, with an added valve at the entrance

The simulation setup is as follows. Initially, the pressure in the two volumes are set to ambient, the compressor speed is set to zero, and the flows are set to zero. The feed flow gradually decreases, eventually causing the system to enter surge. The recycle valve is then opened manually to allow for more mass flow through the system. The higher mass flow encourages a shift to the right in the compressor map, and surge should disappear. The result of the simulation is shown in Figure 4.4. The initialization file is found in Appendix B.2.1 and the SIMULINK diagram is found in Appendix C.2. All the files needed to run the simulation is found in the ZIP-file at "model_recycle".

4.6 Outline of a Recycle Valve Controller

The most common setup in the industry is to PID-control the recycle valve, such as shown in Figure 4.5. The surge control line Ψ_{scl} is linear with an horizontal surge margin to the surge line.

$$\Psi_{scl}(w) = aw + b \tag{4.19}$$

where a and b are the coefficients. When the operating point is right to the surge control line, the controller is off. When the operating point is left to the surge control line, a PID-controller is used to bring the operating point back to the right. Often just a PI-controller is used.

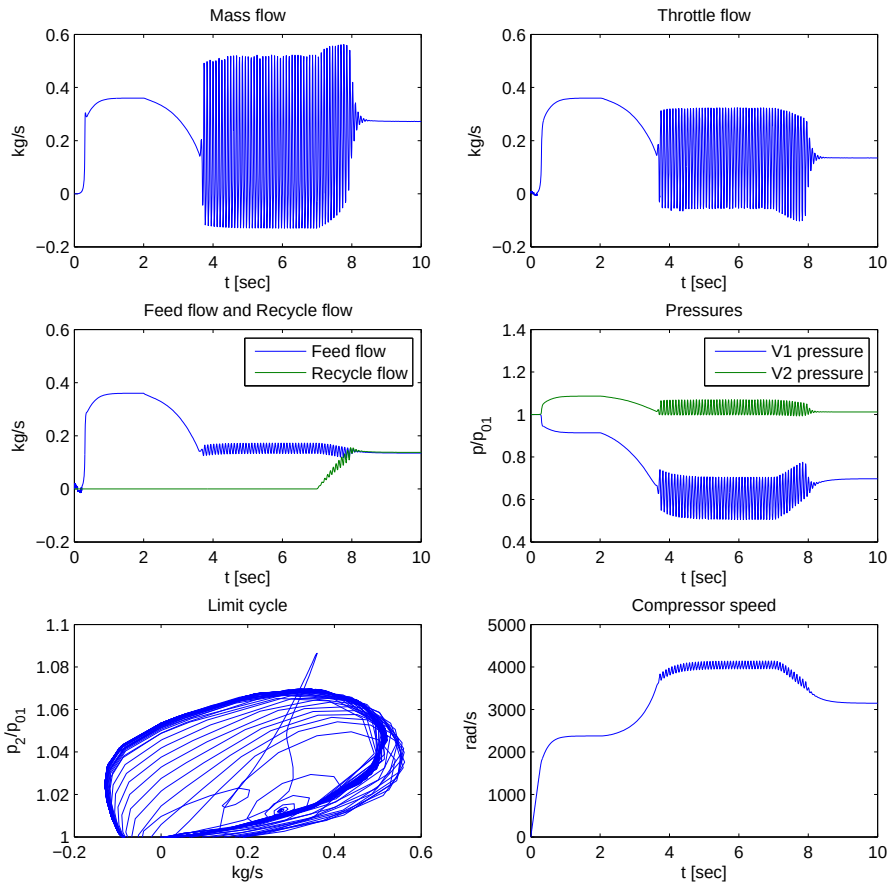

Figure 4.4: The result of a simulation of the open-loop recycle system. Initially, the pressure in the two volumes are set to ambient, the compressor speed is set to zero, and the flows are set to zero.

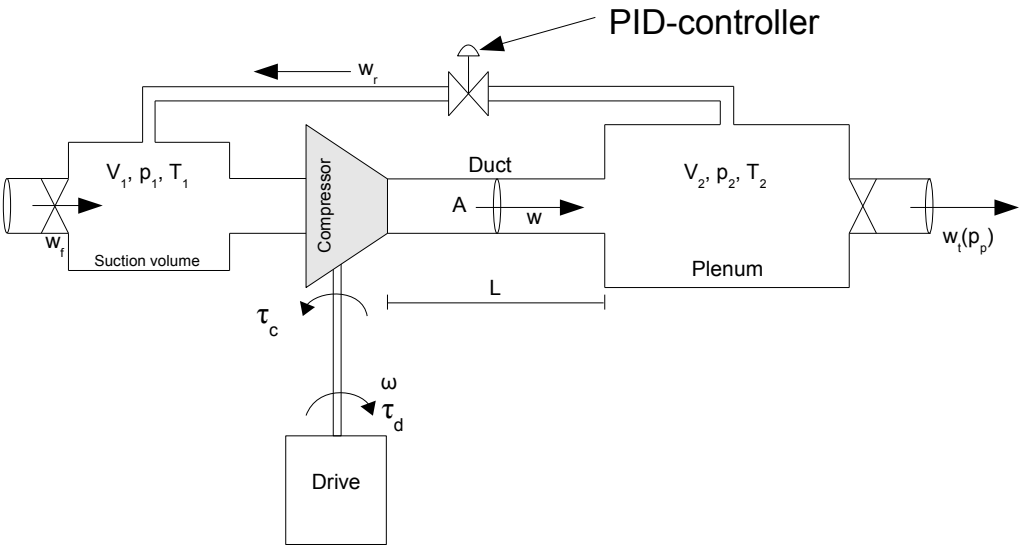

Figure 4.5: Compressor recycle system with PID-control of the recycle valve

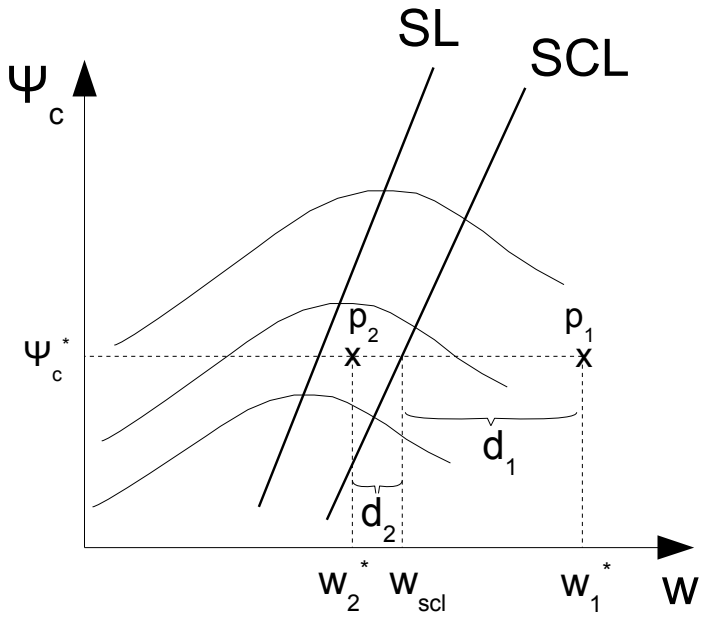

Figure 4.6: Outline of a recycle controller

Defining the distance d as the horizontal difference between the operating point and the surge control line, referring to Figure 4.6,

$$d = w - w_{scl}(\Psi_c) \tag{4.20}$$

where w, Ψ_c is the operating point of the system. $w_{scl}(\Psi_c)$ can be calculated as the inverse of (4.19).

$$w_{scl}(\Psi_c) = \frac{\Psi_{scl}(w) - b}{a} \tag{4.21}$$

Since we are measuring the distance in an horizontal direction, $\Psi_{scl}(w)$ would equal Ψ_c, the pressure rise. (4.21) becomes

$$w_{scl}(\Psi_c) = \frac{\Psi_c - b}{a} \tag{4.22}$$

When the distance is positive, the operating point is located to the right of the control line, and nothing should be done. When the distance is negative, its positive value is used as the error in the controller. The error to be used in the controller would then be

$$e = \begin{cases} 0 & d > 0 \\ -d & \text{otherwise} \end{cases}$$

The PI-controller is given as

$$u = K_p e + K_i \int_0^t e d\tau \tag{4.23}$$

and is controlling the percentage opening, or percentage of flow, of the recycle valve such that

$$w_r = u \cdot A_r \sqrt{p_2 - p_1} \tag{4.24}$$

4.7 Simulation of the Controller

The previously used open-loop model in SIMULINK, is embedded into a subsystem for better overview. This is shown in Appendix C.3. The PI controller outlined above is implemented here. The controller needs to know about the current operating point of the system, and then compare it to the

surge avoidance line. The surge avoidance line is here defined by the MATLAB file in Appendix B.3. It does so by first calculating all the surge points at different speedlines. That is achieved by a "find maximum algorithm", all the details is in the m-file. Then a polynomial of 1st order is fitted to the points such that the surge line becomes linear. The surge avoidance line is defined as this linear line, shifted a percentage (of the mass flow at the surge line) to the right. The result is shown in Figure 4.7.

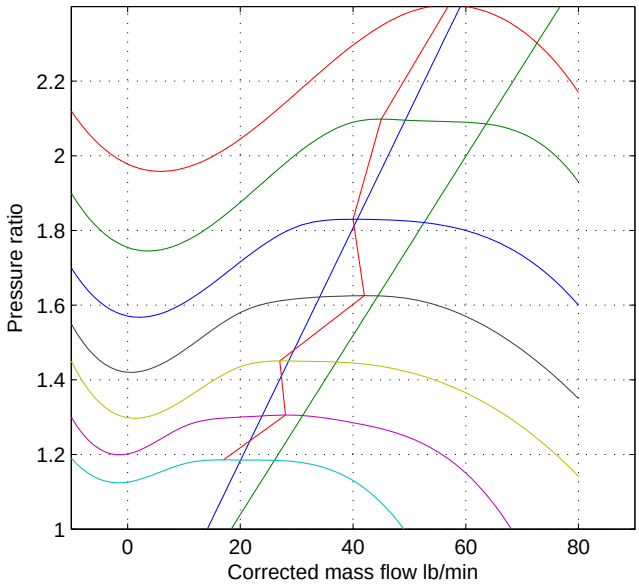

Figure 4.7: The result of defining the surge avoidance line. The jagged line is the true surge points. The leftmost linear line is the surge line, and the rightmost is the avoidance line, or surge control line.

The surge avoidance line is linear and thereby given by two constants, a and b which makes it possible to calculate Equation 4.22. That gives the avoidance point for the current pressure rise. The coefficients a and b, is `PF_avoid(1)` and `PF_avoid(2)` in the m-file, respectively.

The initialization file is found in Appendix B.2.2. Initially, the pressure in the two volumes are set to ambient, the compressor speed is set to zero, and the flows are set to zero. The simulation setup is the same as for the open-loop simulation, the feed flow decreases, and in open-loop, the system entered surge. From Figure 4.8, we can see that an empirically tuned PI-controller with a K_p of 2.5 and a K_i of 5.5 stabilizes the system. The operating point

passes over the control line, the controller goes on and brings it back to the line. Observe that the operating point never reaches the surge line (The operating point is left to the surge line only during startup, which we'll ignore). All the files needed to run the simulation is located in the ZIP-file at "MATLAB/model_recycle_control".

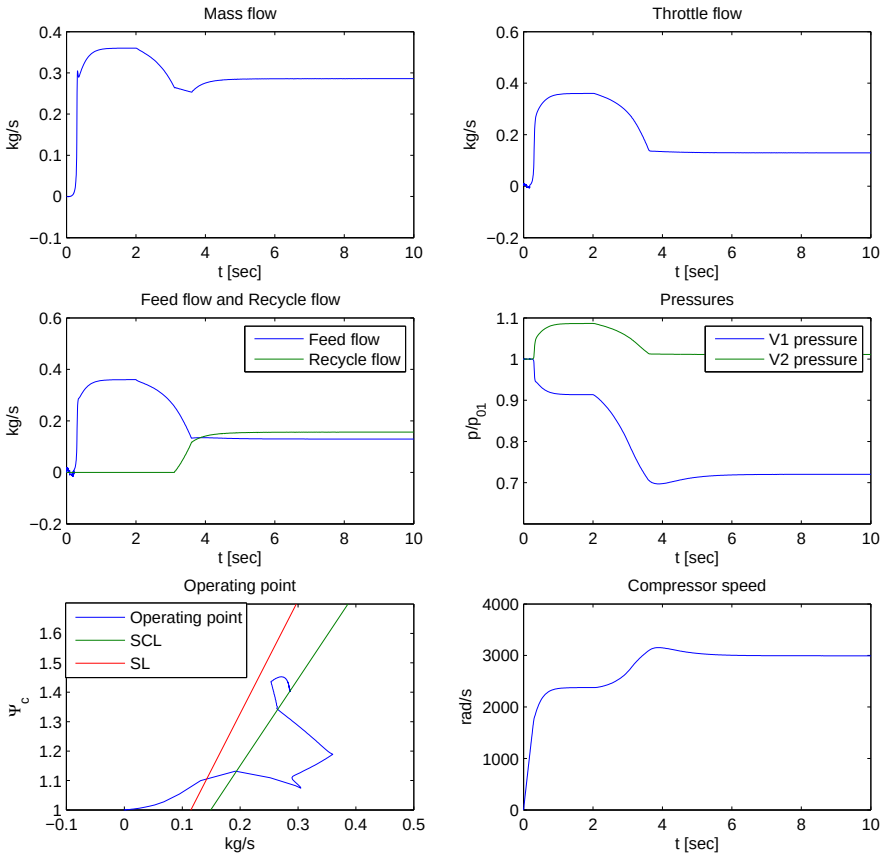

Figure 4.8: The result of a simulation of the closed-loop recycle system. Initially, the pressure in the two volumes are set to ambient, the compressor speed is set to zero, and the flows are set to zero.

Chapter 5

Stability Analysis of the Recycle System

In this chapter a stability analysis for the recycle system will be conducted. Two different models will be investigated, although the last is really an extension of the first. They both uses the pressure rise P_c in the equation for the mass flow, like in Greitzer (1976).

5.1 A New Variant of the Recycle System Model

Consider the differential equation for the time derivative of the mass flow, used in the model of the recycle system presented in the previous chapter.

$$\dot{w} = \frac{A}{L}\left(\Psi_c(w,\omega)p_1 - p_2\right) = f_{\dot{w},1}(\cdot) \tag{5.1}$$

This equation is the result of the momentum balance applied on the duct. The duct is until now defined as the pipe located between the compressor and plenum 2, where the length of it is L, and A is the cross-sectional area. Lets now instead apply the momentum balance on the system shown in Figure 5.1.

When incompressibility is assumed in the two pipes, the result is

$$\dot{w} = \frac{A_c}{L_c}\left(p_1 + P_c(w,\omega) - p_2\right) = f_{\dot{w},2}(\cdot) \tag{5.2}$$

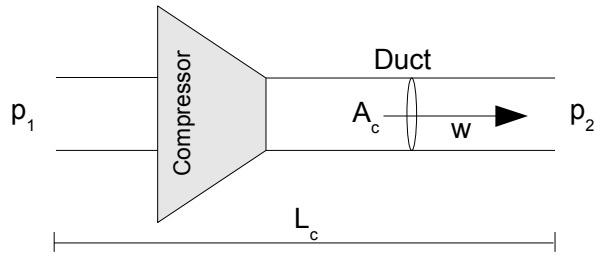

Figure 5.1: Derivation of a new equation for the time derivative of the mass flow

Where $f_{\dot{w},2}(\cdot)$ now is dependent on the pressure rise across the compressor, P_c. (5.2) is identical to Equation 2b in Greitzer (1976), which also used this expression for the time derivative of the mass flow. The new model for the recycle system becomes

$$\begin{aligned}
\dot{p}_1 &= k_1 (w_f + w_r - w) && (5.3)\\
\dot{p}_2 &= k_2 (w - w_r - w_t) && (5.4)\\
\dot{w} &= k_3 (p_1 + P_c(w, \omega) - p_2) && (5.5)\\
\dot{\omega} &= k_4 (\tau_c - \tau_c) && (5.6)
\end{aligned}$$

where $k_1 = \frac{a^2}{V_1}$, $k_2 = \frac{a^2}{V_2}$, $k_3 = \frac{A_c}{L_c}$ and $k_4 = \frac{1}{J}$. The flows described by w_f, w_r and w_t are modeled as

$$\begin{aligned}
w_t &= c_t \sqrt{p_2 - p_{01}} && (5.7)\\
w_f &= c_f \sqrt{p_{upstream} - p_1} && (5.8)\\
w_r &= c_r \sqrt{p_2 - p_1} && (5.9)
\end{aligned}$$

The model can be extended by letting the recycle flow be modeled as

$$\dot{w}_r = k_r (p_2 - P_r - p_1) \qquad (5.10)$$

Where $k_r = \frac{A_r}{L_r}$, A_r and L_r is the cross sectional area and the length of the recycle line, respectively, and P_r is the pressure drop across the recycle valve. It is the result of applying the momentum balance on the recycle line. (5.9) will then be omitted.

5.2 Analysis of the Model

In this section a stability analysis is conducted for the system $[\dot{p}_1\ \dot{p}_2\ \dot{w}]^T = f(\cdot)$ given as

$$\dot{p}_1 = k_1 (w_f + w_r - w) \tag{5.11}$$
$$\dot{p}_2 = k_2 (w - w_r - w_t) \tag{5.12}$$
$$\dot{w} = k_3 (p_1 + P_c(w) - p_2) \tag{5.13}$$

where $k_1 = \frac{a^2}{V_1}$, $k_2 = \frac{a^2}{V_2}$ and $k_3 = \frac{A_c}{L_c}$. The flows described by w_f, w_r and w_t are modeled as

$$w_t = c_t \sqrt{p_2 - p_{01}} \tag{5.14}$$
$$w_f = c_f \sqrt{p_{upstream} - p_1} \tag{5.15}$$
$$w_r = c_r \sqrt{p_2 - p_1} \tag{5.16}$$

5.2.1 Assumptions, Defining a Domain

The first assumption is that we're operating on one speedline. The compressor is running at constant speed, and the equation for the shaft dynamics have been omitted. Secondly, the pressure in volume 2 is assumed higher than the ambient/downstream pressure and the pressure in volume 1. If you think about it, it makes sense. Either the compressor isn't running and the pressure is at least equal to the ambient/volume 1 pressure, or the compressor is running and is compressing air to volume 2. During deep surge, volume 2 is emptying itself out through the compressor, but it is assumed that it does so without the pressure in volume 2 goes below the ambient, or the pressure in volume 1 goes above the pressure in volume 2. Thirdly, the pressure in volume 1 is assumed below the upstream pressure. It also makes sense since when the compressor isn't running, the pressure is at most equal to the upstream pressure, and when the compressor is running, it is of course creating suction. The reasoning stated above implies a domain[1] D for the recycle system (5.11)-(5.13) where $f(\cdot) : D \to R^3$ is a continuously differentiable map. Taking $D = \{\ [p_1\ p_2\ w]^T \in R^3 \mid p_1 < p_{upstream}, p_2 > \max(p_{01}, p_1),$ P_c IS DEFINED$\}$ achieves this locally Lipschitz property of f. Implicitly, the compressor characteristic P_c is assumed continuously differentiable as well.

[1] An open, connected set

5.2.2 Equilibrium Points

Equilibrium points (p_1^*, p_2^*, w^*) for the system (5.11)-(5.13) are given by

$$\begin{aligned} w_f^* + w_r^* &= w^* && (5.17)\\ w_t^* + w_r^* &= w^* && (5.18)\\ p_1^* + P_c(w^*) &= p_2^* && (5.19) \end{aligned}$$

That means that the mass flow is equal to the feed flow plus the recycle flow during an equilibrium. The mass flow is also equal to the throttle flow plus the recycle flow. Implicitly, the feed flow and the throttle flow is equal during an equilibrium. We also have that the discharge pressure is equal to the suction pressure plus the pressure rise. Equilibrium points will have to be shifted to the origin in order to use the nonlinear analysis tools presented in Khalil (2002). It is easy to see that the equilibrium is not centered at the origin. In the model (5.11)-(5.13) the pressure in volume 1 would ideally lie a little under the upstream pressure, and the pressure in volume 2 would be higher than in volume 1. Recall that stable mass flows are found to the right of the surge line, clearly not centered around the origin.

5.2.3 Shift to the Origin

It is desirable to shift the equilibrium to the origin. Defining the deviation from the equilibrium point as

$$\begin{aligned} \hat{p}_1 &= p_1 - p_1^* && (5.20)\\ \hat{p}_2 &= p_2 - p_2^* && (5.21)\\ \hat{w} &= w - w^* && (5.22) \end{aligned}$$

The new equations are then

$$\begin{aligned} \dot{\hat{p}}_1 &= k_1 \left(w_f + w_r - \hat{w} - w^*\right) && (5.23)\\ \dot{\hat{p}}_2 &= k_2 \left(\hat{w} + w^* - w_r - w_t\right) && (5.24)\\ \dot{\hat{w}} &= k_3 \left(\hat{p}_1 + p_1^* + P_c(\hat{w} + w^*) - \hat{p}_2 - p_2^*\right) && (5.25) \end{aligned}$$

Next we want to bring forth a $\hat{P}_c(\hat{w})$ which is centered at the origin. In that case the compressor characteristic would belong to sector $(-\infty, 0)$ for stable

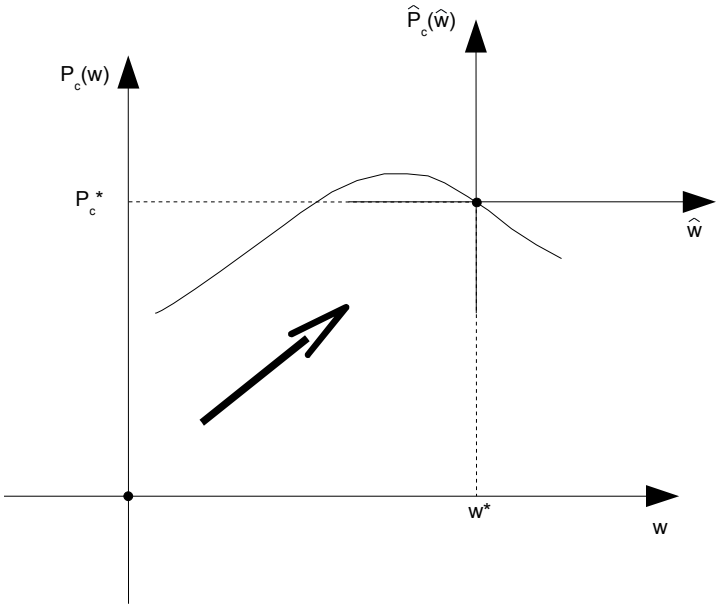

Figure 5.2: Equilibrium shifting of the compressor characteristic

negative slopes, and belong to sector $(0, \infty)$ for unstable positive slopes.[2] In figure 5.2 the shift is shown.

Lets define

$$\hat{P}_c(\hat{w}) \triangleq P_c\left(\hat{w} + w^*\right) - P_c(w^*) \tag{5.26}$$

in which $\hat{P}_c(0) = 0$ proves that it is centered at the origin. Lets further define

$$\begin{aligned}
\hat{w}_t(\hat{p}_2) &\triangleq w_t\left(\hat{p}_2 + p_2^*\right) - w_t(p_2^*) && (5.27)\\
\hat{w}_f(\hat{p}_1) &\triangleq w_f\left(\hat{p}_1 + p_1^*\right) - w_f(p_1^*) && (5.28)\\
\hat{w}_r(\hat{p}_1, \hat{p}_2) &\triangleq w_r\left(\hat{p}_1 + p_1^*, \hat{p}_2 + p_2^*\right) - w_r(p_1^*, p_2^*) && (5.29)
\end{aligned}$$

in which we know that $\hat{w}_t$ belongs to the sector $(0, \infty)$ and $\hat{w}_f$ belongs to sector $(-\infty, 0)$, referring to figure 5.3.

The model (5.23)-(5.25) now becomes

$$\begin{aligned}
\dot{\hat{p}}_1 &= k_1\left(\hat{w}_f(\hat{p}_1) + w_f(p_1^*) + \hat{w}_r(\hat{p}_1, \hat{p}_2) + w_r(p_1^*, p_2^*) - \hat{w} - w^*\right) && (5.30)\\
\dot{\hat{p}}_2 &= k_2\left(\hat{w} + w^* - \hat{w}_r(\hat{p}_1, \hat{p}_2) - w_r(p_1^*, p_2^*) - \hat{w}_t(\hat{p}_2) - w_t(p_2^*)\right) && (5.31)\\
\dot{\hat{w}} &= k_3\left(\hat{p}_1 + p_1^* + \hat{P}_c(\hat{w}) + P_c(w^*) - \hat{p}_2 - p_2^*\right) && (5.32)
\end{aligned}$$

[2]See Appendix A.3 for a review about sector terminology.

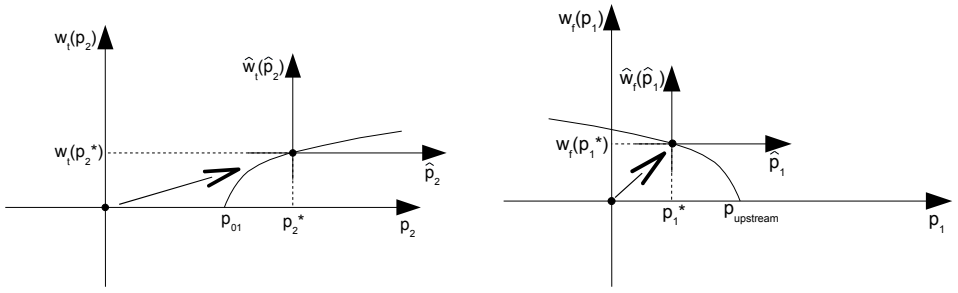

(a) Shift of the throttle flow equilibrium (b) Shift of the feed flow equilibrium

Figure 5.3: Shifting of equilibriums for throttle flow and feed flow

The equilibrium points (5.17)-(5.19) implies that $w_f(p_1^*) - w^* + w_r(p_1^*, p_2^*) = 0$, $w^* - w_r(p_1^*, p_2^*) - w_t(p_2^*) = 0$ and that $p_1^* + P_c(w^*) - p_2^* = 0$. (5.30)-(5.32) becomes

$$\dot{\hat{p}}_1 = k_1 \left(\hat{w}_f(\hat{p}_1) - \hat{w} + \hat{w}_r(\hat{p}_1, \hat{p}_2) \right) \tag{5.33}$$

$$\dot{\hat{p}}_2 = k_2 \left(\hat{w} - \hat{w}_r(\hat{p}_1, \hat{p}_2) - \hat{w}_t(\hat{p}_2) \right) \tag{5.34}$$

$$\dot{\hat{w}} = k_3 \left(\hat{p}_1 + \hat{P}_c(\hat{w}) - \hat{p}_2 \right) \tag{5.35}$$

5.2.4 Lyapunov Analysis

The Lyapunov function

$$V(\hat{p}_1, \hat{p}_2, \hat{w}) = \frac{1}{2k_1}\hat{p}_1^2 + \frac{1}{2k_2}\hat{p}_2^2 + \frac{1}{2k_3}\hat{w}^2 \tag{5.36}$$

is positive definite and radially unbounded. Its derivative along the trajectories of the system (5.33)-(5.35) is

$$\begin{aligned} \dot{V} &= \frac{1}{k_1}\hat{p}_1\dot{\hat{p}}_1 + \frac{1}{k_2}\hat{p}_2\dot{\hat{p}}_2 + \frac{1}{k_3}\hat{w}\dot{\hat{w}} \\ &= \hat{p}_1 \left(\hat{w}_f(\hat{p}_1) - \hat{w} + \hat{w}_r \right) + \hat{p}_2 \left(\hat{w} - \hat{w}_r - \hat{w}_t(\hat{p}_2) \right) + \hat{w} \left(\hat{p}_1 + \hat{P}_c(\hat{w}) - \hat{p}_2 \right) \\ &= \hat{p}_1 \hat{w}_f(\hat{p}_1) - (\hat{p}_2 - \hat{p}_1)\hat{w}_r - \hat{p}_2 \hat{w}_t(\hat{p}_2) + \hat{w}\hat{P}_c(\hat{w}) \end{aligned} \tag{5.37}$$

The sector properties of $\hat{w}_f(\hat{p}_1)$ and $\hat{w}_t(\hat{p}_2)$ implies that $\hat{p}_1 \hat{w}_f(\hat{p}_1) < 0 \ \forall \ \hat{p}_1 \in D - \{\hat{p}_1 = 0\}$ and that $\hat{p}_2 \hat{w}_t(\hat{p}_2) > 0 \ \forall \ \hat{p}_2 \in D - \{\hat{p}_2 = 0\}$. Lets now

investigate the properties of $(\hat{p}_2 - \hat{p}_1)\,\hat{w}_r\,(\hat{p}_1, \hat{p}_2)$. It can be written as

$$\begin{aligned}(\hat{p}_2 - \hat{p}_1)\,\hat{w}_r\,(\hat{p}_1, \hat{p}_2) &= (\hat{p}_2 - \hat{p}_1)\,(w_r(\hat{p}_1 + p_1^*, \hat{p}_2 + p_2^*) - w_r(p_1^*, p_2^*)) \\ &= (\hat{p}_2 - \hat{p}_1)\left(c_r\sqrt{\hat{p}_2 + p_2^* - \hat{p}_1 - p_1^*} - c_r\sqrt{p_2^* - p_1^*}\right) \\ &= c_r X\left(\sqrt{X + p_2^* - p_1^*} - \sqrt{p_2^* - p_1^*}\right) \\ &= c_r X \hat{w}_r(X) \qquad (5.38)\end{aligned}$$

where $X = \hat{p}_2 - \hat{p}_1$. We know that a function on the form $f(x) = \sqrt{x+a} - \sqrt{a}$, where $x > -a$ and $a > 0$, belongs to sector $(0, \infty)$. It implies that $\hat{w}_r(X)$ belongs to sector $(0, \infty)$ since it is a function on that form. That means that (5.38) will be positive definite, $\forall\ X$ in $D - \{\hat{p}_2 - \hat{p}_1 = 0\}$, and positive semidefinite $\forall\ X$ in D. See Figure 5.4 for a graphical illustration. The term $-(\hat{p}_2 - \hat{p}_1)\hat{w}_r$ in $\dot{V}$ will consequently be negative semidefinite, independent on the valve setting c_r.

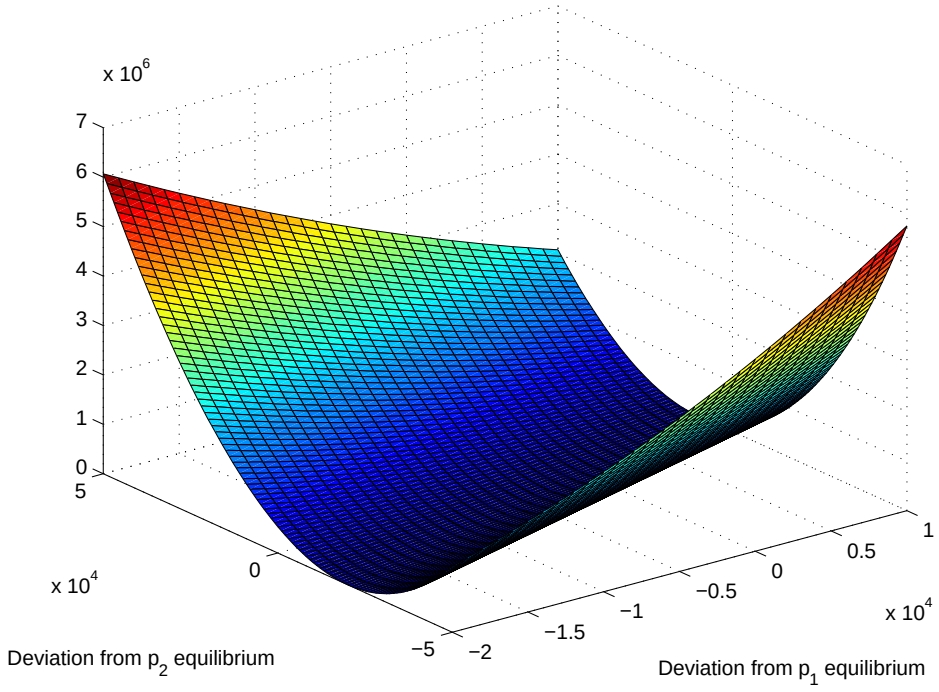

Figure 5.4: Graphical representation of the function $(\hat{p}_2 - \hat{p}_1)\,\hat{w}_r\,(\hat{p}_1, \hat{p}_2)$ for different values of $\hat{p}_1$ and $\hat{p}_2$. A typical value of the pressure rise over the compressor is inserted.

The term $\hat{w}\hat{P}_c(\hat{w})$ is negative definite if $\hat{P}_c(\hat{w})$ belongs to sector $(-\infty, 0)$. And thats the case during operation on a negative slope of the characteristic, or $w > w_{P_c,max}$. The result is that $\dot{V} < 0$ in $D' - \{0\}$, where $D' = \{ [p_1\ p_2\ w]^T \in R^3 \mid p_1 < p_{upstream},\ p_2 > \max(p_{01}, p_1),\ w_{\Psi_c,max} < w < w_{stonewall}\}$, and that the origin of the recycle system (5.33)-(5.35) is asymptotically stable. (Theorem 4.1, Khalil (2002)) So we can conclude and say that the origin of the recycle system (5.33)-(5.35) is asymptotically stable, independent of recycle flow, as long as we're operating on a negative slope of the compressor characteristic.

Lemma 5.1 *Consider the recycle system* (5.33)-(5.35). *It is asymptotically stable in the domain D', independent on the recycle valve setting c_r.* ◇

5.3 Analysis of the Extended Model

The extended model of the recycle system is given as

$$\begin{aligned} \dot{p}_1 &= k_1 (w_f + w_r - w) && (5.39)\\ \dot{p}_2 &= k_2 (w - w_r - w_t) && (5.40)\\ \dot{w} &= k_3 (p_1 + P_c(w) - p_2) && (5.41)\\ \dot{w}_r &= k_r (p_2 - P_r - p_1) && (5.42) \end{aligned}$$

where P_r is the pressure drop across the recycle valve. P_r is used as the input to the system. Transformed to the origin, the system becomes

$$\begin{aligned} \dot{\hat{p}}_1 &= k_1 (\hat{w}_f + \hat{w}_r - \hat{w}) && (5.43)\\ \dot{\hat{p}}_2 &= k_2 (\hat{w} - \hat{w}_r - \hat{w}_t) && (5.44)\\ \dot{\hat{w}} &= k_3 \left(\hat{p}_1 + \hat{P}_c(\hat{w}) - \hat{p}_2\right) && (5.45)\\ \dot{\hat{w}}_r &= k_r \left(\hat{p}_2 - \hat{P}_r - \hat{p}_1\right) && (5.46) \end{aligned}$$

Using the Lyapunov function

$$V(\hat{p}_1, \hat{p}_2, \hat{w}, \hat{w}_r) = \frac{1}{2k_1}\hat{p}_1^2 + \frac{1}{2k_2}\hat{p}_2^2 + \frac{1}{2k_3}\hat{w}^2 + \frac{1}{2k_r}\hat{w}_r^2 \qquad (5.47)$$

which is positive definite and radially unbounded, its derivative along the trajectories of the system becomes

$$\dot{V} = \hat{p}_1\hat{w}_f(\hat{p}_1) - \hat{p}_2\hat{w}_t(\hat{p}_2) + \hat{w}\hat{P}_c(\hat{w}) - \hat{w}_r\hat{P}_r \qquad (5.48)$$

(5.48) is negative semidefinite if

$$\hat{w}\hat{P}_c(\hat{w}) - \hat{w}_r\hat{P}_r < 0 \quad \forall \quad \hat{w} \neq 0 \tag{5.49}$$

Lets say we can choose $\hat{P}_r$ such that the term $-\hat{w}_r\hat{P}_r$ can overcome the positiveness of $\hat{w}\hat{P}_c(\hat{w})$. By choosing $\hat{P}_r = \frac{1}{2}k\hat{w}^3$, the requirement (5.49) becomes

$$\hat{w}\left(\hat{P}_c(\hat{w}) - \frac{1}{2}k\hat{w}_r\hat{w}^2\right) < 0 \tag{5.50}$$

(5.50) holds if

$$\hat{P}_c(\hat{w}) - \frac{1}{2}k\hat{w}_r\hat{w}^2\Big|_{\hat{w}=0} = 0 \tag{5.51}$$

$$\frac{\partial}{\partial\hat{w}}\left(\hat{P}_c(\hat{w}) - \frac{1}{2}k\hat{w}_r\hat{w}^2\right) < 0 \tag{5.52}$$

Obviously, (5.51) holds. The last requirement can be written as

$$\frac{\partial\hat{P}_c}{\partial\hat{w}} < k\hat{w}_r\hat{w} \tag{5.53}$$

It is seen that the last requirement is that the slope of the characteristic should be less than some value dependent on the states $\hat{w}_r$ and $\hat{w}$. It turns out that it is a very difficult task to choose a k which fulfills this requirement. Motivated by the result above, backstepping methods for finding a stabilizing input is investigated in the next sections.

5.4 Finding a Stabilizing Input I

The differential equations

$$\dot{\hat{w}} = k_3 \left(\hat{p}_1 + \hat{P}_c(\hat{w}) - \hat{p}_2 \right) \tag{5.54}$$

$$\dot{\hat{p}}_1 = k_1 \left(\hat{w}_f + \hat{w}_r - \hat{w} \right) \tag{5.55}$$

$$\dot{\hat{p}}_2 = k_2 \left(\hat{w} - \hat{w}_r - \hat{w}_t \right) \tag{5.56}$$

are present in both the main model of the recycle system, and in the extended model, used in this chapter. To successfully apply backstepping, an expression for $\hat{w}_r$ must be found which stabilizes the origin of these three equations. The equations can be written as

$$\dot{\hat{w}} = f_1(\hat{w}, \hat{p}_1, \hat{p}_2) \tag{5.57}$$

$$\dot{\hat{p}}_1 = f_2(\hat{w}, \hat{p}_1, \hat{w}_r) \tag{5.58}$$

$$\dot{\hat{p}}_2 = f_3(\hat{w}, \hat{p}_2, \hat{w}_r) \tag{5.59}$$

$\dot{\hat{p}}_1$ and $\dot{\hat{p}}_2$ aren't interdependent, although they really are in the main model by the expression for $\hat{w}_r$, but it is in this case just viewed as an input to the system for simplicity. (5.57)-(5.59) is not a *strict-feedback* system.[3] The reason for this is that (5.57) is dependent on both $\hat{p}_1$ and $\hat{p}_2$, and (5.58) and (5.59) both are dependent on $\hat{w}$. The result is that the normal recursive application of backstepping can't be used. The system (5.57)-(5.59) is not a general system in the backstepping context either, since two of the equations depend on the input $\hat{w}_r$. Of these reasons, backstepping methods such that in Krstic and Kokotovic (1995) and Bøhagen and Gravdahl (2005) will be difficult to conduct. However, *block backstepping* (Khalil, 2002) could be attempted, by partly viewing the system as multiinput.

Theorem 5.1 *The control law*

$$\hat{w}_r = -k_c k_3 \left(\hat{P}_c(\hat{w}) - k_c(k_1 + 3k_2)\hat{w} - \hat{p}_1 + \hat{p}_2 \right) \tag{5.60}$$

where

$$k_c > \frac{2 \sup_{\hat{w}} \left\{ \frac{\partial \hat{P}_c}{\partial \hat{w}} \right\}}{k_1 + k_2}, \quad \frac{\partial \hat{w}_f}{\partial \hat{p}_1} < -\frac{1}{k_c k_1}, \quad \frac{\partial \hat{w}_t}{\partial \hat{p}_2} > \frac{1}{k_c k_2} \tag{5.61}$$

renders the origin of (5.54) - (5.56) *semiglobally asymptotically stable.* ◇

[3] See appendix A.4 for an explanation of strict-feedback systems

Proof:

Step 1:

Using

$$\begin{bmatrix} \hat{p}_1 \\ \hat{p}_2 \end{bmatrix} = \phi(\hat{w}) = \begin{bmatrix} -k_c k_1 \hat{w} \\ k_c k_2 \hat{w} \end{bmatrix}$$

as the input in the first equation, (5.54) becomes

$$\dot{\hat{w}} = k_3 \left(\hat{P}_c(\hat{w}) - k_c(k_1 + k_2)\hat{w} \right) \tag{5.62}$$

Using the Lyapunov function $V(\hat{w}) = \frac{1}{2k_3}\hat{w}^2$, its derivative is

$$\begin{aligned} \dot{V} &= \hat{w} \left(\hat{P}_c(\hat{w}) - k_c(k_1 + k_2)\hat{w} \right) \\ &= \hat{w} \left(\hat{P}_c(\hat{w}) - \theta k_c(k_1 + k_2)\hat{w} \right) - (1-\theta)k_c(k_1 + k_2)\hat{w}^2 \\ &\leq -(1-\theta)k_c(k_1 + k_2)\hat{w}^2 \end{aligned} \tag{5.63}$$

For some constant $0 < \theta < 1$. For (5.63) to hold, the following must hold

$$\hat{P}_c(\hat{w}) - \theta k_c(k_1 + k_2)\hat{w}\Big|_{\hat{w}=0} = 0 \tag{5.64}$$

$$\frac{\partial}{\partial \hat{w}} \left(\hat{P}_c(\hat{w}) - \theta k_c(k_1 + k_2)\hat{w} \right) < 0 \tag{5.65}$$

Obviously, (5.64) holds. (5.65) becomes

$$\frac{\partial \hat{P}_c}{\partial \hat{w}} < \theta k_c(k_1 + k_2) \tag{5.66}$$

Choosing k_c according to

$$k_c > \frac{\sup_{\hat{w}} \left\{ \frac{\partial \hat{P}_c}{\partial \hat{w}} \right\}}{\theta(k_1 + k_2)} \tag{5.67}$$

guarantees that (5.66), and thereby (5.63) holds. Hence, the origin of $\dot{\hat{w}}$ is exponentially stable where $\hat{P}_c$ is defined. (Theorem 4.10, Khalil (2002))

Step 2:

The change of variables

$$z = \begin{bmatrix} \hat{p}_1 \\ \hat{p}_2 \end{bmatrix} - \phi(\hat{w}) = \begin{bmatrix} \hat{p}_1 + k_c k_1 \hat{w} \\ \hat{p}_2 - k_c k_2 \hat{w} \end{bmatrix}$$

transforms the system into

$$\dot{\hat{w}} = k_3 \left(\hat{P}_c(\hat{w}) - 2k_c(k_1+k_2)\hat{w} \right) + gz \tag{5.68}$$

$$\dot{z}_1 = k_1 \left(\hat{w}_f + \hat{w}_r - \hat{w} \right) + k_c k_1 \left(k_3 \left(\hat{P}_c(\hat{w}) - 2k_c(k_1+k_2)\hat{w} \right) + gz \right) \tag{5.69}$$

$$\dot{z}_2 = k_2 \left(\hat{w} - \hat{w}_r - \hat{w}_t \right) - k_c k_2 \left(k_3 \left(\hat{P}_c(\hat{w}) - 2k_c(k_1+k_2)\hat{w} \right) + gz \right) \tag{5.70}$$

where $g = [k_3 \ -k_3]$. Taking

$$V_c = \frac{1}{2k_3}\hat{w}^2 + \frac{1}{2k_1}z_1^2 + \frac{1}{2k_2}z_2^2 \tag{5.71}$$

as a composite Lyapunov function, we obtain

$$\begin{aligned}
\dot{V}_c &= \hat{w} \left(\hat{P}_c(\hat{w}) - \theta k_c(k_1+k_2)\hat{w} \right) - (1-\theta)k_c(k_1+k_2)\hat{w}^2 + \frac{1}{k_3}\hat{w}gz \\
&\quad + z_1 \left(\hat{w}_f + \hat{w}_r - \hat{w} \right) + k_c z_1 \left(k_3 \left(\hat{P}_c(\hat{w}) - 2k_c(k_1+k_2)\hat{w} \right) + gz \right) \\
&\quad + z_2 \left(\hat{w} - \hat{w}_r - \hat{w}_t \right) - k_c z_2 \left(k_3 \left(\hat{P}_c(\hat{w}) - 2k_c(k_1+k_2)\hat{w} \right) + gz \right) \\
&= \hat{w} \left(\hat{P}_c(\hat{w}) - \theta k_c(k_1+k_2)\hat{w} \right) - (1-\theta)k_c(k_1+k_2)\hat{w}^2 \\
&\quad + z_1 \left(\hat{w}_f + \hat{w}_r \right) + k_c z_1 \left(k_3 \left(\hat{P}_c(\hat{w}) - 2k_c(k_1+k_2)\hat{w} \right) + gz \right) \\
&\quad + z_2 \left(-\hat{w}_r - \hat{w}_t \right) - k_c z_2 \left(k_3 \left(\hat{P}_c(\hat{w}) - 2k_c(k_1+k_2)\hat{w} \right) + gz \right) \\
&= \hat{w} \left(\hat{P}_c(\hat{w}) - \theta k_c(k_1+k_2)\hat{w} \right) - (1-\theta)k_c(k_1+k_2)\hat{w}^2 + \hat{p}_1\hat{w}_f - \hat{p}_2\hat{w}_t \\
&\quad + k_c k_1 \hat{w}\hat{w}_f + z_1\hat{w}_r + k_c z_1 \left(k_3 \left(\hat{P}_c(\hat{w}) - 2k_c(k_1+k_2)\hat{w} \right) + gz \right) \\
&\quad - k_c k_2 \hat{w}\hat{w}_t - z_2\hat{w}_r - k_c z_2 \left(k_3 \left(\hat{P}_c(\hat{w}) - 2k_c(k_1+k_2)\hat{w} \right) + gz \right)
\end{aligned} \tag{5.72}$$

By using Young's inequality[4], $\dot{V}_c$ can be upper bounded as

$$\begin{aligned}
\dot{V}_c \;\leq\;& \hat{w}\left(\hat{P}_c(\hat{w}) - \theta k_c(k_1+k_2)\hat{w}\right) - (1-\theta)k_c(k_1+k_2)\hat{w}^2 + \hat{p}_1\hat{w}_f - \hat{p}_2\hat{w}_t \\
&+k_c k_1\left(\frac{1}{2\varepsilon}\hat{w}^2 + \frac{\varepsilon}{2}\hat{w}_f^2\right) + k_c z_1\left(\frac{1}{k_c}\hat{w}_r + k_3\left(\hat{P}_c(\hat{w}) - 2k_c(k_1+k_2)\hat{w}\right) + gz\right) \\
&+k_c k_2\left(\frac{1}{2\varepsilon}\hat{w}^2 + \frac{\varepsilon}{2}\hat{w}_t^2\right) - k_c z_2\left(\frac{1}{k_c}\hat{w}_r + k_3\left(\hat{P}_c(\hat{w}) - 2k_c(k_1+k_2)\hat{w}\right) + gz\right) \\
\leq\;& \hat{w}\left(\hat{P}_c(\hat{w}) - \theta k_c(k_1+k_2)\hat{w}\right) - k_c(k_1+k_2)\left\{1-\theta-\frac{1}{2\varepsilon}\right\}\hat{w}^2 \\
&+\hat{p}_1\hat{w}_f + k_c k_1\frac{\varepsilon}{2}\hat{w}_f^2 - \hat{p}_2\hat{w}_t + k_c k_2\frac{\varepsilon}{2}\hat{w}_t^2 \\
&+k_c z_1\left(\frac{1}{k_c}\hat{w}_r + k_3\left(\hat{P}_c(\hat{w}) - 2k_c(k_1+k_2)\hat{w}\right) + gz\right) \\
&-k_c z_2\left(\frac{1}{k_c}\hat{w}_r + k_3\left(\hat{P}_c(\hat{w}) - 2k_c(k_1+k_2)\hat{w}\right) + gz\right) \\
\leq\;& \hat{w}\left(\hat{P}_c(\hat{w}) - \theta k_c(k_1+k_2)\hat{w}\right) - k_c(k_1+k_2)\left\{1-\theta-\frac{1}{2\varepsilon}\right\}\hat{w}^2 \\
&+\left\{\hat{p}_1 + k_c k_1\frac{\varepsilon}{2}\hat{w}_f\right\}\hat{w}_f + \left\{-\hat{p}_2 + k_c k_2\frac{\varepsilon}{2}\hat{w}_t\right\}\hat{w}_t \\
&+k_c z_1\left(\frac{1}{k_c}\hat{w}_r + k_3\left(\hat{P}_c(\hat{w}) - 2k_c(k_1+k_2)\hat{w}\right) + gz\right) \\
&-k_c z_2\left(\frac{1}{k_c}\hat{w}_r + k_3\left(\hat{P}_c(\hat{w}) - 2k_c(k_1+k_2)\hat{w}\right) + gz\right)
\end{aligned} \tag{5.73}$$

Recall that k_c is chosen such that the first term in (5.73) is negative definite. For the next three terms to be negative definite, the following requirements must hold

$$1-\theta-\frac{1}{2\varepsilon} \;>\; 0 \tag{5.74}$$

$$\hat{p}_1 + k_c k_1\frac{\varepsilon}{2}\hat{w}_f\Big|_{\hat{w}_f=0} \;=\; 0 \tag{5.75}$$

$$\frac{\partial}{\partial \hat{w}_f}\left(\hat{p}_1 + k_c k_1\frac{\varepsilon}{2}\hat{w}_f\right) \;<\; 0 \tag{5.76}$$

$$-\hat{p}_2 + k_c k_2\frac{\varepsilon}{2}\hat{w}_t\Big|_{\hat{w}_t=0} \;=\; 0 \tag{5.77}$$

$$\frac{\partial}{\partial \hat{w}_t}\left(-\hat{p}_2 + k_c k_2\frac{\varepsilon}{2}\hat{w}_t\right) \;<\; 0 \tag{5.78}$$

[4]See Appendix A.5 for a formal definition

The first requirement holds if $\varepsilon > \frac{1}{2(1-\theta)}$. The second and fourth requirements obviously holds, because $\hat{p}_1$ is zero when $\hat{w}_f$ is zero, and $\hat{p}_2$ is zero when $\hat{w}_t$ is zero, due to the expressions for $\hat{w}_f$ and $\hat{w}_t$. The last two requirements can be written as

$$\frac{\partial \hat{p}_1}{\partial \hat{w}_f} < -k_c k_1 \frac{\varepsilon}{2} \tag{5.79}$$

$$\frac{\partial \hat{p}_2}{\partial \hat{w}_t} > k_c k_2 \frac{\varepsilon}{2} \tag{5.80}$$

Choosing $\varepsilon = 2$ transforms the requirements into

$$\theta < \frac{3}{4} \tag{5.81}$$

$$\frac{\partial \hat{w}_f}{\partial \hat{p}_1} < -\frac{1}{k_c k_1} \tag{5.82}$$

$$\frac{\partial \hat{w}_t}{\partial \hat{p}_2} > \frac{1}{k_c k_2} \tag{5.83}$$

Taking

$$\begin{aligned} \hat{w}_r &= k_c \left(-k_3 \left(\hat{P}_c(\hat{w}) - 2k_c(k_1 + k_2)\hat{w} \right) - gz \right) \\ &= -k_c k_3 \left(\hat{P}_c(\hat{w}) - k_c(k_1 + 3k_2)\hat{w} - \hat{p}_1 + \hat{p}_2 \right) \end{aligned} \tag{5.84}$$

and $\theta = \frac{1}{2}$ yields

$$\begin{aligned} \dot{V}_c \leq\ & \hat{w} \left(\hat{P}_c(\hat{w}) - \frac{1}{2} k_c(k_1 + k_2)\hat{w} \right) - \frac{1}{4} k_c(k_1 + k_2)\hat{w}^2 \\ & + \{\hat{p}_1 + k_c k_1 \hat{w}_f\}\, \hat{w}_f + \{-\hat{p}_2 + k_c k_2 \hat{w}_t\}\, \hat{w}_t \end{aligned} \tag{5.85}$$

Hence, the origin is asymptotically stable in the domain $D = \{\ [p_1\ p_2\ w]^T \in R^3 \mid p_1 < p_{upstream},\ p_2 > p_{01},\ P_c$ IS DEFINED$\}$ if the requirements are met. (Theorem 4.9, Khalil (2002)) We're defining this as semiglobally asymptotically stable. □

5.5 Finding a Stabilizing Input II

The backstepping procedure in the previous chapter resulted in a control law for the recycle system which is dependent on all the states. The law is also dependent on the compressor characteristic P_c, which is not very well known as discussed in previous chapters. Implementing this controller on a real system would be a difficult task. Motivated by this, our quest for a simpler controller continues.

The differential equations which must be stabilized are

$$\dot{\hat{w}} = k_3 \left(\hat{p}_1 + \hat{P}_c(\hat{w}) - \hat{p}_2 \right) \tag{5.86}$$

$$\dot{\hat{p}}_1 = k_1 \left(\hat{w}_f + \hat{w}_r - \hat{w} \right) \tag{5.87}$$

$$\dot{\hat{p}}_2 = k_2 \left(\hat{w} - \hat{w}_r - \hat{w}_t \right) \tag{5.88}$$

Theorem 5.2 *The control law*

$$\hat{w}_r = -k(\hat{p}_1 - \hat{p}_2) \tag{5.89}$$

where k is a positive tuning parameter, renders the origin of (5.86) - (5.88) *semiglobally exponentially stable.* ◇

Proof:

Step 1:

Using

$$\begin{bmatrix} \hat{p}_1 \\ \hat{p}_2 \end{bmatrix} = \phi(\hat{w}) = \begin{bmatrix} -k_c k_1 \hat{w} \\ -k_c k_2 \hat{w} \end{bmatrix}$$

as the input in the first equation, (5.86) becomes

$$\dot{\hat{w}} = k_3 \left(\hat{P}_c(\hat{w}) - k_c(k_1 - k_2)\hat{w} \right) \tag{5.90}$$

Using the Lyapunov function $V(\hat{w}) = \frac{1}{2k_3}\hat{w}^2$, its derivative is

$$\begin{aligned} \dot{V} &= \hat{w} \left(\hat{P}_c(\hat{w}) - k_c(k_1 - k_2)\hat{w} \right) \\ &= \hat{w} \left(\hat{P}_c(\hat{w}) - k_c(k_1 - k_2)\theta\hat{w} \right) - k_c(k_1 - k_2)(1-\theta)\hat{w}^2 \\ &\leq -k_c(k_1 - k_2)(1-\theta)\hat{w}^2 \end{aligned} \tag{5.91}$$

For some constant $0 < \theta < 1$. For (5.91) to hold, the following must hold

$$\hat{P}_c(\hat{w}) - k_c(k_1 - k_2)\theta\hat{w}\Big|_{\hat{w}=0} = 0 \tag{5.92}$$

$$\frac{\partial}{\partial\hat{w}}\left(\hat{P}_c(\hat{w}) - k_c(k_1 - k_2)\theta\hat{w}\right) < 0 \tag{5.93}$$

Obviously, (5.92) holds. (5.93) becomes

$$\frac{\partial\hat{P}_c}{\partial\hat{w}} < k_c(k_1 - k_2)\theta \tag{5.94}$$

Choosing k_c according to

$$k_c(k_1 - k_2)\theta > \sup_{\hat{w}}\left\{\frac{\partial\hat{P}_c}{\partial\hat{w}}\right\} \tag{5.95}$$

guarantees that (5.94), and thereby (5.91) holds. Observe that the sign of k_c is not determined at this point. It is dependent on which of k_1 and k_2 is the greatest, and will have the same sign as $(k_1 - k_2)$. Hence, the origin of $\dot{\hat{w}}$ is exponentially stable as long as P_c is defined.

Step 2:

The change of variables

$$z = \begin{bmatrix} \hat{p}_1 \\ \hat{p}_2 \end{bmatrix} - \phi(\hat{w}) = \begin{bmatrix} \hat{p}_1 + k_c k_1 \hat{w} \\ \hat{p}_2 + k_c k_2 \hat{w} \end{bmatrix}$$

transforms the system into

$$\dot{\hat{w}} = k_3\left(\hat{P}_c(\hat{w}) - k_c(k_1 - k_2)\hat{w}\right) + gz \tag{5.96}$$

$$\dot{z}_1 = k_1\left(\hat{w}_f + \hat{w}_r - \hat{w}\right) + k_c k_1\left(k_3\left(\hat{P}_c(\hat{w}) - k_c(k_1 - k_2)\hat{w}\right) + gz\right) \tag{5.97}$$

$$\dot{z}_2 = k_2\left(\hat{w} - \hat{w}_r - \hat{w}_t\right) + k_c k_2\left(k_3\left(\hat{P}_c(\hat{w}) - k_c(k_1 - k_2)\hat{w}\right) + gz\right) \tag{5.98}$$

where $g = [k_3 \; -k_3]$. As a composite Lyapunov function, V_c is taken as

$$V_c = \frac{1}{2}\begin{bmatrix} \hat{w} & z_1 & z_2 \end{bmatrix} \underbrace{\begin{bmatrix} \frac{1}{k_3} & -k_c & -k_c \\ -k_c & \frac{1}{k_1} & 0 \\ -k_c & 0 & \frac{1}{k_2} \end{bmatrix}}_{P} \begin{bmatrix} \hat{w} \\ z_1 \\ z_2 \end{bmatrix}$$

V_c is positive definite if the symmetric matrix P is positive definite. For P to be positive definite, all its leading principal minors must be positive. The leading principal minors are

$$\left|\frac{1}{k_3}\right|, \quad \begin{vmatrix} \frac{1}{k_3} & -k_c \\ -k_c & \frac{1}{k_1} \end{vmatrix}, \quad \begin{vmatrix} \frac{1}{k_3} & -k_c & -k_c \\ -k_c & \frac{1}{k_1} & 0 \\ -k_c & 0 & \frac{1}{k_2} \end{vmatrix}$$

So we have the following requirements for V_c to be positive definite

$$\frac{1}{k_3} > 0 \tag{5.99}$$

$$\frac{1}{k_1}\frac{1}{k_3} - k_c^2 > 0 \tag{5.100}$$

$$\frac{1}{k_1}\frac{1}{k_2}\frac{1}{k_3} - k_c^2\left(\frac{1}{k_1} + \frac{1}{k_2}\right) > 0 \tag{5.101}$$

The requirements result in a least upper bound for k_c, given as

$$k_c < \sqrt{\frac{1}{k_3(k_1 + k_2)}} \tag{5.102}$$

V_c can be written as

$$V_c = \frac{1}{2k_3}\hat{w}^2 + \frac{1}{2k_1}z_1^2 + \frac{1}{2k_2}z_2^2 - k_c z_1 \hat{w} - k_c z_2 \hat{w} \tag{5.103}$$

Its derivative along the trajectories of the system (5.96)-(5.98) is

$$\begin{aligned}
\dot{V}_c &= \hat{w}\left(\hat{P}_c(\hat{w}) - k_c(k_1-k_2)\hat{w}\right) + \frac{1}{k_3}\hat{w}gz \\
&\quad + z_1\left(\hat{w}_f + \hat{w}_r - \hat{w}\right) + k_c z_1\dot{\hat{w}} + z_2\left(\hat{w} - \hat{w}_r - \hat{w}_t\right) + k_c z_2\dot{\hat{w}} \\
&\quad - k_c\dot{z}_1\hat{w} - k_c\dot{z}_2\hat{w} - k_c z_1\dot{\hat{w}} - k_c z_2\dot{\hat{w}} \\
&= \hat{w}\left(\hat{P}_c(\hat{w}) - k_c(k_1-k_2)\hat{w}\right) \\
&\quad + z_1\left(\hat{w}_f + \hat{w}_r\right) + z_2\left(-\hat{w}_r - \hat{w}_t\right) - k_c\dot{z}_1\hat{w} - k_c\dot{z}_2\hat{w} \\
&= \hat{w}\left(\hat{P}_c(\hat{w}) - k_c(k_1-k_2)\hat{w}\right) \\
&\quad + \hat{p}_1\hat{w}_f - \hat{p}_2\hat{w}_t + k_c k_1\hat{w}\hat{w}_f - k_c k_2\hat{w}\hat{w}_t + \frac{1}{k_3}gz\hat{w}_r - k_c\dot{z}_1\hat{w} - k_c\dot{z}_2\hat{w} \\
&= \hat{w}\left(\hat{P}_c(\hat{w}) - k_c(k_1-k_2)\hat{w}\right) \\
&\quad + \hat{p}_1\hat{w}_f - \hat{p}_2\hat{w}_t + k_c k_1\hat{w}\hat{w}_f - k_c k_2\hat{w}\hat{w}_t + \frac{1}{k_3}gz\hat{w}_r \\
&\quad - k_c\left(k_1(\hat{w}_f + \hat{w}_r - \hat{w}) + k_c k_1\dot{\hat{w}}\right)\hat{w} - k_c\left(k_2(\hat{w} - \hat{w}_r - \hat{w}_t) + k_c k_2\dot{\hat{w}}\right)\hat{w} \\
&= \hat{w}\left(\hat{P}_c(\hat{w}) - k_c(k_1-k_2)\hat{w}\right) + \hat{p}_1\hat{w}_f - \hat{p}_2\hat{w}_t + \frac{1}{k_3}gz\hat{w}_r \\
&\quad - k_c k_1\left(\hat{w}_r - \hat{w} + k_c\dot{\hat{w}}\right)\hat{w} - k_c k_2\left(\hat{w} - \hat{w}_r + k_c\dot{\hat{w}}\right)\hat{w} \\
&= \hat{w}\left(\hat{P}_c(\hat{w}) - k_c(k_1-k_2)\hat{w}\right) \\
&\quad + \hat{p}_1\hat{w}_f - \hat{p}_2\hat{w}_t + \frac{1}{k_3}gz\hat{w}_r - k_c^2(k_1+k_2)k_3\hat{w}\left(\hat{P}_c(\hat{w}) - k_c(k_1-k_2)\hat{w}\right) \\
&\quad - k_c k_1\left(\hat{w}_r - \hat{w} + k_c gz\right)\hat{w} - k_c k_2\left(\hat{w} - \hat{w}_r + k_c gz\right)\hat{w} \\
&= \left\{1 - k_c^2(k_1+k_2)k_3\right\}\hat{w}\left(\hat{P}_c(\hat{w}) - k_c(k_1-k_2)\hat{w}\right) + \hat{p}_1\hat{w}_f - \hat{p}_2\hat{w}_t \\
&\quad + \frac{1}{k_3}gz\hat{w}_r - k_c k_1\left(\hat{w}_r - \hat{w} + k_c gz\right)\hat{w} - k_c k_2\left(\hat{w} - \hat{w}_r + k_c gz\right)\hat{w} \\
&= \left\{1 - k_c^2(k_1+k_2)k_3\right\}\hat{w}\left(\hat{P}_c(\hat{w}) - k_c(k_1-k_2)\hat{w}\right) + \hat{p}_1\hat{w}_f - \hat{p}_2\hat{w}_t \\
&\quad - k_c^2(k_1+k_2)gz\hat{w} + \frac{1}{k_3}gz\hat{w}_r - k_c k_1\left(\hat{w}_r - \hat{w}\right)\hat{w} - k_c k_2\left(\hat{w} - \hat{w}_r\right)\hat{w} \\
&= \left\{1 - k_c^2(k_1+k_2)k_3\right\}\hat{w}\left(\hat{P}_c(\hat{w}) - k_c(k_1-k_2)\hat{w}\right) + \hat{p}_1\hat{w}_f - \hat{p}_2\hat{w}_t \\
&\quad - k_c^2(k_1+k_2)gz\hat{w} + \frac{1}{k_3}gz\hat{w}_r - k_c(k_1-k_2)\hat{w}_r\hat{w} + k_c(k_1-k_2)\hat{w}^2 \\
&= \left\{1 - k_c^2(k_1+k_2)k_3\right\}\hat{w}\left(\hat{P}_c(\hat{w}) - k_c(k_1-k_2)\hat{w}\right) + \hat{p}_1\hat{w}_f - \hat{p}_2\hat{w}_t \\
&\quad - k_c^2(k_1+k_2)gz\hat{w} + \left(z_1 - z_2 - k_c(k_1-k_2)\hat{w}\right)\hat{w}_r + k_c(k_1-k_2)\hat{w}^2
\end{aligned} \tag{5.104}$$

$$\begin{aligned}
\dot{V}_c &= \left\{1 - k_c^2(k_1+k_2)k_3\right\}\hat{w}\left(\hat{P}_c(\hat{w}) - k_c(k_1-k_2)\hat{w}\right) + \hat{p}_1\hat{w}_f - \hat{p}_2\hat{w}_t \\
&\quad -k_c^2(k_1+k_2)k_3(\hat{p}_1-\hat{p}_2+k_c(k_1-k_2)\hat{w})\hat{w} + (z_1 - z_2 - k_c(k_1-k_2)\hat{w})\,\hat{w}_r \\
&\quad +k_c(k_1-k_2)\hat{w}^2 \\
&= \left\{1 - k_c^2(k_1+k_2)k_3\right\}\hat{w}\left(\hat{P}_c(\hat{w}) - k_c(k_1-k_2)\hat{w}\right) + \hat{p}_1\hat{w}_f - \hat{p}_2\hat{w}_t \\
&\quad -k_c^2(k_1+k_2)k_3(\hat{p}_1-\hat{p}_2)\hat{w} - k_c^2(k_1+k_2)k_3k_c(k_1-k_2)\hat{w}^2 \\
&\quad +(z_1 - z_2 - k_c(k_1-k_2)\hat{w})\,\hat{w}_r + k_c(k_1-k_2)\hat{w}^2 \qquad (5.105)
\end{aligned}$$

Taking

$$\hat{w}_r = -k\left(z_1 - z_2 - k_c(k_1-k_2)\hat{w}\right) \qquad (5.106)$$

yields

$$\begin{aligned}
\dot{V}_c &= \left\{1 - k_c^2(k_1+k_2)k_3\right\}\hat{w}\left(\hat{P}_c(\hat{w}) - k_c(k_1-k_2)\hat{w}\right) + \hat{p}_1\hat{w}_f - \hat{p}_2\hat{w}_t \\
&\quad -k_c^2(k_1+k_2)k_3(\hat{p}_1-\hat{p}_2)\hat{w} - k_c^2(k_1+k_2)k_3k_c(k_1-k_2)\hat{w}^2 \\
&\quad -k\left(z_1 - z_2 - k_c(k_1-k_2)\hat{w}\right)^2 + k_c(k_1-k_2)\hat{w}^2 \qquad (5.107)
\end{aligned}$$

We know that $\hat{w}\left(\hat{P}_c(\hat{w}) - k_c(k_1-k_2)\hat{w}\right)$ is negative definite with k_c proper set. That means that we can upper bound this term, locally.

$$\hat{w}\left(\hat{P}_c(\hat{w}) - k_c(k_1-k_2)\hat{w}\right) \leq -\delta\hat{w}^2 \qquad (5.108)$$

Since $\hat{P}_c$ only is defined for a given range of $\hat{w}$, we can always choose δ small enough such that (5.108) holds. $\dot{V}_c$ can now be upper bounded as

$$\begin{aligned}
\dot{V}_c &\leq -\left\{1 - k_c^2(k_1+k_2)k_3\right\}\delta\hat{w}^2 + \hat{p}_1\hat{w}_f - \hat{p}_2\hat{w}_t \\
&\quad -k_c^2(k_1+k_2)k_3(\hat{p}_1-\hat{p}_2)\hat{w} - k_c^2(k_1+k_2)k_3k_c(k_1-k_2)\hat{w}^2 \\
&\quad -k\left(z_1 - z_2 - k_c(k_1-k_2)\hat{w}\right)^2 + k_c(k_1-k_2)\hat{w}^2 \\
&\leq -\left\{(1 - k_c^2(k_1+k_2)k_3)\delta - k_c(k_1-k_2)\right\}\hat{w}^2 + \hat{p}_1\hat{w}_f - \hat{p}_2\hat{w}_t \\
&\quad -k_c^2(k_1+k_2)k_3(\hat{p}_1-\hat{p}_2)\hat{w} - k_c^2(k_1+k_2)k_3k_c(k_1-k_2)\hat{w}^2 \\
&\quad -k\left(z_1 - z_2 - k_c(k_1-k_2)\hat{w}\right)^2 \qquad (5.109)
\end{aligned}$$

Now comes the trick of letting $\hat{p}_1\hat{w}_f$ and $-\hat{p}_2\hat{w}_t$ take some of the "badness" away from the term $-k_c^2(k_1+k_2)k_3(\hat{p}_1-\hat{p}_2)\hat{w}$. By using Young's inequality,

$\dot{V}_c$ can be upper bounded as

$$\begin{aligned}\dot{V}_c &\leq -\left\{(1-k_c^2(k_1+k_2)k_3)\delta - k_c(k_1-k_2)\right\}\hat{w}^2 + \hat{p}_1\hat{w}_f - \hat{p}_2\hat{w}_t \\ &\quad +k_c^2(k_1+k_2)k_3\left\{\frac{1}{2\varepsilon}\hat{p}_1^2 + \frac{\varepsilon}{2}\hat{w}^2 + \frac{1}{2\varepsilon}\hat{p}_2^2 + \frac{\varepsilon}{2}\hat{w}^2\right\} \\ &\quad -k_c^2(k_1+k_2)k_3k_c(k_1-k_2)\hat{w}^2 - k\left(z_1 - z_2 - k_c(k_1-k_2)\hat{w}\right)^2\end{aligned} \tag{5.110}$$

Choosing $\varepsilon = k_c(k_1-k_2)$ yields

$$\begin{aligned}\dot{V}_c &\leq -\left\{(1-k_c^2(k_1+k_2)k_3)\delta - k_c(k_1-k_2)\right\}\hat{w}^2 + \hat{p}_1\hat{w}_f - \hat{p}_2\hat{w}_t \\ &\quad +k_c^2(k_1+k_2)k_3\left\{\frac{1}{2\varepsilon}\hat{p}_1^2 + \frac{1}{2\varepsilon}\hat{p}_2^2\right\} - k\left(z_1 - z_2 - k_c(k_1-k_2)\hat{w}\right)^2 \\ &\leq -\left\{(1-k_c^2(k_1+k_2)k_3)\delta - k_c(k_1-k_2)\right\}\hat{w}^2 + \hat{p}_1\hat{w}_f - \hat{p}_2\hat{w}_t \\ &\quad +\frac{k_c(k_1+k_2)k_3}{2(k_1-k_2)}\left\{\hat{p}_1^2 + \hat{p}_2^2\right\} - k\left(z_1 - z_2 - k_c(k_1-k_2)\hat{w}\right)^2 \\ &\leq -\left\{(1-k_c^2(k_1+k_2)k_3)\delta - k_c(k_1-k_2)\right\}\hat{w}^2 \\ &\quad +\hat{p}_1\left(\hat{w}_f + \frac{k_c(k_1+k_2)k_3}{2(k_1-k_2)}\hat{p}_1\right) + \hat{p}_2\left(-\hat{w}_t + \frac{k_c(k_1+k_2)k_3}{2(k_1-k_2)}\hat{p}_2\right) \\ &\quad -k\left(z_1 - z_2 - k_c(k_1-k_2)\hat{w}\right)^2\end{aligned} \tag{5.111}$$

Lets now investigate the terms in (5.111). The two terms in the middle are negative definite if

$$\hat{w}_f + k_e\hat{p}_1|_{\hat{p}_1=0} = 0 \tag{5.112}$$

$$-\hat{w}_t + k_e\hat{p}_2|_{\hat{p}_2=0} = 0 \tag{5.113}$$

$$\frac{\partial}{\partial\hat{p}_1}\left(\hat{w}_f + k_e\hat{p}_1\right) < 0 \tag{5.114}$$

$$\frac{\partial}{\partial\hat{p}_2}\left(-\hat{w}_t + k_e\hat{p}_2\right) < 0 \tag{5.115}$$

where $k_e = \frac{k_c(k_1+k_2)k_3}{2(k_1-k_2)}$. The two first requirements obviously holds, the latter two can be written as

$$\frac{\partial\hat{w}_f}{\partial\hat{p}_1} < -k_e \tag{5.116}$$

$$\frac{\partial\hat{w}_t}{\partial\hat{p}_2} > k_e \tag{5.117}$$

As long as the positive constant δ is chosen such that

$$(1 - k_c^2(k_1 + k_2)k_3)\delta > k_c(k_1 - k_2) \tag{5.118}$$

$\dot{V}_c$ is negative definite. The requirements stated above implies that

$$\hat{p}_1 \left(\hat{w}_f + \frac{k_c(k_1 + k_2)k_3}{2(k_1 - k_2)} \hat{p}_1 \right) < -\delta_1 \hat{p}_1^2 \tag{5.119}$$

$$\hat{p}_2 \left(-\hat{w}_t + \frac{k_c(k_1 + k_2)k_3}{2(k_1 - k_2)} \hat{p}_2 \right) < -\delta_2 \hat{p}_2^2 \tag{5.120}$$

As long as there is an upper and a lower bound for $\hat{p}_1$ and $\hat{p}_2$, δ_1 and δ_2 can always be chosen small enough such that (5.119) and (5.120) holds. $\dot{V}_c$ can now be upper bounded as

$$\begin{aligned} \dot{V}_c \leq & -\left\{ (1 - k_c^2(k_1 + k_2)k_3)\delta - k_c(k_1 - k_2) \right\} \hat{w}^2 \\ & -\delta_1 \hat{p}_1^2 - \delta_2 \hat{p}_2^2 - k \left(z_1 - z_2 - k_c(k_1 - k_2)\hat{w} \right)^2 \triangleq -W_c \end{aligned} \tag{5.121}$$

Hence, the feedback law

$$\hat{w}_r = -k \left(z_1 - z_2 - k_c(k_1 - k_2)\hat{w} \right) = -k(\hat{p}_1 - \hat{p}_2) \tag{5.122}$$

renders the the origin of the system (5.86)-(5.88) exponentially stable in the domain $D = \{ [p_1 \ p_2 \ w]^T \in R^3 \mid p_1 < p_{upstream}, \ p_{2,max} > p_2 > p_{01}, \ P_c \text{ IS DEFINED} \}$ if the requirements are met. (Theorem 4.10, Khalil (2002)) We're defining this as semiglobally exponentially stable. □

5.5.1 Verification by Simulation

Of course, the simple controller proven to be stable in the section above seems nearly too good to be true. To verify that the controller is working, a simulation is conducted. The simulation setup is as follows. The speed is set constant to 4000 rads/sec. At 2 seconds, the feed flow gradually decreases and the system enters deep surge. At 6 seconds the controller is enabled, and stabilizes the system in the unstable area. Correct values for the desired equilibrium points are inserted into the control law. All the files needed to conduct the verification is found in the ZIP-file at "control_law_verification".

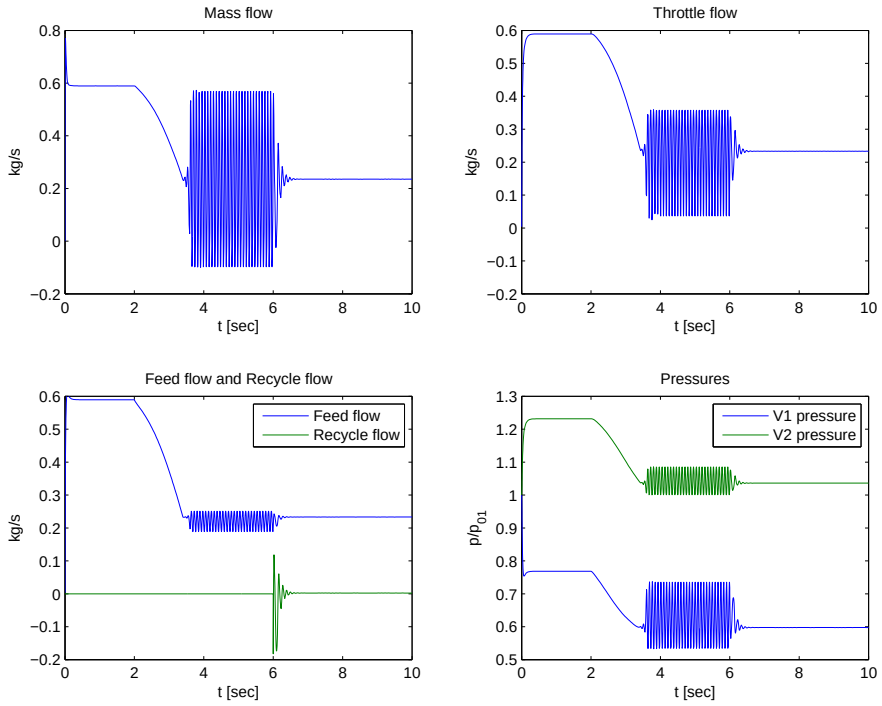

Figure 5.5: Verification of the stabilizing input by simulation. The speed is constant. Initially, the pressure in both volumes are set to ambient, and all the flows are zero.

One thing that is left out of the discussion is the question whether the recycle line has the capability of stabilizing the system in the way conducted above. First of all, we'll need some kind of actuation in the recycle line which actually can produce $\hat{w}_r = -k(\hat{p}_1 - \hat{p}_2)$. It can be difficult with an ordinary recycle valve, since it only can produce flow in one direction. Figure 5.5 reveals that the flow through the recycle line fluctuates around zero to stabilize the system.

5.6 Finding a Stabilizing Input III

Motivated by the inability of recycle valves to produce negative flow, another step of the backstepping procedure is attempted. The extended system is now investigated, given as

$$\dot{\hat{p}}_1 = k_1 (\hat{w}_f + \hat{w}_r - \hat{w}) \tag{5.123}$$

$$\dot{\hat{p}}_2 = k_2 (\hat{w} - \hat{w}_r - \hat{w}_t) \tag{5.124}$$

$$\dot{\hat{w}} = k_3 \left(\hat{p}_1 + \hat{P}_c(w) - \hat{p}_2 \right) \tag{5.125}$$

$$\dot{\hat{w}}_r = k_r \left(\hat{p}_2 - \hat{P}_r - \hat{p}_1 \right) \tag{5.126}$$

where the inclusion of the last equation makes it possible to obtain an expression for the pressure drop over the recycle valve, $\hat{P}_r$.

Theorem 5.3 *The control law*

$$\hat{P}_r = -(k_1 + k_2)\hat{w} - k_1\hat{w}_f + k_2\hat{w}_t - (k_1 + k_2)k_r(\hat{p}_1 - \hat{p}_2) + k'(\hat{w}_r - k_r(\hat{p}_1 - \hat{p}_2)) \tag{5.127}$$

where k' is a positive tuning parameter, renders the origin of (5.123) - (5.126) *semiglobally exponentially stable.* ◇

Proof:

We're continuing the backstepping procedure of the previous chapter. Assume that the positive constant of the feedback law is k_r, that is

$$\hat{w}_r = -k_r (z_1 - z_2 - k_c(k_1 - k_2)\hat{w}) = \phi(z, \hat{w}) \tag{5.128}$$

Step 3:

The change of variables

$$x = \hat{w}_r - \phi(z, \hat{w}) = \hat{w}_r + k_r (z_1 - z_2 - k_c(k_1 - k_2)\hat{w})$$

transforms the system into

$$\begin{aligned}
\dot{\hat{w}} &= k_3\left(\hat{P}_c(\hat{w}) - k_c(k_1-k_2)\hat{w}\right) + gz && (5.129)\\
\dot{z} &= f(z,\hat{w}) + g_2 x && (5.130)\\
\dot{x} &= \dot{\hat{w}}_r + k_r(\dot{z}_1 - \dot{z}_2 - k_c(k_1-k_2)\dot{\hat{w}}) && (5.131)
\end{aligned}$$

where $g_2 = [k_1 \ -k_2]$ and

$$f(z,\hat{w}) = \begin{bmatrix} k_1\left(\hat{w}_f - k_r\left(z_1 - z_2 - k_c(k_1-k_2)\hat{w}\right) - \hat{w}\right) \\ +k_c k_1\left(k_3\left(\hat{P}_c(\hat{w}) - k_c(k_1-k_2)\hat{w}\right) + gz\right) \\ \\ k_2\left(\hat{w} + k_r\left(z_1 - z_2 - k_c(k_1-k_2)\hat{w}\right) - \hat{w}_t\right) \\ +k_c k_2\left(k_3\left(\hat{P}_c(\hat{w}) - k_c(k_1-k_2)\hat{w}\right) + gz\right) \end{bmatrix}$$

The total composite Lyapunov function is taken as

$$V_{c,tot} = V_c + \frac{1}{2k_r}x^2 \qquad (5.132)$$

Its derivative can be upper bounded as

$$\begin{aligned}
\dot{V}_{c,tot} &\leq -W_c + xz_1 - xz_2 - k_c k_1 x\hat{w} + k_c k_2 x\hat{w} + \frac{1}{k_r}x\dot{x}\\
&\leq -W_c + xz_1 - xz_2 - k_c k_1 x\hat{w} + k_c k_2 x\hat{w}\\
&\quad +x\left(\hat{p}_2 - \hat{P}_r - \hat{p}_1\right) + x\left(\dot{z}_1 - \dot{z}_2 - k_c(k_1-k_2)\dot{\hat{w}}\right)\\
&\leq -W_c + xz_1 - xz_2 - k_c k_1 x\hat{w} + k_c k_2 x\hat{w}\\
&\quad +x\left(z_2 - k_c k_2\hat{w} - \hat{P}_r - z_1 + k_c k_1\hat{w}\right) + x\left(\dot{z}_1 - \dot{z}_2 - k_c(k_1-k_2)\dot{\hat{w}}\right)\\
&\leq -W_c - x\hat{P}_r + x\left(\dot{z}_1 - \dot{z}_2 - k_c(k_1-k_2)\dot{\hat{w}}\right)\\
&\leq -W_c + x\left(k_1\left(\hat{w}_f - k_r\left(z_1 - z_2 - k_c(k_1-k_2)\hat{w}\right) - \hat{w}\right)\right.\\
&\quad \left.-k_2\left(\hat{w} + k_r\left(z_1 - z_2 - k_c(k_1-k_2)\hat{w}\right) - \hat{w}_t\right) - \hat{P}_r\right)\\
&\leq -W_c + x\left(k_1\left(\hat{w}_f - k_r\left(\hat{p}_1 - \hat{p}_2\right) - \hat{w}\right)\right.\\
&\quad \left.-k_2\left(\hat{w} + k_r\left(\hat{p}_1 - \hat{p}_2\right) - \hat{w}_t\right) - \hat{P}_r\right) \qquad (5.133)
\end{aligned}$$

Taking

$$\hat{P}_r = k_1\left[\hat{w}_f - k_r(\hat{p}_1 - \hat{p}_2) - \hat{w}\right] - k_2\left[\hat{w} + k_r(\hat{p}_1 - \hat{p}_2) - \hat{w}_t\right] + k'x \qquad (5.134)$$

yields

$$\dot{V}_{c,tot} \leq -W_c - k'x^2 \tag{5.135}$$

Hence, the origin is exponentially stable in $D = \{\ [p_1\ p_2\ w]^T \in R^3 \mid p_1 < p_{upstream},\ p_{2,max} > p_2 > p_{01},\ P_c$ IS DEFINED$\}$. (Theorem 4.10, Khalil (2002)) We're defining this as semiglobally exponentially stable. □

Chapter 6

Final Discussion

This chapter provides a final discussion of the results obtained in this thesis. The cubic bivariate spline approximation is discussed first, followed by a discussion of the recycle system and the new SIMULINK model. At last, the new variant of the recycle system model and the analysis are discussed.

6.1 The Cubic Bivariate Spline as the Characteristic

The cubic bivariate spline approximation demonstrated to-the-point accuracy with regards to measurement points. Modeling the compressor characteristic with it would result in a more correct simulation than any other approximation method. Methods which uses a third order polynomial fit or a variant of it, fails to capture the exact location of the measurement points, which can be critical when determining when the system reaches instability. The bivariate spline characteristic is very complex. It transforms the compressor map into a grid, where each cell has its own third order approximation. Because of this, any mathematical stability analysis would be very difficult. The bivariate spline characteristic would be most valuable during simulations, when e.g. the surge control line should be determined, or controllers should be verified. It would allow for more correct decisions about stabilizing inputs. However, most mathematical analysis concerning compressor control uses the Moore-Greitzer approximation of the characteristic. It would be an idea to tune those results during simulations with the more advanced bivariate spline characteristic. The chapter concerning the bivariate spline approximation is

very practical with its MATLAB code, and there's a reason for it. It has been developed first and foremost for simulation purposes.

6.2 The Recycle System

Initially in the model of the recycle system, the feed flow is set to constant. It would mean that the feed flow is not dependent on the compressor, and would make the pressure in the suction volume misbehave. The recycle model is extended with a valve at the feed flow intake to overcome this problem.¨The new model in SIMULINK of the recycle system seems to be working very well (Appendix C.3). It uses the bivariate spline as the compressor characteristic, and can simulate different speeds of the compressor. Different controllers can easily be tested on the model. Not only can controllers for the recycle valve be tested, but also torque-controllers, throttle valve controllers, and feed flow controllers can be tested. The simplicity of modifying the cubic bivariate spline to fit another compressor type makes it possible to simulate a lot of recycle systems.

The typical recycle valve controller outlined in Chapter 4 worked as expected. When the mass flow gets too low, the recycle valve opens and stimulates more mass flow. The controller parameters will have to be rather powerfully tuned to deal with sudden disturbances. The surge line is often determined with considerable margin. 10 to 20 percent is not unusual. Lesser margin means more powerful controllers, to ensure that the operating point not slides over into the surge area.

6.3 The Stability Analysis

Analysis of the model which uses the compressor ratio Ψ_c as the compressor characteristic in its mass flow equation proved to be very difficult. The appendix contains a whole chapter with these incomplete stability proofs. Instead, modeling the mass flow equation with the pressure rise P_c as the characteristic, gave many valuable results concerning stability. This is how Greitzer done it, in Greitzer (1976). It is well known that the recycle system is stable with regards to surge, independent of anything, as long as the operating point of the compressor is located on a negative slope of the characteristic. The first goal of the stability analysis was to prove just this, with Lyapunov's method. The result is summed up in a lemma which states

that the recycle system is asymptotically stable, independent on the recycle valve setting, as long we're operating on a negative slope of the characteristic. Thats why there is no need to recycle right of the surge line. The importance of the compressor characteristic once again appears.

The second goal of the stability analysis was to find a stabilizing input for the recycle system. This is where the recycle system is evaluated in the active surge/stall control scheme. The possibility of stabilizing the unstable regime left to the surge line with the recycle line is investigated. With a clever variant of backstepping, three control laws are found which semiglobally stabilizes the system. The first and the second control law is an expression for the recycle flow $\hat{w}_r$. They'll both be difficult to implement, since the actuation in the recycle line almost always is a valve. A valve placed in the recycle line will just be able to let the flow travel from the high pressure volume to the low. Active surge/stall stabilization with the recycle line involves flow in both directions. The choice of actuation in the recycle line to achieve this remains an open question. However, the second control law is pretty simple, given as

$$\hat{w}_r = -k(\hat{p}_1 - \hat{p}_2) \tag{6.1}$$

The equation almost resembles the equation most frequently used to model a valve, the equation for flow through an orifice. It could be possible to use such a special valve which we can model as the control law. The third control law is an expression for the pressure drop over the recycle valve, $\hat{P}_r$. It could have been the easiest implementable of the three, hadn't it been for the long expression and the dependency on all the states.

Semiglobal asymptotic stability is proven for the recycle system with the use of the first control law. For the two others, semiglobal exponential stability was proven. That the result is semiglobal, and not global, simply means that we have some restrictions on the states. The mass flow will have to be in the set where the compressor characteristic is defined, and pressure can't be negative. There is also upper bounds on the pressure states at times.

There should also be noted that the recycle system and its various models presented in this thesis not is suitable for feedback linearization. This is due to the fact that the system is not feedback linearizable.

Chapter 7

Conclusion

The main focus of this thesis has been to conduct research about the compressor recycle system. It is old, and has been in use for decades in the industry, but it has actually not been proven to be stable mathematically. The goal of this thesis has been to find out if there exists clever control laws for the recycle system, through a thorough mathematical analysis.

7.1 Concluding Remarks

There has been considerable research into the active surge/stall control scheme over the last years. Several control laws which stabilizes the unstable regime left to the surge line have been proposed. Some of them uses the drive torque as input, some uses a close coupled valve, and some of them uses the throttle. Still, recycle systems are used in the industry. Recycle systems are trusted and have been working for many decades, and companies are not willing to risk safety and durability for something they do not trust yet. It is well known that active surge/stall control schemes outperformes surge/stall avoidance schemes with regards to efficiency.

This thesis shows that its possible to use the recycle line as an active surge/stall control actuation device. Two of the control laws derived may need another form for actuation in the line, due to the two-way flow. The replacement for the valve is yet to be determined. The third law is a control law for the pressure drop over the recycle valve. The simplest law were simulated, and it stabilized an unstable operating point.

The main conclusions of this thesis can be summarized as:

- Modeling the compressor characteristic with the cubic bivariate spline approximation yields more correct simulation results. It will allow for real measurements to be embedded into the model, two-dimensionally. It is also a fast performer with SIMULINK, with regards to all the information it holds.

- Modeling the recycle system with the pressure rise as the characteristic in the mass flow equation was critical with regards to successful mathematical analysis of the system.

- Three control laws was derived. The simplest one of them semiglobally exponentially stabilizes the recycle system at all operating points, both stable and unstable. The use of such a law, compared to the classic use of the recycle line, would yield a drastic improvement of the efficiency of the system.

7.2 Contributions Provided by This Thesis

To the author's knowledge a cubic bivariate spline approximation has never been used as the compressor characteristic, at least not in such a practical way. There's one paper concerning splines (Drummond and Davison, 2009), but not a cubic bivariate one.

The previously modeled recycle model by Egeland and Gravdahl (2002) has been extended with a valve at the entrance of the feed flow, to make the feed flow dependent on the compressor. The recycle model is then modeled in another way, with the mass flow equation dependent on the compressor pressure rise, instead of the ratio.

To the author's knowledge, nobody has ever conducted a successful stability analysis of the recycle system. Four results are presented in this paper. The first is that the recycle system is asymptotically stable independent of recycle flow as long as the operating point is located on a negative slope of the characteristic. The next three results are different stabilizing control laws, which in theory will allow the recycle system to operate in the active surge/stall control scheme.

7.3 Suggestions for Further Work

- Investigation of the importance of the length of the recycle line, the area, the type of duct, and the actuation device in it for use with active surge/stall control.
- "Domain control." Define a domain around the equilibrium point which extends to the surge line. The idea is that a controller can be found which guarantees that the operating point stays in this domain. It is a new and more efficient surge/stall avoidance method.

Bibliography

Badmus, O. O., Nett, C. N., and Schork, F. J. (1991). An integrated, full-range surge control/rotating stall avoidance compressor control system. In *American Control Conference*, pages 3173–3180.

Bøhagen, B. (2007). *Active surge control of centrifugal compression systems.* PhD thesis, NTNU.

Bøhagen, B. and Gravdahl, J. T. (2005). Active control of compression systems using drive torque; a backstepping approach. In *Proceedings of the 44th IEEE Conference on Decision and Control, and the European Control Conference 2005.*

Botros, K. K. and Henderson, J. F. (1994). Developments in centrifugal compressor surge control-a technology assessment. In *Journal of turbomachinery 116*, pages 240–249.

de Boor, C. (2010). Spline toolbox user's guide. *For Use with Matlab, Version*, 3.

Drummond, C. and Davison, C. R. (2009). Improved compressor maps using approximate solutions to the moore greitzer model. In *Proceedings of ASME Turbo Expo.*

Egeland, O. and Gravdahl, J. T. (2002). *Modeling and Simulation for Automatic Control.* Tapir Trykkeri, Trondheim, Norway.

Fink, D. A., Cumpsty, N. A., and Greitzer, E. M. (1992). Surge dynamics in a free-spool centrifugal compressor system. In *Journal of Turbomachinery.*

Gravdahl, J. T. and Egeland, O. (1999). *Compressor Surge and Rotating Stall: Modeling and Control.* London: Springer Verlag.

Greitzer, E. M. (1976). Surge and rotating stall in axial flow compressors, part 1: Theoretical compression system model. In *Journal of Engineering for Power.*

Gu, G., Sparks, A., and Banda, S. S. (1999). An overview of rotating stall and surge control for axial flow compressors. In *IEEE Transactions on Control Systems Technology*, volume 7, pages 639–647.

Hansen, K. E., Jørgensen, P., and Larsen, P. S. (1981). Experimental and theoretical study of surge in a small centrifugal compressor. In *Journal of Fluids Engineering.*

Khalil, H. K. (2002). *Nonlinear Systems.* Prentice Hall, third edition.

Koff, S. G. (1983). Stalled flow characteristics for axial compressors. Master's thesis, Massachusetts Institute of Technology, Department of Mechanical Engineering.

Koff, S. G. and Greitzer, E. M. (1984). Stalled flow performance for axial compressors, part 1: Axisymmetric characteristics. *ASME Paper No. 84-GT-93*.

Krstic, M. and Kokotovic, P. V. (1995). Lean backstepping design for a jet engine compressor model. In *Proceedings of the 4th IEEE Conference on Control Applications*, pages 1047–1052.

Lüdtke, K. H. (2004). *Process centrifugal compressors: basics, function, operation, design, application*. Springer Verlag.

Moore, F. K. and Greitzer, E. M. (1986). A theory of post-stall transients in a axial compressor system, part 1: Development of equations. In *Journal of Engineering for Gas Turbines and Power*.

Nisenfeld, A. E. (1982). *Centrifugal Compressors*. Research Triangle Park, N.C. : Instrument Society of America.

Staroselsky, N. and Ladin, L. (1979). Improved surge control for centrifugal compressors. *Chemical engineering*, pages 175–184.

White, F. M. (2008). *Fluid Mechanics*. McGraw-Hill, sixth edition.

Willems, F., Heemels, M., de Jager, B., and Stoorvogel, A. (1999). Positive feedback stabilization of compressor surge. In *Conference on Decision & Control*.

Appendix A

Mathematical Review

A.1 Derivation of Incompressible Flow Through an Orifice

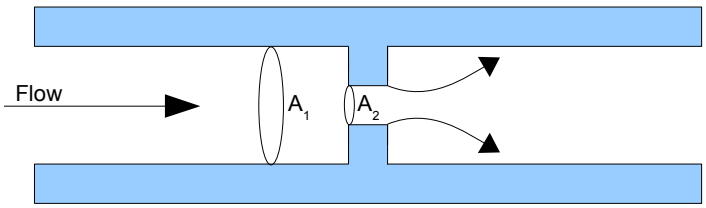

Figure A.1.1: Flow through an orifice

By assuming incompressible flow through the orifice, the continuity equation yields

$$v_1 A_1 = v_2 A_2 = q \tag{A.1}$$

That is, the volumetric flow is constant. By further assuming stationary and frictionless (inviscid) flow, the Bernoulli equation (2.2) yields

$$\frac{v_1^2}{2} + \frac{p_1}{\rho} = \frac{v_2^2}{2} + \frac{p_2}{\rho} \tag{A.2}$$

From (A.1) we have $v_1 = \frac{q}{A_1}$ and $v_2 = \frac{q}{A_2}$. (A.2) becomes

$$\begin{aligned} \frac{q^2}{2A_1^2} + \frac{p_1}{\rho} &= \frac{q^2}{2A_2^2} + \frac{p_2}{\rho} \\ \Rightarrow q &= A_2 \sqrt{\frac{2}{\rho} \frac{(p_1 - p_2)}{(1 - (A_2/A_1)^2)}} \\ \Rightarrow q &= A_2 \sqrt{\frac{1}{1 - (d_2/d_1)^4}} \sqrt{\frac{2}{\rho}(p_1 - p_2)} \end{aligned} \tag{A.3}$$

Introducing the coefficient of discharge C_d in $C = C_d \sqrt{\frac{1}{1-(d_2/d_1)^4}}$, (A.3) becomes

$$q = C A_2 \sqrt{\frac{2}{\rho}(p_1 - p_2)} \tag{A.4}$$

Equating (A.4) with the density to get the mass flow

$$w = \rho q = C A_2 \sqrt{2\rho (p_1 - p_2)} \tag{A.5}$$

A.2 Derivation of Compressible Nozzle Flow

Consider the nozzle in figure A.2.1.

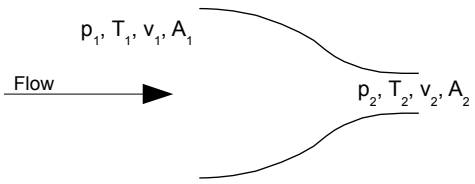

Figure A.2.1: Nozzle flow

Lets now assume the gas to be ideal. That is, ignoring intermolecular forces and the size of the molecules. Generally, real gases behave like an ideal gas at high temperatures and low pressures. The flow through the nozzle is

$$w = \rho_2 v_2 A_2 = \rho_2 M_2 a_2 A_2 = \rho_2 M_2 \sqrt{\kappa R T_2} A_2 = \frac{p_2 M_2 A_2 \kappa}{\sqrt{\kappa R T_2}} \tag{A.6}$$

where $M = \frac{v}{a}$ is the mach number, a is the speed of sound and for an ideal gas we have $a = \sqrt{\kappa RT}$ (eq. 9.16 in White (2008)) and $\rho = \frac{p}{RT}$. The heat capacity ratio $\kappa = \frac{c_p}{c_v}$ of a gas is the ratio of the heat capacity c_p at constant pressure to the heat capacity c_v at constant volume. Lets further assume that the flow is isentropic, that is, there is no losses due to heat conduction or viscosity. The following relation can be used (equation 9.28a in White (2008))

$$\frac{p_1}{p_2} = \frac{T_1}{T_2}^{\frac{\kappa}{\kappa-1}} \tag{A.7}$$

Rewriting (A.6) as

$$\begin{aligned}
w &= \frac{p_1}{\frac{T_1}{T_2}^{\frac{\kappa}{\kappa-1}}} \frac{M_2 A_2 \kappa}{\sqrt{\kappa R T_2}} \\
\Rightarrow w &= \frac{p_1}{\frac{T_1}{T_2}^{\frac{\kappa}{\kappa-1}}} \frac{M_2 A_2 \kappa}{\sqrt{\kappa R T_2}} \sqrt{\frac{T_1}{T_1}} \\
\Rightarrow w &= \frac{p_1}{\frac{T_1}{T_2}^{\frac{\kappa}{\kappa-1}}} \frac{M_2 A_2 \kappa}{\sqrt{\kappa R T_1}} \sqrt{\frac{T_1}{T_2}} \\
\Rightarrow w &= \frac{p_1 M_2 A_2 \kappa}{\sqrt{\kappa R T_1}} \frac{\left(\frac{T_1}{T_2}\right)^{\frac{1}{2}}}{\left(\frac{T_1}{T_2}\right)^{\frac{\kappa}{\kappa-1}}} \\
\Rightarrow w &= \frac{p_1 M_2 A_2 \kappa}{\sqrt{\kappa R T_1}} \left(\frac{T_1}{T_2}\right)^{\frac{-\kappa-1}{2(\kappa-1)}}
\end{aligned} \tag{A.8}$$

Using (A.7) again in (A.8) yields

$$\begin{aligned}
w &= \frac{p_1 M_2 A_2 \kappa}{\sqrt{\kappa R T_1}} \left(\frac{p_1}{p_2}\right)^{\left(\frac{\kappa-1}{\kappa}\right)\left(\frac{-\kappa-1}{2(\kappa-1)}\right)} = \frac{p_1 M_2 A_2 \kappa}{\sqrt{\kappa R T_1}} \left(\frac{p_1}{p_2}\right)^{\frac{-(\kappa+1)}{2\kappa}} \\
\Rightarrow\ & w = \frac{A_2 p_1}{\sqrt{\kappa R T_1}} \kappa \left(\frac{p_2}{p_1}\right)^{\frac{\kappa+1}{2\kappa}} M_2
\end{aligned} \tag{A.9}$$

An expression for the mach number at the throat can be found from the energy balance. The energy balance in its general form is taken from White (2008) equation 3.63, which is

$$\dot{Q} - \dot{W}_s - \dot{W}_v = \frac{d}{dt}\left[\iiint_{CV} \left(\hat{u} + \frac{1}{2}V^2 + gz\right) \rho dV\right] + \iint_{CS} \left(\hat{h} + \frac{1}{2}V^2 + gz\right) \rho(\vec{V} \cdot \vec{n}) dA \tag{A.10}$$

With no heat transfer, no work done by the system and stationary conditions, (A.10) becomes

$$\begin{aligned} \iint_{CS} \left(\hat{h} + \frac{1}{2}V^2 + gz\right) \rho(\vec{V} \cdot \vec{n}) dA &= 0 \\ \Rightarrow -(\hat{h}_1 + \frac{1}{2}v_1^2)\rho_1 v_1 A_1 + (\hat{h}_2 + \frac{1}{2}v_2^2)\rho_2 v_2 A_2 &= 0 \end{aligned} \tag{A.11}$$

From the continuity equation we have that the mass flow is $w = \rho_1 v_1 A_1 = \rho_2 v_2 A_2$. (A.11) becomes

$$\hat{h}_1 + \frac{1}{2}v_1^2 = \hat{h}_2 + \frac{1}{2}v_2^2 \tag{A.12}$$

Assuming that the speed v_1 is close to zero, and using that $\hat{h} = c_p T$ where c_p is the specific heat at constant pressure, (A.12) becomes

$$\begin{aligned} c_p T_1 &= c_p T_2 + \frac{1}{2}v_2^2 \\ \Rightarrow c_p T_1 &= c_p T_2 + \frac{1}{2}M_2^2 a_2^2 \\ \Rightarrow c_p T_1 &= c_p T_2 + \frac{1}{2}M_2^2 \kappa R T_2 \\ \Rightarrow T_1 &= T_2 + \frac{1}{2}M_2^2 \kappa \frac{R}{c_p} T_2 \end{aligned} \tag{A.13}$$

Equation 9.4 in White (2008) gives $\frac{R}{c_p} = \frac{\kappa - 1}{\kappa}$. (A.13) becomes

$$\begin{aligned} T_1 &= T_2 + \frac{1}{2}M_2^2 \kappa \frac{\kappa - 1}{\kappa} T_2 \\ \Rightarrow T_1 &= T_2 \left(1 + M_2^2 \frac{\kappa - 1}{2}\right) \\ \Rightarrow \frac{T_1}{T_2} &= 1 + M_2^2 \frac{\kappa - 1}{2} \\ \Rightarrow M_2^2 &= \left(\frac{T_1}{T_2} - 1\right) \frac{2}{\kappa - 1} \\ \Rightarrow M_2 &= \sqrt{\frac{2}{\kappa - 1}\left(\left(\frac{p_1}{p_2}\right)^{\frac{\kappa - 1}{\kappa}} - 1\right)} \end{aligned} \tag{A.14}$$

Insertion of (A.14) into (A.9) yields

$$\begin{aligned}
w &= \frac{A_2 p_1}{\sqrt{\kappa R T_1}} \kappa \left(\frac{p_2}{p_1}\right)^{\frac{\kappa+1}{2\kappa}} \sqrt{\frac{2}{\kappa-1}\left(\left(\frac{p_1}{p_2}\right)^{\frac{\kappa-1}{\kappa}} - 1\right)} \\
\Rightarrow w &= \frac{A_2 p_1}{\sqrt{R T_1}} \sqrt{\frac{2\kappa}{\kappa-1}\left(\frac{p_2}{p_1}\right)^{\frac{\kappa+1}{\kappa}}\left(\left(\frac{p_1}{p_2}\right)^{\frac{\kappa-1}{\kappa}} - 1\right)} \\
\Rightarrow w &= \frac{A_2 p_1}{\sqrt{R T_1}} \sqrt{\frac{2\kappa}{\kappa-1}\left(\frac{p_2}{p_1}\right)^{\frac{\kappa+1}{\kappa}}\left(\left(\frac{p_2}{p_1}\right)^{-\frac{\kappa-1}{\kappa}} - 1\right)} \\
\Rightarrow w &= \frac{A_2 p_1}{\sqrt{R T_1}} \sqrt{\frac{2\kappa}{\kappa-1}\frac{\left(\frac{p_2}{p_1}\right)^{\frac{\kappa+1}{\kappa}}}{\left(\frac{p_2}{p_1}\right)^{\frac{\kappa-1}{\kappa}}}\left(\left(\frac{p_2}{p_1}\right)^{-\frac{\kappa-1}{\kappa}} - 1\right)\left(\frac{p_2}{p_1}\right)^{\frac{\kappa-1}{\kappa}}} \\
\Rightarrow w &= \frac{A_2 p_1}{\sqrt{R T_1}} \sqrt{\frac{2\kappa}{\kappa-1}\left(\frac{p_2}{p_1}\right)^{\frac{2}{\kappa}}\left(1 - \left(\frac{p_2}{p_1}\right)^{\frac{\kappa-1}{\kappa}}\right)}
\end{aligned} \tag{A.15}$$

which is the expression for isentropic nozzle flow of an ideal gas.

A.3 Sector Terminology

Consider the function h. It belongs to sector $[0, \infty]$ if

$$u^T h(t, u) \geq 0 \tag{A.16}$$

for all (t, u). For the scalar case, the graph of the $u - h$ relation must lie in the first and third quadrants. The graphical representation is valid even when h is time varying. Zero and infinity are the slopes of the boundaries of the first-third quadrant region, hence sector $[0, \infty]$.

In case the inequality (A.16) is strict, we write the sector as $(0, \infty)$. Similarly, we say that h belongs to the sector $[-\infty, 0]$ if

$$u^T h(t, u) \leq 0 \tag{A.17}$$

for all(t, u). For the scalar case, the graph of the $u-h$ relation must lie in the second and fourth quadrants, where $-\infty$ and 0 are the slopes of the boundaries of the second-fourth quadrant region. In case the inequality (A.17) is strict, we write the sector as $(-\infty, 0)$.

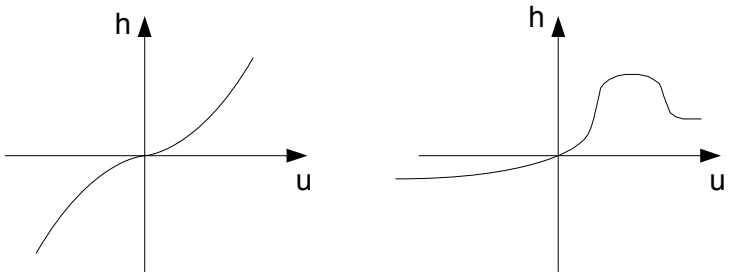

Figure A.3.1: Two examples of $u - h$ characteristics in which h belongs to the sector $[0, \infty]$

A.4 Strict-Feedback Systems

Consider a system on the form

$$\begin{aligned}
\dot{x} &= f_0(x) + g_0(x)z_1 \\
\dot{z}_1 &= f_1(x, z_1) + g_1(x, z_1)z_2 \\
\dot{z}_2 &= f_2(x, z_1, z_2) + g_2(x, z_1, z_2)z_3 \\
&\vdots \\
\dot{z}_{k-1} &= f_{k-1}(x, z_1, \ldots, z_{k-1}) + g_{k-1}(x, z_1, \ldots, z_{k-1})z_k \\
\dot{z}_k &= f_k(x, z_1, \ldots, z_k) + g_k(x, z_1, \ldots, z_k)u
\end{aligned}$$

where $x \in R^n$, z_1 to z_k are scalars, and f_0 to f_k vanish at the origin. It is called a *strict-feedback* system because the nonlinearities f_i and g_i in the $\dot{z}_i$-equation $(i = 1, \ldots, k)$ depend only on $x, z_1, \ldots, z_i$; that is, on the state variables that are "fed back."

A.5 Young's Inequality

Young's inequality states that for any real numbers a and b,

$$\pm ab \leq \frac{a^2}{2\varepsilon} + \frac{\varepsilon b^2}{2} \tag{A.18}$$

for any $\varepsilon > 0$.

Appendix B

MATLAB Files

B.1 Spline Approximation

B.1.1 approximation_spline.m

```
%% COMPRESSOR CHARACTERISTIC APPROXIMATION
%%
%% MATLAB file which generates a bivariate spline.  This spline is stored
%% in the file "psic_data" in the current directory and can be accessed by the
%% command "pp = load('psic_data')".
%% From this spline the value of the compressor characteristic can be returned
%% for all speeds and massflows.
%%
%% AUTHOR: Bjørn Ove Barstad



% STEP 1 - collect points from the compressor map
x_corrected = {};
y = {};

%points for the speedline 20000 rpm
x_corrected(1) = {[10 20 30 40]};
y(1) = {[1.175 1.185 1.18 1.13]};

%points for the speedline 25000 rpm
```

```
22 x_corrected(2) = {[10 20 30 40 50 60]};
23 y(2) = {[1.275 1.30 1.305 1.285 1.245 1.15]};
24
25 %points for the speedline 30000 rpm
26 x_corrected(3) = {[20 30 40 50 60]};
27 y(3) = {[1.435 1.45 1.445 1.42 1.365]};
28
29 %points for the speedline 35000 rpm
30 x_corrected(4) = {[20 30 40 50 60 70]};
31 y(4) = {[1.58 1.617 1.625 1.617 1.57 1.48]};
32
33 %points for the speedline 40000 rpm
34 x_corrected(5) = {[30 40 50 60 70]};
35 y(5) = {[1.81 1.83 1.825 1.8 1.733]};
36
37 %points for the speedline 45000 rpm
38 x_corrected(6) = {[40 50 60 70 80]};
39 y(6) = {[2.09 2.095 2.09 2.06 1.93]};
40
41 %points for the speedline 50000 rpm
42 x_corrected(7) = {[50 60 70 80]};
43 y(7) = {[2.385 2.4 2.335 2.17]};
44
45 %plot
46 X_CORRECTED = [];
47 Y = [];
48 for i = 1 : length(x_corrected)
49     for j = 1 : length(x_corrected{i})
50         X_CORRECTED = [X_CORRECTED x_corrected{i}(j)];
51         Y = [Y y{i}(j)];
52     end
53 end
54 scrsz = get(0,'ScreenSize');
55 figure(1)
56 set(1,'Position',[(scrsz(3)/2 - 466/2) (scrsz(4)/2 - 411/2)
       466 411]);
57 plot(X_CORRECTED, Y,'+'),grid,axis([-10 90 1.0 2.4])
58 xlabel('Corrected mass flow lb/min')
59 ylabel('Pressure ratio')
60
61
62
63 % STEP 2 - augment the points with zero flow - and negative
       flow points
64
65 %kappa = c_p / c_v, air
66 kappa = 1.4;
67 %sonic velocity
68 c_plenum = 343;
```

```
%ambient temperature 30 deg C
T_01 = 303.15;
%inducer diameter
D1 = 0.079;
%impeller perimeter diameter
D2 = 0.113;

%speedvector
N = [20000 25000 30000 35000 40000 45000 50000]; %RPM

%zero flow pressure ratio
PSI_czero = [];
for i = 1 : length(N)
    PSI_czero = [PSI_czero (1 + (pi^2* (N(i)/60)^2 *(D2^2 - D1
        ^2))/(2*c_plenum*T_01))^(kappa/(kappa - 1))];
end

%negative flow pressure ratio
PSI_cneg = [1.19 1.30 1.45 1.55 1.70 1.90 2.12];

%augment
for i = 1 : length(x_corrected)
    x_corrected(i) = {[-10 0 x_corrected{i}]};
    y(i) = {[PSI_cneg(i) PSI_czero(i) y{i}]};
end

%generate new points to plot
X_CORRECTED = [];
Y = [];
for i = 1 : length(x_corrected)
    for j = 1 : length(x_corrected{i})
        X_CORRECTED = [X_CORRECTED x_corrected{i}(j)];
        Y = [Y y{i}(j)];
    end
end



% STEP 3 - cubic bivariate spline interpolation and
    extrapolation based on tensor product splines

%generate a cubic spline in ppform for each speedline
PP = [];
for i = 1 : length(x_corrected)
    PP = [PP spline(x_corrected{i}, y{i})];
end

%prepare grid {w, omega} = {massflow, speed}
w = -10 : 10 : 100;
```

```
116 omega = 20000 : 5000 : 50000;
117
118 %construct the z-matrix z(i,j) = f( w(i) , omega(j) ) ( =
       PSI_c )
119 %from the one-dim splines
120 z = [];
121 for i = 1 : length(omega)
122     for j = 1 : length(w)
123         z(j,i) = fnval(PP(i), w(j));
124     end
125 end
126
127 %cubic bivariate spline in ppform generation
128 pp = csape({w, omega}, z,{'clamped', 'clamped'});
129
130 %gather lines to draw
131 w = -10 : 1 : 80;
132 clear PP
133 PP = [];
134 for i = 1 : length(N)
135     PP = [PP fnval(pp, {w, N(i)})];
136 end
137 PP(:,8) = fnval(pp, {w, 29500});
138
139 %plot points and approximated speedlines
140 scrsz = get(0,'ScreenSize');
141 figure(2)
142 set(2,'Position',[(scrsz(3)/2 - 466/2) (scrsz(4)/2 - 411/2)
       466 411]);
143 plot(X_CORRECTED, Y,'+', w, PP(:,1), w, PP(:,2), w, PP(:,3), w
       , PP(:,4), w, PP(:,5), w, PP(:,6), w, PP(:,7)),grid,axis
       ([-10 90 1.0 2.4])
144 xlabel('Corrected mass flow lb/min')
145 ylabel('Pressure ratio')
146
147
148
149 % STEP 4 - save the only data needed, pp, in a file
150 save('psic_data','-struct','pp');
151 clear all
```

B.1.2 getPsic.m

```
function [ pcic ] = getPsic( w_correctedlbmin, omega_rpm )
%   getPsic Returns the compressor characteristic for
    different mass flows and
%   speeds.
%
%   Author: Bjørn Ove Barstad

persistent pp;
if isempty(pp)
    'loading psic_data'
    pp = load('psic_data');
end

pcic = fnval(pp, {w_correctedlbmin, omega_rpm});

if pcic < 1
    pcic = 1;
end
```

B.2 Init Files

B.2.1 init_vortech_plain.m

```
clear all

%speed of sound in plenum and volume
a_p = 343; %m/s
V_p = 0.1; %m^3

%duct area and length
d_duct = 0.07; %70 mm
A = pi/4 * d_duct^2; %0.0038 m^2
L = 2.85; %m

%ambient pressure and temperature
p_01 = 101325; %Pascals
T_01 = 20; %Celcius

%density air, 20 deg C
rho_AIR = 1.204; %kg/m^3
% %density air, 30 deg C
% rho_AIR = 1.164;

%energy transfer coeff
mu = 0.99;

%impeller inertia
J = 5e-4; %kg m^2

%impeller perimeter radius
D2 = 0.119;
r_2 = D2 / 2;

%orifice opening
A_t = A;

%conversion factors
T_01_rankine = (T_01 +  273.15) * 9/5;
p_01_hg = p_01 / 3375;
si_to_corrected = sqrt(T_01_rankine/545) / (p_01_hg/28.4) *
    60/0.4536;
rads_to_rpm = 60/(2*pi);

%sgn(p1 - p2) = lim(zeta -> inf) tanh(zeta(p1 - p2))
zeta = 1000;
```

B.2.2 init_vortech_recon.m

```
clear all

%speed of sound in plenum and volume
a_p = 343; %m/s
V_2 = 0.1; %m^3 (original plenum)
V_1 = 0.05;

%duct area and length
d_duct = 0.07; %70 mm
A = pi/4 * d_duct^2; %0.0038 m^2
L = 2.85; %m

%ambient pressure and temperature
p_01 = 101325; %Pascals
T_01 = 20; %Celcius

%density air, 20 deg C
rho_AIR = 1.204; %kg/m^3
% %density air, 30 deg C
% rho_AIR = 1.164;

%energy transfer coeff
mu = 0.99;

%impeller inertia
J = 5e-4; %kg m^2

%impeller perimeter radius
D2 = 0.119;
r_2 = D2 / 2;

%orifice opening
A_t = A;

%conversion factors
T_01_rankine = (T_01 +  273.15) * 9/5;
p_01_hg = p_01 / 3375;
si_to_corrected = sqrt(T_01_rankine/545) / (p_01_hg/28.4) *
    60/0.4536;
rads_to_rpm = 60/(2*pi);

%sgn(p1 - p2) = lim(zeta -> inf) tanh(zeta(p1 - p2))
zeta = 1000;

%loading surge control line
```

```
45 load('scl.mat');
46
47 %RECYCLE PI-controller settings
48 Kp_recycle = 2.5;
49 Ki_recycle = 5.5;
```

B.3 Defining the Surge Line; define_scl.m

```
% DEFINES THE SURGE AVOIDANCE LINE
%
% Author: Bjørn Ove Barstad

%surge margin
surge_margin = .3;

%define the speedlines
speedvector = 20000 : 5000 : 50000;

%obtain the bivariate cubic spline
%which contains all the data for
%the compressor characteristic
pp = load('psic_data');

%generate the speedlines
y = [];
w = -10 : 80;
for i = 1 : length(speedvector)
    y(i,:) = fnval(pp, {w, speedvector(i)});
end

%directional derivative of the bivariate
%cubic spline in the mass flow direction
dp = fndir(pp, [1; 0]);

%find maximum algorithm
MAX = zeros(2, length(speedvector));
for i = 1 : length(speedvector)
    max = -inf;
    for j = 1 : length(w)
        deriv = fnval(dp, {w(j), speedvector(i)});
        if abs(deriv) < 1e-4 %derivative ¬ zero
            if max == -inf
                max = [w(j); fnval(pp, {w(j), speedvector(i)})
                    ];
            else
                try_max = [w(j); fnval(pp, {w(j), speedvector(
                    i)})];
                if try_max(2) > max(2)
                    max = try_max;
                end
            end
        end
    end
```

```
44      MAX(:,i) = max;
45  end
46
47  %makes the surge line defined by MAX linear
48  PF_surge = polyfit(MAX(1,:), MAX(2,:), 1);
49  save('sl','PF_surge');
50  y_surgeline = PF_surge(1).*w + PF_surge(2);
51
52  %along with the surge avoidance line
53  PF_avoid = polyfit(MAX(1,:).*(1 + surge_margin), MAX(2,:), 1);
54  save('scl','PF_avoid');
55  y_avoid = PF_avoid(1).*w + PF_avoid(2);
56
57  %draw
58  scrsz = get(0,'ScreenSize');
59  figure(2)
60  set(2,'Position',[(scrsz(3)/2 - 466/2) (scrsz(4)/2 - 411/2)
        466 411]);
61  plot(w, y_surgeline, w, y_avoid, MAX(1,:), MAX(2,:), w, y(1,:)
        , w, y(2,:), w, y(3,:), w, y(4,:), w, y(5,:), w, y(6,:), w
        , y(7,:)),grid,axis([-10 90 1.0 2.4])
62  xlabel('Corrected mass flow lb/min')
63  ylabel('Pressure ratio')
```

Appendix C

SIMULINK Diagrams

C.1 model_plain.mdl

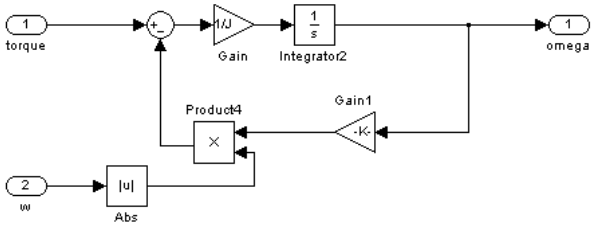

Figure C.1.1: Subsystem: Drive

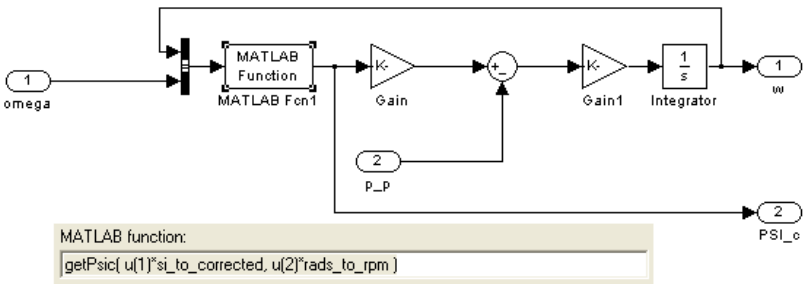

Figure C.1.2: Subsystem: Compressor and duct

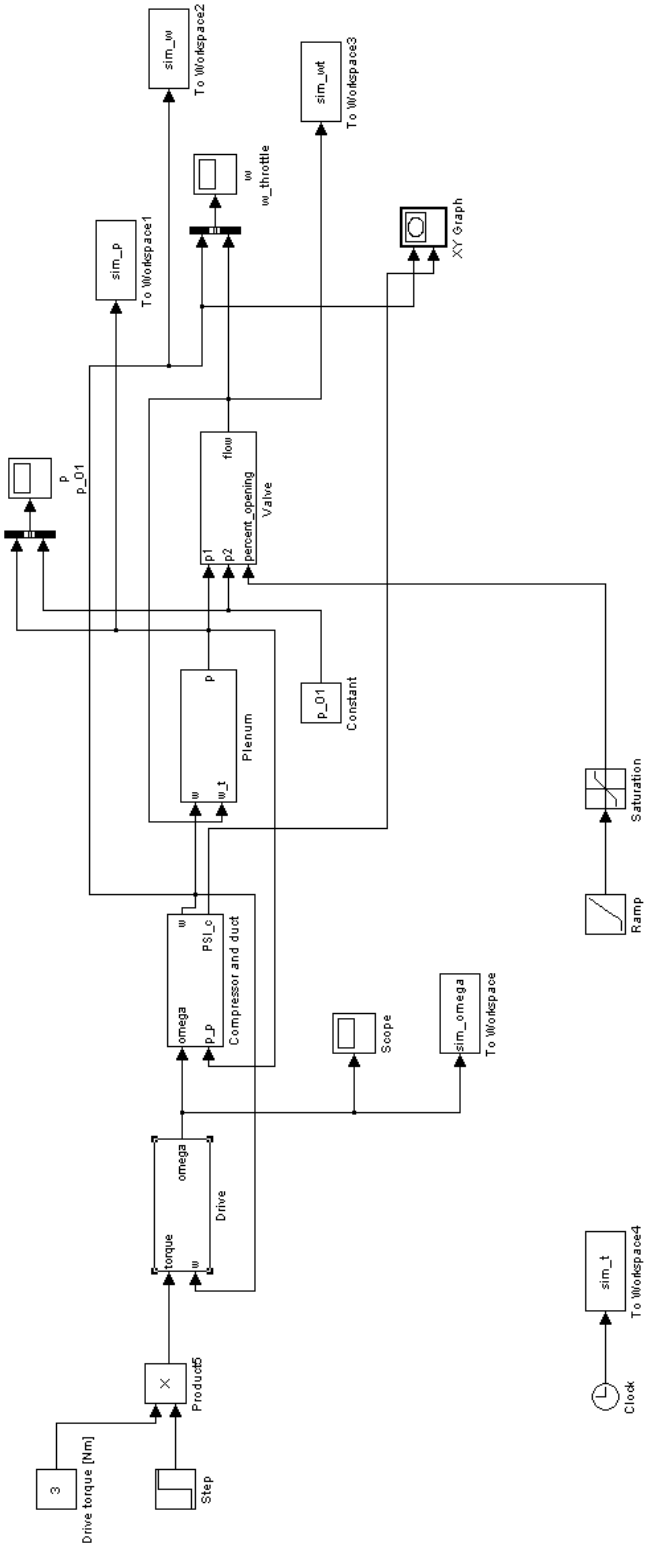

Figure C.1.3: Main model

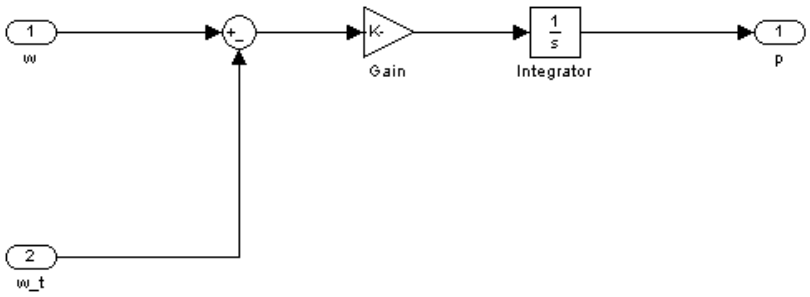

Figure C.1.4: Subsystem: Plenum

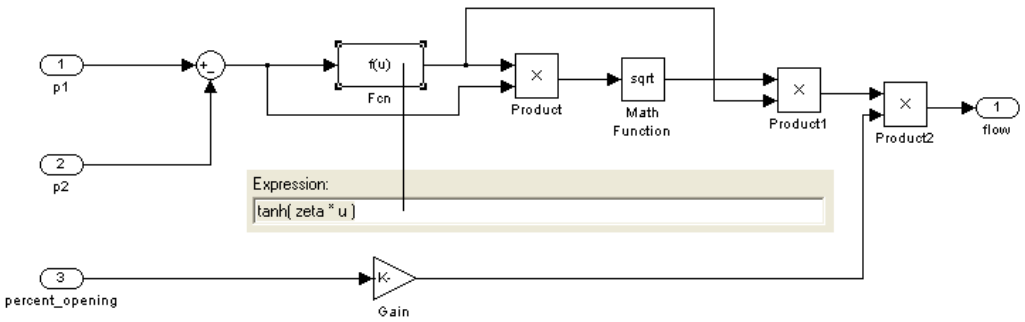

Figure C.1.5: Subsystem: Valve

C.2 model_recycle.mdl

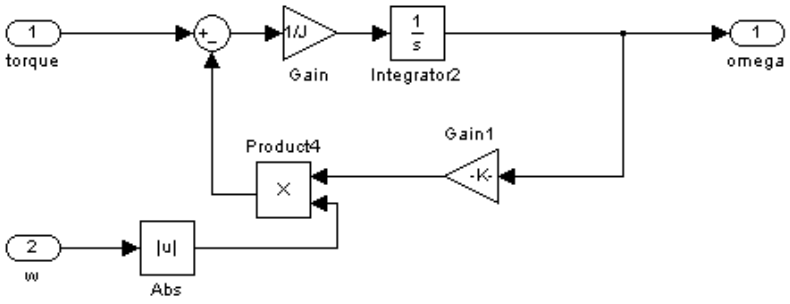

Figure C.2.1: Subsystem: Drive

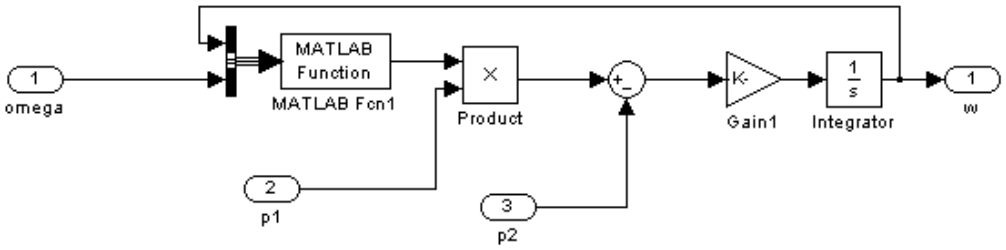

Figure C.2.2: Subsystem: Compressor and duct

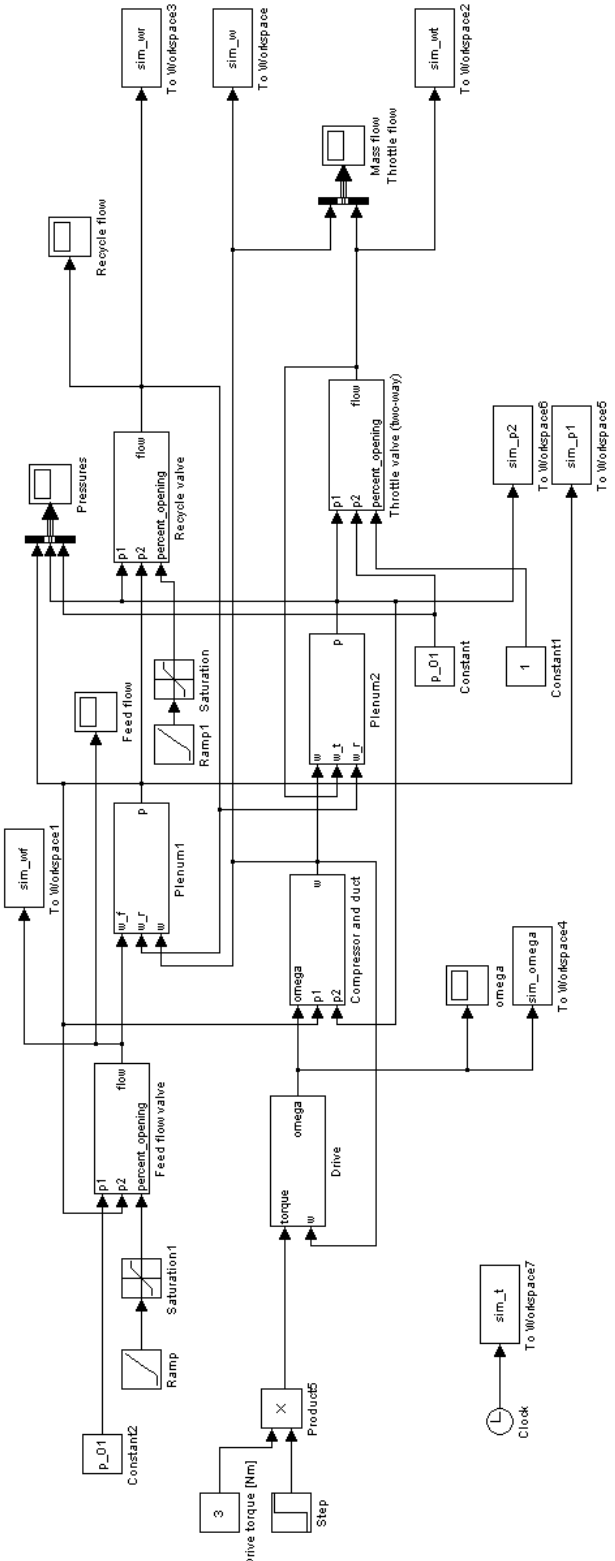

Figure C.2.3: Main model

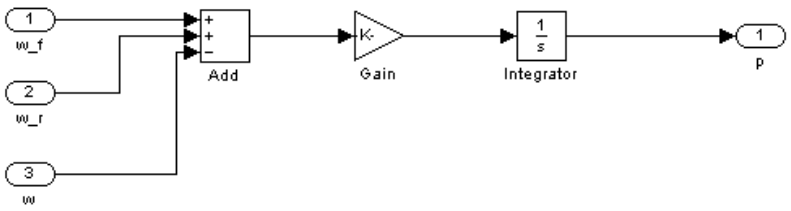

Figure C.2.4: Subsystem: Plenum1

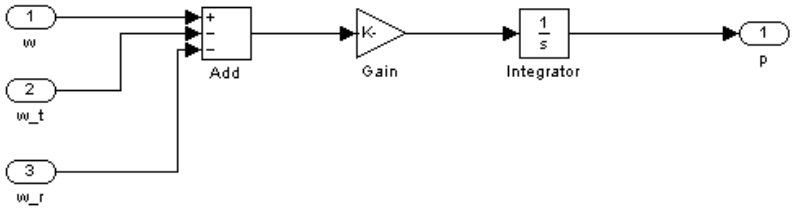

Figure C.2.5: Subsystem: Plenum2

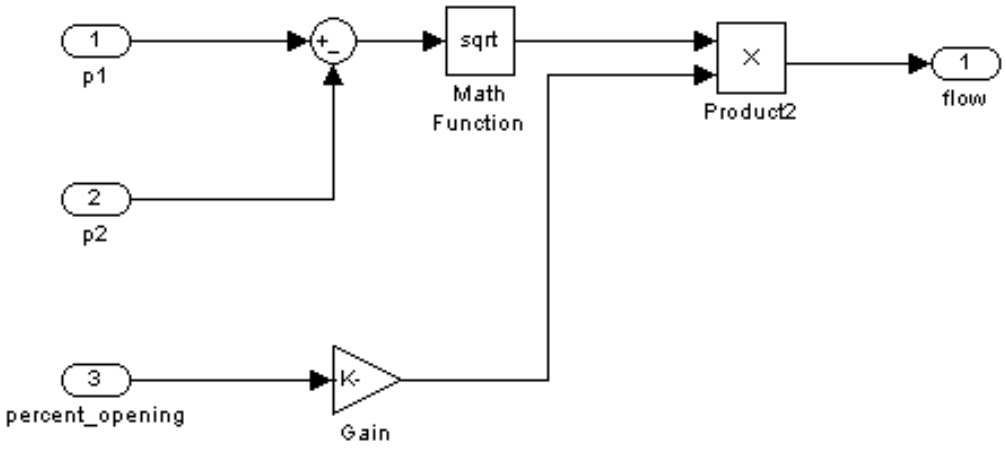

Figure C.2.6: Subsystem: Feed flow valve

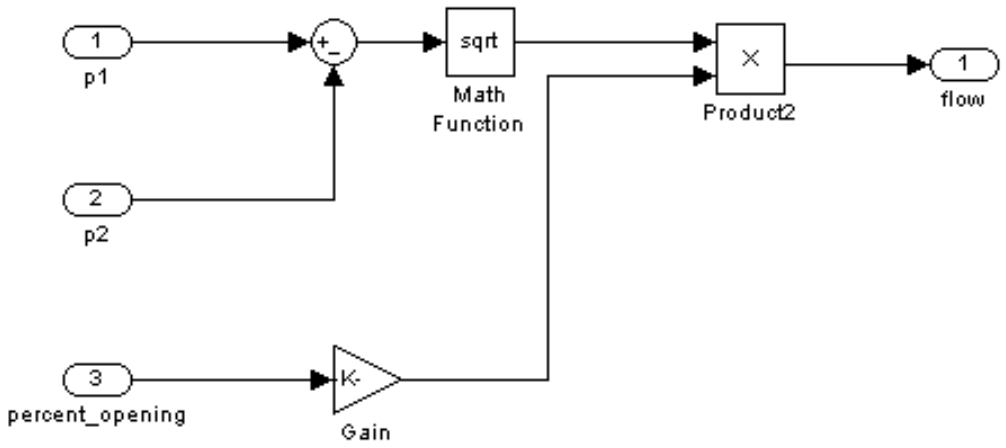

Figure C.2.7: Subsystem: Recycle valve

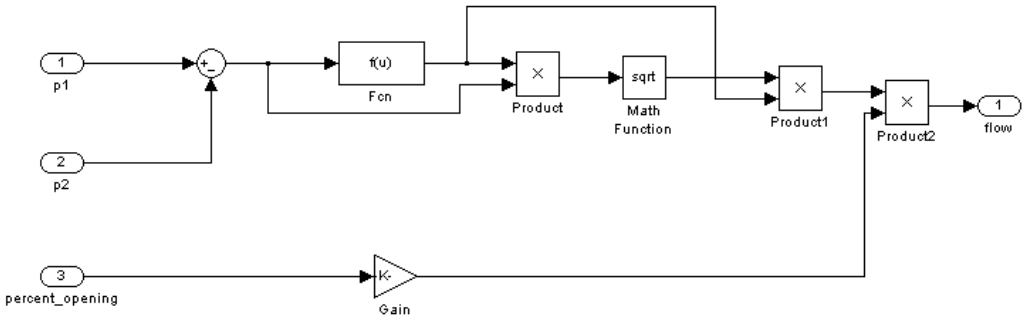

Figure C.2.8: Subsystem: Throttle valve

C.3 model_recycle_control.mdl

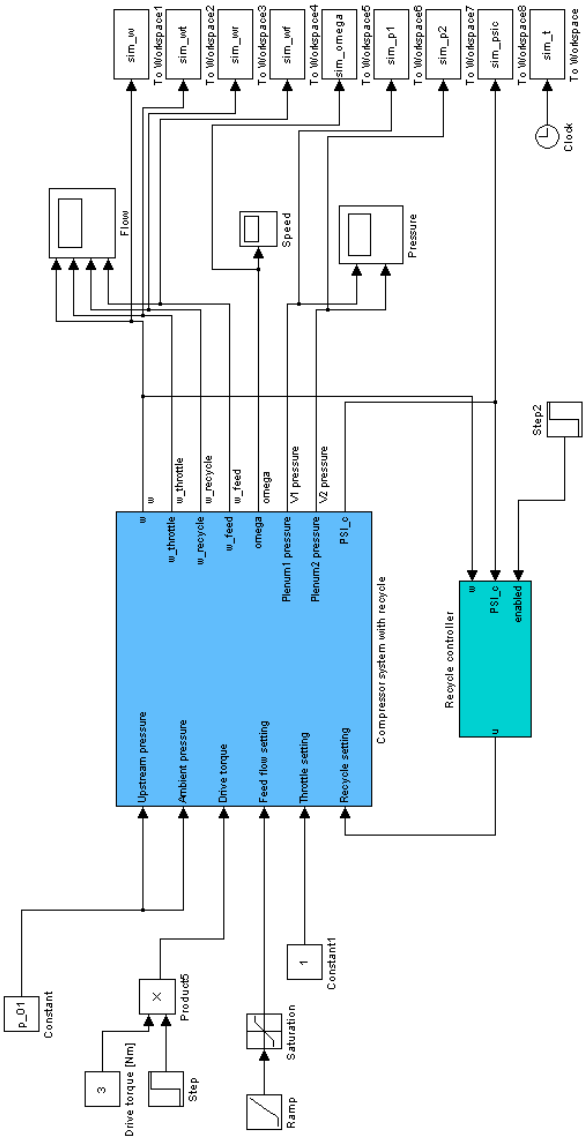

Figure C.3.1: Main model

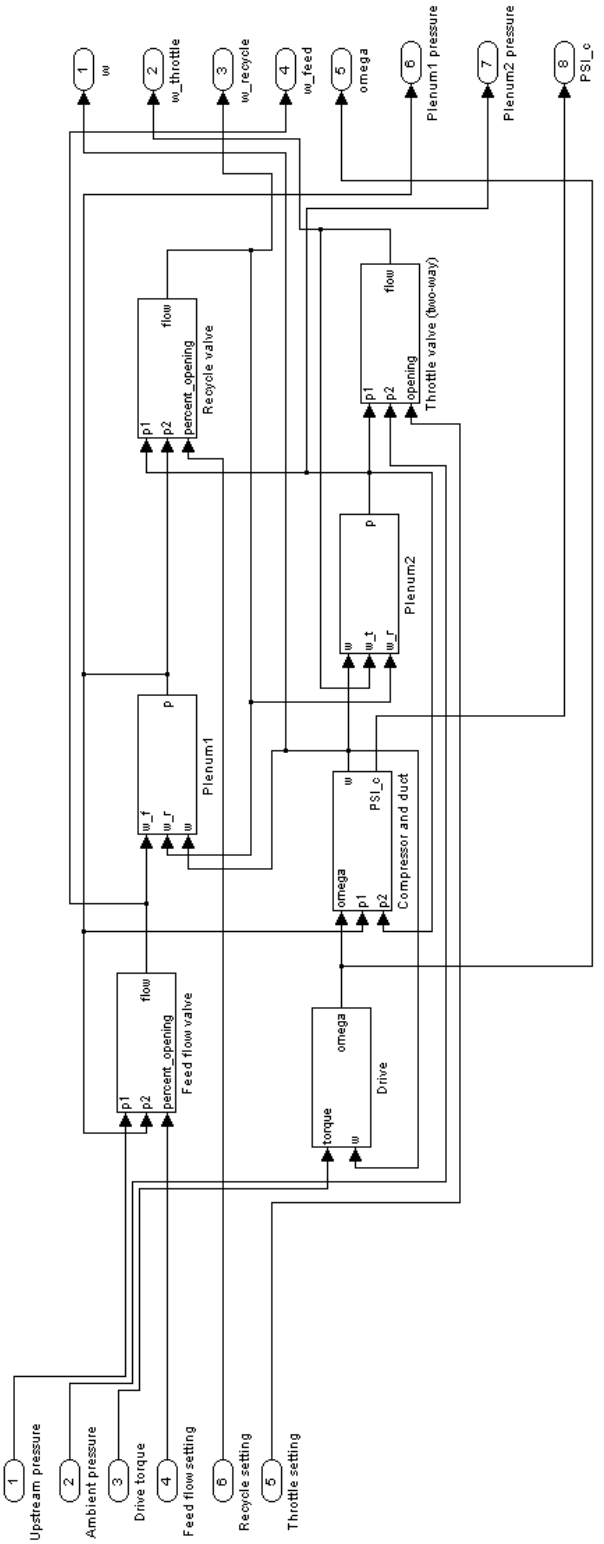

Figure C.3.2: Subsystem: Compressor system with recycle. Within this diagram, all the subsystems are the same as in C.2.

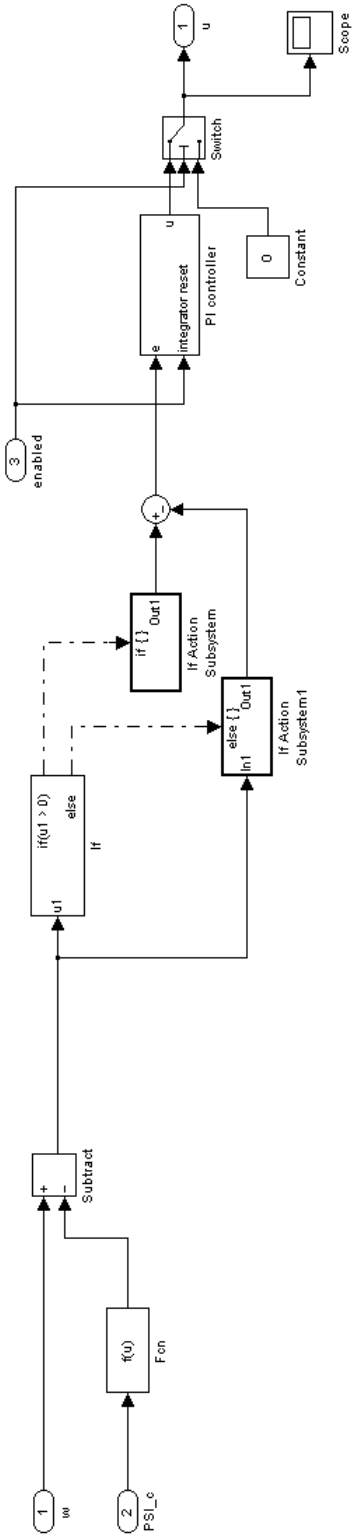

Figure C.3.3: Subsystem: Recycle controller

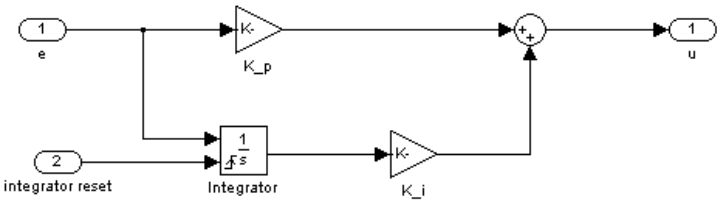

Figure C.3.4: Subsystem: Recycle controller; Subsystem: PI controller

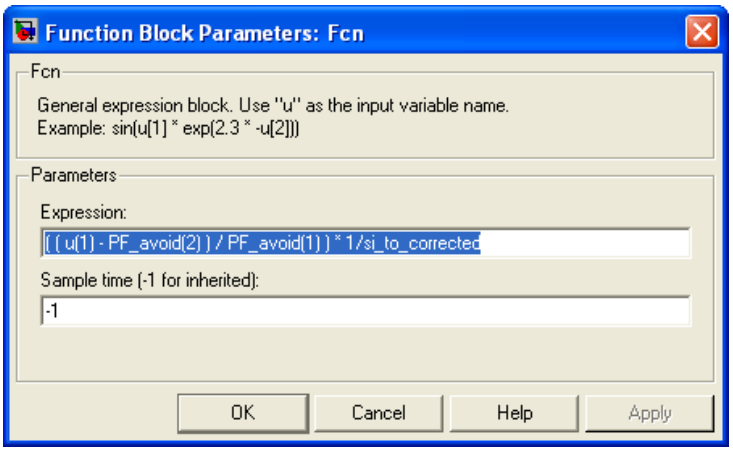

Figure C.3.5: Subsystem: Recycle controller; Fcn

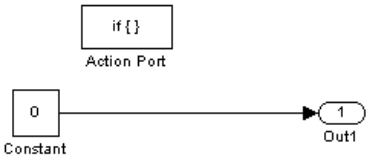

Figure C.3.6: Subsystem: Recycle controller; If Action Subsystem

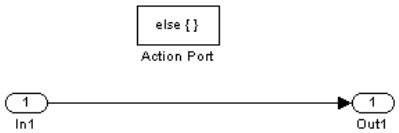

Figure C.3.7: Subsystem: Recycle controller; If Action Subsystem1

Appendix D

Incomplete Stability Proofs of the Recycle System

D.1 Foreword

This appendix contains multiple attempts in proving that the recycle system is stable. They have one thing in common, all the attempts have been conducted with the use of the compressor ratio Ψ_c as the compressor characteristic. The model where the flow through the throttle, the flow through the recycle line, and the flow through the entrance to the suction volume are modeled as $w = const \cdot \sqrt{\Delta p}$ have been used. The same assumptions as in Section 5.2 is also used here.

D.2 The System

The system we're trying to prove stability for is

$$\dot{p}_1 = \frac{a^2}{V_1}(w_f + w_r - w) \tag{D.1}$$

$$\dot{p}_2 = \frac{a^2}{V_2}(w - w_t - w_r) \tag{D.2}$$

$$\dot{w} = \frac{A}{L}(\Psi_c(w, \omega)\, p_1 - p_2) \tag{D.3}$$

where the last equation is modeled in pressure ratio form. The valves are

modeled as

$$w_t = c_t\sqrt{p_2 - p_{01}} \tag{D.4}$$
$$w_f = c_f\sqrt{p_{upstream} - p_1} \tag{D.5}$$
$$w_r = c_r\sqrt{p_2 - p_1} \tag{D.6}$$

Defining the constants $k_1 = \frac{a^2}{V_1}$, $k_2 = \frac{a^2}{V_2}$, $k_3 = \frac{A}{L}$, the model (D.1)-(D.3) becomes

$$\dot{p}_1 = k_1\left(w_f - w + w_r\right) = f_1(\cdot) \tag{D.7}$$
$$\dot{p}_2 = k_2\left(w - w_r - w_t\right) = f_2(\cdot) \tag{D.8}$$
$$\dot{w} = k_3\left(\Psi_c\left(w\right)p_1 - p_2\right) = f_3(\cdot) \tag{D.9}$$

The domain where the equations are continuously differentiable is $D = \{ [p_1\ p_2\ w]^T \in R^3 \mid p_1 < p_{upstream},\ p_2 > \max(p_{01}, p_1),\ w_{deepsurge,min} < w < w_{stonewall}\}$. The compressor characteristic Ψ_c is assumed continuously differentiable as well.

D.3 Equilibrium Points

Equilibrium points (p_1^*, p_2^*, w^*) for the system (D.7)-(D.9) are given by

$$w_f^* + w_r^* = w^* \tag{D.10}$$
$$w_t^* + w_r^* = w^* \tag{D.11}$$
$$\Psi_c(w^*) = \frac{p_2^*}{p_1^*} \tag{D.12}$$

D.4 Shift to the Origin

Defining the deviation from the equilibrium point as

$$\hat{p}_1 = p_1 - p_1^* \tag{D.13}$$
$$\hat{p}_2 = p_2 - p_2^* \tag{D.14}$$
$$\hat{w} = w - w^* \tag{D.15}$$

The new equations are then

$$\dot{\hat{p}}_1 = k_1 \left(w_f - (\hat{w} + w^*) + w_r \right) \tag{D.16}$$
$$\dot{\hat{p}}_2 = k_2 \left(\hat{w} + w^* - w_r - w_t \right) \tag{D.17}$$
$$\dot{\hat{w}} = k_3 \left(\Psi_c \left(\hat{w} + w^* \right) \left(\hat{p}_1 + p_1^* \right) - \left(\hat{p}_2 + p_2^* \right) \right) \tag{D.18}$$

We can center $\hat{\Psi}_c(\hat{w})$ at the origin in the same way as the characteristic in the pressure rise form. That is because they both have the S-form. The compressor characteristic would belong to sector $(-\infty, 0)$ for stable negative slopes, and belong to sector $(0, \infty)$ for unstable positive slopes. In Figure D.4.1 the shift is shown.

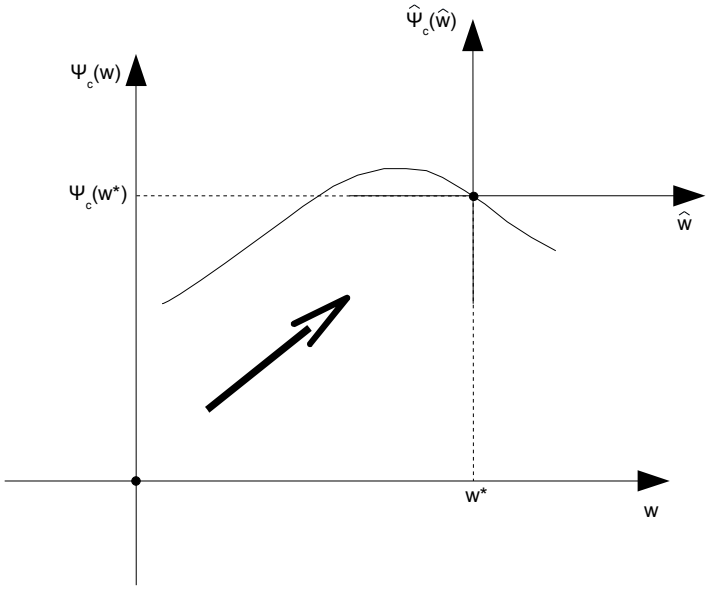

Figure D.4.1: Equilibrium shifting of the compressor characteristic

Lets define

$$\hat{\Psi}_c(\hat{w}) \triangleq \Psi_c \left(\hat{w} + w^* \right) - \Psi_c(w^*) \tag{D.19}$$

in which $\hat{\Psi}_c(0) = 0$ proves that it is centered at the origin. Lets further define

$$\hat{w}_t(\hat{p}_2) \triangleq w_t \left(\hat{p}_2 + p_2^* \right) - w_t(p_2^*) \tag{D.20}$$
$$\hat{w}_f(\hat{p}_1) \triangleq w_f \left(\hat{p}_1 + p_1^* \right) - w_f(p_1^*) \tag{D.21}$$
$$\hat{w}_r(\hat{p}_1, \hat{p}_2) \triangleq w_r \left(\hat{p}_1 + p_1^*, \hat{p}_2 + p_2^* \right) - w_r(p_1^*, p_2^*) \tag{D.22}$$

in which we know that $\hat{w}_t$ belongs to the sector $(0, \infty)$ and $\hat{w}_f$ belongs to sector $(-\infty, 0)$. The model (D.16)-(D.18) now becomes

$$\begin{aligned}
\dot{\hat{p}}_1 &= k_1 \left(\hat{w}_f(\hat{p}_1) + w_f(p_1^*) - \hat{w} - w^* + \hat{w}_r(\hat{p}_1, \hat{p}_2) + w_r(p_1^*, p_2^*)\right) && \text{(D.23)} \\
\dot{\hat{p}}_2 &= k_2 \left(\hat{w} + w^* - \hat{w}_r(\hat{p}_1, \hat{p}_2) - w_r(p_1^*, p_2^*) - \hat{w}_t(\hat{p}_2) - w_t(p_2^*)\right) && \text{(D.24)} \\
\dot{\hat{w}} &= k_3 \left(\left[\hat{\Psi}_c(\hat{w}) + \Psi_c(w^*)\right] (\hat{p}_1 + p_1^*) - (\hat{p}_2 + p_2^*) \right) && \text{(D.25)}
\end{aligned}$$

The equilibrium points (D.10)-(D.12) implies that $w_f(p_1^*) - w^* + w_r(p_1^*, p_2^*) = 0$, $w^* - w_r(p_1^*, p_2^*) - w_t(p_2^*) = 0$ and that $\Psi_c(w^*)p_1^* - p_2^* = 0$. (D.23)-(D.25) becomes

$$\begin{aligned}
\dot{\hat{p}}_1 &= k_1 \left(\hat{w}_f(\hat{p}_1) - \hat{w} + \hat{w}_r(\hat{p}_1, \hat{p}_2)\right) && \text{(D.26)} \\
\dot{\hat{p}}_2 &= k_2 \left(\hat{w} - \hat{w}_r(\hat{p}_1, \hat{p}_2) - \hat{w}_t(\hat{p}_2)\right) && \text{(D.27)} \\
\dot{\hat{w}} &= k_3 \left(\hat{\Psi}_c(\hat{w})(\hat{p}_1 + p_1^*) + \Psi_c(w^*)\hat{p}_1 - \hat{p}_2 \right) && \text{(D.28)}
\end{aligned}$$

D.5 Lyapunov Analysis for Zero Recycle Flow

The Lyapunov function

$$V(\hat{p}_1, \hat{p}_2, \hat{w}) = \frac{1}{2}\Psi_c^* \frac{k_2 k_3}{k_1} \hat{p}_1^2 + \frac{1}{2} k_3 \hat{p}_2^2 + \frac{1}{2} k_2 \hat{w}^2 \qquad \text{(D.29)}$$

where $\Psi_c^* = \Psi_c(w^*)$, is positive definite and radially unbounded. Its derivative along the trajectories of the system (D.26)-(D.28) is

$$\begin{aligned}
\dot{V} &= \frac{k_2 k_3}{k_1} \Psi_c^* \hat{p}_1 \dot{\hat{p}}_1 + k_3 \hat{p}_2 \dot{\hat{p}}_2 + k_2 \hat{w} \dot{\hat{w}} \\
&= k_2 k_3 \Psi_c^* \hat{p}_1 \left[\hat{w}_f(\hat{p}_1) - \hat{w} + \hat{w}_r(\hat{p}_1, \hat{p}_2)\right] \\
&\quad + k_2 k_3 \hat{p}_2 \left[\hat{w} - \hat{w}_r(\hat{p}_1, \hat{p}_2) - \hat{w}_t(\hat{p}_2)\right] \\
&\quad + k_2 k_3 \hat{w} \left[\hat{\Psi}_c(\hat{w})(\hat{p}_1 + p_1^*) + \Psi_c^* \hat{p}_1 - \hat{p}_2\right] \\
&= k_2 k_3 \left[\Psi_c^* \hat{p}_1 \hat{w}_f(\hat{p}_1) + (\Psi_c^* \hat{p}_1 - \hat{p}_2)\, \hat{w}_r(\hat{p}_1, \hat{p}_2)\right. \\
&\quad \left. - \hat{p}_2 \hat{w}_t(\hat{p}_2) + \hat{w} \hat{\Psi}_c(\hat{w})(\hat{p}_1 + p_1^*)\right] \qquad \text{(D.30)}
\end{aligned}$$

Zero change in recycle means $\hat{w}_r = 0$, and that

$$\dot{V} = k_2 k_3 \left[\Psi_c^* \hat{p}_1 \hat{w}_f(\hat{p}_1) - \hat{p}_2 \hat{w}_t(\hat{p}_2) + \hat{w} \hat{\Psi}_c(\hat{w})(\hat{p}_1 + p_1^*)\right] \qquad \text{(D.31)}$$

We know that $k_2, k_3, \Psi_c^* > 0$ and that $\hat{p}_1 + p_1^* > 0 \ \forall \ \hat{p}_1 \in D$. The sector properties of $\hat{w}_f(\hat{p}_1)$ and $\hat{w}_t(\hat{p}_2)$ implies that $\hat{p}_1\hat{w}_f(\hat{p}_1) < 0 \ \forall \ \hat{p}_1 \in D - \{\hat{p}_1 = 0\}$ and that $\hat{p}_2\hat{w}_t(\hat{p}_2) > 0 \ \forall \ \hat{p}_2 \in D - \{\hat{p}_2 = 0\}$. The term $\hat{w}\hat{\Psi}_c(\hat{w})$ is negative definite if $\hat{\Psi}_c(\hat{w})$ belongs to sector $(-\infty, 0)$. And thats the case during operation on a negative slope of the characteristic, or $w > w_{\Psi_c,max}$. The result is that $\dot{V} < 0$ in $D' - \{0\}$, where $D' = \{ \ [p_1 \ p_2 \ w]^T \in R^3 \mid p_1 < p_{upstream}, \ p_2 > \max(p_{01}, p_1), \ w_{\Psi_c,max} < w < w_{stonewall}\}$, and that the origin of the recycle system (D.26)-(D.28) is asymptotically stable. (Theorem 4.1, Khalil (2002)) The simple result is summed up in the lemma below.

Lemma D.1 *Given the recycle system*

$$\dot{p}_1 = k_1 (w_f - w + w_r) \tag{D.32}$$
$$\dot{p}_2 = k_2 (w - w_r - w_t) \tag{D.33}$$
$$\dot{w} = k_3 (\Psi_c (w) p_1 - p_2) \tag{D.34}$$

independent of recycle flow w_r, with zero change in it, the system is asymptotically stable as long as the operating point of the compressor characteristic is located in the negative slope area.

◇

The result we're after is that the recycle system is asymptotically stable, independent of change in recycle flow, as long as we're operating on a negative slope. We were not able to prove this here.

D.6 General Lyapunov Analysis

In the previous section we could only prove asymptotic stability when operating on a negative slope for zero change in recycle flow. During simulations, it seems like the recycle system is asymptotically stable, also during change in recycle flow, as long as we're operating on a negative slope of the characteristic. But the system is very complex, and everything is dependent on each other. Decreasing the recycle flow would move the operating point towards the surge line. It means that operating in the safe area on the characteristic would implicitly mean that the recycle flow and the throttle flow are "safely" tuned. Therefore, in this section, a more general stability conclusion is attempted. Lets make another equilibrium shift of the compressor characteristic

$$\hat{\Psi}_c'(\hat{w}, \hat{p}_1) \triangleq \Psi_c (\hat{w} + w^*) - \frac{\Psi_c^* p_1^* + \hat{p}_1}{\hat{p}_1 + p_1^*} \tag{D.35}$$

and it is seen that this function has some interesting properties. It is two-dimensionally centered at the origin, $\hat{\Psi}'_c(0,0) = \Psi^*_c - \Psi^*_c = 0$, and it reduces to (D.19) when $\hat{p}_1 = 0$.

The model (D.16)-(D.18) now becomes

$$\begin{aligned}
\dot{\hat{p}}_1 &= k_1 \left(\hat{w}_f(\hat{p}_1) + w_f(p_1^*) - \hat{w} - w^* + \hat{w}_r(\hat{p}_1, \hat{p}_2) + w_r(p_1^*, p_2^*)\right) && \text{(D.36)}\\
\dot{\hat{p}}_2 &= k_2 \left(\hat{w} + w^* - \hat{w}_r(\hat{p}_1, \hat{p}_2) - w_r(p_1^*, p_2^*) - \hat{w}_t(\hat{p}_2) - w_t(p_2^*)\right) && \text{(D.37)}\\
\dot{\hat{w}} &= k_3 \left(\left[\hat{\Psi}'_c(\hat{w}, \hat{p}_1) + \frac{\Psi^*_c p_1^* + \hat{p}_1}{\hat{p}_1 + p_1^*} \right] (\hat{p}_1 + p_1^*) - (\hat{p}_2 + p_2^*) \right) && \text{(D.38)}
\end{aligned}$$

And the equilibrium points implies along with some calculation that

$$\begin{aligned}
\dot{\hat{p}}_1 &= k_1 \left(\hat{w}_f(\hat{p}_1) - \hat{w} + \hat{w}_r(\hat{p}_1, \hat{p}_2)\right) && \text{(D.39)}\\
\dot{\hat{p}}_2 &= k_2 \left(\hat{w} - \hat{w}_r(\hat{p}_1, \hat{p}_2) - \hat{w}_t(\hat{p}_2)\right) && \text{(D.40)}\\
\dot{\hat{w}} &= k_3 \left(\hat{\Psi}'_c(\hat{w}, \hat{p}_1)(\hat{p}_1 + p_1^*) + \hat{p}_1 - \hat{p}_2 \right) && \text{(D.41)}
\end{aligned}$$

Using the Lyapunov function

$$V(\hat{p}_1, \hat{p}_2, \hat{w}) = \frac{1}{2}\frac{k_2 k_3}{k_1}\hat{p}_1^2 + \frac{1}{2}k_3\hat{p}_2^2 + \frac{1}{2}k_2\hat{w}^2 \qquad \text{(D.42)}$$

which is positive definite and radially unbounded, the derivative along the trajectories of the system is now

$$\begin{aligned}
\dot{V} &= \frac{k_2 k_3}{k_1}\hat{p}_1\dot{\hat{p}}_1 + k_3\hat{p}_2\dot{\hat{p}}_2 + k_2\hat{w}\dot{\hat{w}}\\
&= k_2 k_3 \hat{p}_1 \left[\hat{w}_f(\hat{p}_1) - \hat{w} + \hat{w}_r(\hat{p}_1, \hat{p}_2)\right]\\
&\quad + k_2 k_3 \hat{p}_2 \left[\hat{w} - \hat{w}_r(\hat{p}_1, \hat{p}_2) - \hat{w}_t(\hat{p}_2)\right]\\
&\quad + k_2 k_3 \hat{w} \left[\hat{\Psi}'_c(\hat{w}, \hat{p}_1)(\hat{p}_1 + p_1^*) + \hat{p}_1 - \hat{p}_2\right]\\
&= k_2 k_3 \left[\hat{p}_1 \hat{w}_f(\hat{p}_1) - (\hat{p}_2 - \hat{p}_1)\, \hat{w}_r(\hat{p}_1, \hat{p}_2)\right.\\
&\quad \left. - \hat{p}_2 \hat{w}_t(\hat{p}_2) + \hat{w}\hat{\Psi}'_c(\hat{w}, \hat{p}_1)(\hat{p}_1 + p_1^*)\right] \qquad \text{(D.43)}
\end{aligned}$$

We know from before that $\hat{p}_1\hat{w}_f(\hat{p}_1)$ is negative definite and that $-\hat{p}_2\hat{w}_t(\hat{p}_2)$ is negative definite. Lets now investigate the properties of $(\hat{p}_2 - \hat{p}_1)\,\hat{w}_r(\hat{p}_1, \hat{p}_2)$. It can be written as

$$\begin{aligned}
(\hat{p}_2 - \hat{p}_1)\,\hat{w}_r(\hat{p}_1, \hat{p}_2) &= (\hat{p}_2 - \hat{p}_1)\left(w_r(\hat{p}_1 + p_1^*, \hat{p}_2 + p_2^*) - w_r(p_1^*, p_2^*)\right)\\
&= (\hat{p}_2 - \hat{p}_1)\left(c_r\sqrt{\hat{p}_2 + p_2^* - \hat{p}_1 - p_1^*} - c_r\sqrt{p_2^* - p_1^*}\right)\\
&= c_r X \left(\sqrt{X + p_2^* - p_1^*} - \sqrt{p_2^* - p_1^*}\right)\\
&= c_r X \hat{w}_r(X) \qquad \text{(D.44)}
\end{aligned}$$

where $X = \hat{p}_2 - \hat{p}_1$. We know that a function on the form $f(x) = \sqrt{x+a} - \sqrt{a}$, where $x > -a$ and $a > 0$, belongs to sector $(0, \infty)$. It implies that $\hat{w}_r(X)$ belongs to sector $(0, \infty)$ since it is a function on that form. That means that (D.44) will be positive, $\forall\ X$ in $D - \{\hat{p}_2 - \hat{p}_1 = 0\}$, and positive semidefinite $\forall\ X$ in D.

The last term inside the brackets of (D.43), which contains the two-dimensional shifted compressor characteristic, can be written as

$$\begin{aligned}
\hat{w}\hat{\Psi}_c'(\hat{w}, \hat{p}_1)\,(\hat{p}_1 + p_1^*) &= \hat{w}\left(\Psi_c(\hat{w} + w^*) - \frac{\Psi_c^* p_1^* + \hat{p}_1}{\hat{p}_1 + p_1^*}\right)(\hat{p}_1 + p_1^*) \\
&= \hat{w}\,(\Psi_c(\hat{w} + w^*)(\hat{p}_1 + p_1^*) - \Psi_c^* p_1^* - \hat{p}_1) \\
&= \hat{w}\,(\Psi_c(w)\hat{p}_1 + \Psi_c(\hat{w} + w^*)p_1^* - \Psi_c^* p_1^* - \hat{p}_1) \\
&= \hat{w}\,((\Psi_c(\hat{w} + w^*) - \Psi_c^*)\,p_1^* + (\Psi_c(w) - 1)\,\hat{p}_1) \\
&= \hat{w}\left(\hat{\Psi}_c(\hat{w})p_1^* + k_c\hat{p}_1\right) \qquad \text{(D.45)}
\end{aligned}$$

We know that the compressor characteristic $\Psi_c(w)$ is always greater than 1 with our assumptions. That is, $\Psi_c(w) > 1 \Rightarrow \Psi_c(w) - 1 > 0 \Rightarrow k_c > 0$. When the pressure in volume 1 is not changing, $\hat{p}_1 = 0$, (D.45) is negative definite if $\hat{\Psi}_c(\hat{w})$ belongs to sector $(-\infty, 0)$. That is negative slope, as before.

There is another story when p_1 is allowed to change. The question arises, what kind of conditions will have to be imposed in order for (D.45) to be negative definite? First of all, lets continue to assume that we're operating on a negative slope and that $\hat{\Psi}_c(\hat{w})$ belongs to sector $(-\infty, 0)$. When $\hat{w}$ is negative $\hat{\Psi}_c(\hat{w})p_1^*$ will be positive. And as long as $\hat{\Psi}_c(\hat{w})p_1^* > -k_c\hat{p}_1$, (D.45) will be negative. Similarly, when $\hat{w}$ is positive $\hat{\Psi}_c(\hat{w})p_1^*$ will be negative. And as long as $\hat{\Psi}_c(\hat{w})p_1^* < -k_c\hat{p}_1$, (D.45) will be negative. In other words, when $\hat{w}$ is negative, $k_c\hat{p}_1$ will have to be lower bounded, and when $\hat{w}$ is positive, $k_c\hat{p}_1$ will have to be upper bounded. It can be summed up as $|k_c\hat{p}_1| < |\hat{\Psi}_c(\hat{w})|p_1^*$ $\forall\ \hat{p}_1,\ \hat{w} \in D - \{\hat{p}_1 = 0, \hat{w} = 0\}$. The result is a bound on $\hat{p}_1$,

$$|\hat{p}_1| < \frac{1}{k_c}|\hat{\Psi}_c(\hat{w})|p_1^* \qquad \text{(D.46)}$$

Of course, a bound on $\hat{p}_1$ is not appropriate. However, there is a possibility that (D.46) is a general property of the system (D.26)-(D.28).

D.7 Coordinate Transformation

Consider the coordinate transformation

$$x_1 = \frac{1}{k_1}\hat{p}_1 + \frac{1}{k_2}\hat{p}_2 \tag{D.47}$$

$$x_2 = \frac{1}{k_3}\hat{w} \tag{D.48}$$

$$x_3 = \frac{1}{k_2}\hat{p}_2 \tag{D.49}$$

of the system (D.26)-(D.28). It makes the input we're going to use, w_r, only appear in one of the equations. This is achieved while conserving the dynamics of the system by saving $\dot{\hat{p}}_2$. The new equations become

$$\dot{x}_1 = \hat{w}_f(k_1(x_1 - x_3)) - \hat{w}_t(k_2 x_3) \tag{D.50}$$

$$\dot{x}_2 = \hat{\Psi}_c(k_3 x_2)(k_1(x_1 - x_3) + p_1^*) + \Psi_c^* k_1(x_1 - x_3) - k_2 x_3 \tag{D.51}$$

$$\dot{x}_3 = k_3 x_2 - \hat{w}_r(k_1(x_1 - x_3), k_2 x_3) - \hat{w}_t(k_2 x_3) \tag{D.52}$$

By using a Lyapunov function on the form

$$V(z) = \frac{1}{2}k_1(x_1 - x_3)^2 + \frac{1}{2}k_3 x_2^2 \tag{D.53}$$

this procedure also failed to show stability of any kind.